MISSOURI S&T

CENTER FOR TRANSPORTATION INFRASTRUCTURE AND SAFETY

Design for FRP Systems for Strengthening Concrete Girders in Shear

by

Abdeldjelil Belarbi
Sang-Wook Bae
Ashraf Ayoub
Daniel Kuchma
Amir Mirmiran
Ayman Okeil

NUTC R197

A National University Transportation Center at Missouri University of Science and Technology

Disclaimer

The contents of this report reflect the views of the author(s), who are responsible for the facts and the accuracy of information presented herein. This document is disseminated under the sponsorship of the Department of Transportation, University Transportation Centers Program and the Center for Transportation Infrastructure and Safety NUTC program at the Missouri University of Science and Technology, in the interest of information exchange. The U.S. Government and Center for Transportation Infrastructure and Safety assumes no liability for the contents or use thereof.

Technical Report Documentation Page

1. Report No.	2. Government Accession No.	3. Recipient's Catalog No.
NUTC R197		

4. Title and Subtitle	5. Report Date
Design for FRP Systems for Strengthening Concrete Girders in Shear	June 2011
	6. Performing Organization Code

7. Author/s	8. Performing Organization Report No.
Abdeldjelil Belarbi, Sang-Wook Bae, Ashraf Ayoub, Daniel Kuchma, Amir Mirmiran and Ayman Okeil	00017550

9. Performing Organization Name and Address	10. Work Unit No. (TRAIS)
Center for Transportation Infrastructure and Safety/NUTC program Missouri University of Science and Technology 220 Engineering Research Lab Rolla, MO 65409	11. Contract or Grant No. DTRT06-G-0014

12. Sponsoring Organization Name and Address	13. Type of Report and Period Covered
U.S. Department of Transportation Research and Innovative Technology Administration 1200 New Jersey Avenue, SE Washington, DC 20590	Final
	14. Sponsoring Agency Code

15. Supplementary Notes

16. Abstract

FRP systems have been used on a project-specific basis for the last two decades. They are now becoming a widely accepted method of strengthening concrete structures. The acceptance and utilization of these new strengthening techniques depend on the availability of clear design guidelines, installation procedures and construction specifications. Standard specifications exist for all commonly used traditional materials in civil engineering structures. At this time, design specifications for FRP use are still under development. The results of several experimental investigations have shown that FRP systems can be effective for increasing ductility and strength to structural members such as columns and girders. As most of the research focused on strengthening of axial members of flexural members, there are less experimental and analytical data on the use of FRP systems for shear strengthening of girders. Shear strengthening with FRP is still under investigation and the results obtained thus far are scarce and sometimes controversial. Even in traditional reinforced concrete members without FRP, the shear design is a complex challenge and uses more empirical methods as compared to axial and flexural design methods. Adding FRP to the equation, with its specific design issues, would bring another level of complication in the design. These FRP-related shear design issues and lack of comprehensive analytical and experimental models are the main motivation for this research project. Thus, a thorough understanding of the shear design problem along with the development of an AASHTO design method for FRP shear strengthening of concrete girders are needed.

As such, the objective of this project is to develop design methods, specifications, and examples for design of FRP systems for strengthening concrete girders in shear. The proposed specifications will be in LRFD format and will be suitable for recommendation to the AASHTO Highway Subcommittee on Bridges and Structures for adoption.

17. Key Words	18. Distribution Statement
Bridge, Bridge Girders, FRP Strengthening	No restrictions. This document is available to the public through the National Technical Information Service, Springfield, Virginia 22161.

19. Security Classification (of this report)	20. Security Classification (of this page)	21. No. Of Pages	22. Price
unclassified	unclassified	124	

FOREWORD

By Amir N. Hanna
Staff Officer
Transportation Research Board

This report presents design guidelines for concrete girders strengthened in shear using externally bonded Fiber-Reinforced Polymer (FRP) systems. These guidelines address the strengthening schemes and application of the FRP systems and their contribution to shear capacity of reinforced and prestressed concrete girders. The guidelines are supplemented by design examples to illustrate their use for concrete beams strengthened with different FRP systems. The guidelines are presented in AASHTO LRFD format to facilitate use and incorporation into the *AASHTO LRFD Bridge Design Specifications.* Also, the report presents recommended changes to the *AASHTO LRFD Bridge Design Specifications* to introduce provisions pertaining to the use of FRP systems for strengthening concrete girders in shear. The material contained in the report should be of immediate interest to state bridge engineers and those involved in the strengthening and repair of concrete structures using FRP systems.

Use of externally bonded FRP systems for the repair and strengthening of reinforced and prestressed concrete bridge structures has become accepted practice by some state highway agencies because of their technical and economic benefits. Such FRP systems are lightweight, exhibit high tensile strength, and are easy to install; these features facilitate handling and help expedite repair or construction. Extensive research has shown that FRP systems improve both short- and long-term flexural behavior of concrete girders. Several analytical studies have dealt with the shear behavior of concrete girders strengthened with FRP systems and a number of models were developed to predict such behavior. However, limited experimental studies have investigated the validity of these models. Nevertheless, some of these studies have shown that FRP systems can provide an effective means for increasing the shear capacity of concrete girders. Currently, there are no widely accepted guidelines for the design of concrete girders strengthened in shear using externally bonded FRP systems. Thus, research was needed to review available information, conduct analytical and experimental investigations to evaluate the contributions of FRP systems to shear capacity, and develop design guidelines for concrete girders strengthened in shear using externally bonded FRP systems. These guidelines will provide highway agencies with the information necessary for considering externally bonded FRP systems for shear strengthening of concrete girders to expedite repair and yield economic and other benefits.

Under NCHRP Project 12-75, "Design of FRP Systems for Strengthening Concrete Girders in Shear," Missouri University of Science and Technology of Rolla, conducted a review of the existing information and practices relevant to the strengthening of concrete girders in shear using FRP systems; identified the factors that influence the design of such girders; evaluated available design methods and the shear design parameters that account for the FRP strengthening; and conducted laboratory tests to evaluate the effect of important factors on

girder response and shear strengthening. Results of this work provided a basis for developing guidelines and proposed changes to the *AASHTO LRFD Bridge Design Specifications*. The guidelines and proposed changes are accompanied by commentaries that are necessary for explaining the background, applicability, and limitations of the respective provisions. In addition, design examples are provided to illustrate use of the guidelines for designing FRP systems for strengthening reinforced and prestressed concrete beams.

The guidelines presented in this report will be particularly useful to highway agencies because they facilitate consideration of FRP systems among the options available for the shear strengthening of concrete girders and help select options that are expected to yield economic and other benefits. The incorporation of the recommended design guidelines into the *AASHTO LRFD Bridge Design Specifications* will provide easy access to the information needed for the design of externally bonded FRP systems for the strengthening of concrete girders in shear.

The appendix contained in the research agency's final report provides further elaboration on the work performed in this project. This appendix titled "Research Description and Findings" is not published herein; but it is available on the *NCHRP Report 678* summary webpage at http://www.trb.org/Main/Blurbs/164622.aspx.

CONTENTS

1 Summary

4 **Chapter 1** Introduction
4 1.1 Background
4 1.2 Research Objectives
4 1.3 Research Plan and Methodology
4 1.4 Organization of the Report

7 **Chapter 2** Summary of Major Findings
7 2.1 Use of FRP for Shear Strengthening of Concrete Girders
7 2.2 Field Applications
8 2.3 Existing Analytical Models
8 2.4 Experimental Investigations Reported in the Literature
21 2.5 Current Codes/Guidelines/Specifications
22 2.6 Factors Affecting the Design of FRP Shear Strengthening
32 2.7 Performance Evaluation of Existing Design Methods
33 2.8 Suggestions for Improved Design Methods
35 2.9 Reliability Assessment

37 **Chapter 3** Application and Implementation
37 3.1 Approaches for Relevant Changes to AASHTO LRFD Bridge Design Specifications
38 3.2 Design Guidelines
38 3.3 Design Examples

39 **Chapter 4** Summary of Findings and Recommendations for Future Research
39 4.1 Summary of Findings
40 4.2 Suggestions for Future Research

41 Notations

47 References

51 **Attachment A** Recommended Changes to AASHTO LRFD Bridge Design Specifications

59 **Attachment B** Recommended Design Guidelines for Concrete Girders Strengthened in Shear with RFP

Note: Many of the photographs, figures, and tables in this report have been converted from color to grayscale for printing. The electronic version of the report (posted on the Web at www.trb.org) retains the color versions.

SUMMARY

Design of FRP Systems for Strengthening Concrete Girders in Shear

Background

Fiber-reinforced polymer (FRP) systems have been used for more than 20 years and are becoming a widely accepted method of strengthening concrete structures. The use of FRP composites in rehabilitating structures has grown in popularity due to its advantages over conventional materials and wide range of structural applications. FRP systems for strengthening reinforced or prestressed concrete girders consist of externally bonded laminates or near-surface mounted bars. These systems may contain either carbon or glass fibers. Because of their light-weight and exceptional formability, FRP reinforcements can be quickly and easily bonded to even the most curved and irregular surfaces. The high strength-to-weight ratio of FRP composites makes them more structurally efficient than traditional strengthening materials. In addition, FRP composites are noncorrosive, nonmagnetic, nonconductive, and generally resistant to chemicals.

Externally bonded FRP systems composites are generally used for flexural strengthening, confinement and improvement of ductility in columns, or shear strengthening. Although flexure is typically the limiting mode of failure in bridge girder design, shear failure may dominate in cases where the transverse reinforcement has severely corroded or the flexural strength has been increased due to flexural strengthening. In such cases, the shear capacity should be enhanced to avoid catastrophic failures. A significant amount of research has been conducted on flexural and axial strengthening but limited investigations have been conducted on the use of externally bonded FRP for shear strengthening. Nevertheless, several models have been proposed for predicting the shear contribution of externally bonded FRP. These models are diverse in their approach and in many cases contradictory in their estimates of strength increase. FRP reinforcement configurations include the selection of surfaces to be bonded (side bonding, U-wrap, complete wrap), continuous reinforcement or a series of discrete strips, and orientation of the primary direction of fibers. The bond characteristics between the FRP and concrete substrate add to the complexity in understanding the FRP shear contribution. The effectiveness of the strengthening method has been found to depend on the mode of failure.

The use of FRPs for external strengthening of concrete structures has been hindered by the lack of comprehensive design provisions. Design of FRP strengthening systems has been based on system- or project-specific research. The AASHTO LRFD Bridge Design Specifications (AASHTO, 2008) include no provisions for the design of externally bonded FRP systems. NCHRP Project 12-75 was initiated to develop a recommended design method for shear strengthening of concrete girders using FRP systems.

Project Objectives and Scope

The objective of this project was to develop design methods, specifications, and examples for the design of FRP systems for strengthening concrete girders in shear. The proposed specifications are intended for incorporation into the AASHTO LRFD Bridge Design Specifications (AASHTO, 2008). Such specifications will provide design engineers with the information needed for considering externally bonded FRP systems for shear strengthening of existing structures. To accomplish this objective, the research involved the following tasks:

- Study and review relevant practices, existing models and specifications, and research findings from both foreign and domestic sources regarding the use of externally bonded FRP for shear strengthening of concrete girders.
- Identify and evaluate criteria that influence the performance of FRP shear strengthening systems based on review of the literature (including the development of a database of tests related to FRP shear strengthening).
- Evaluate the performance of existing design methods.
- Investigate in full-scale tests, the key parameters affecting the shear performance of externally bonded FRP for both reinforced concrete (RC) and prestressed concrete (PC) girders.
- Recommended provisions and specifications for incorporation into the AASHTO LRFD Bridge Design Specifications.

Overview

To develop design provisions for shear strengthening with externally bonded FRP systems, the parameters affecting the behavior of such systems were identified first through review of the existing literature. Also, a database of the reported test results on the use of externally bonded FRP for shear strengthening was compiled. An experimental program was then developed to further study parameters that were considered to have not been sufficiently investigated in earlier tests, including the effects of pre-cracking, continuity (negative moment), long-term conditioning (such as fatigue loading and corrosion of internal steel reinforcement), and prestressing. The experimental program included full-scale tests on RC T-beams and AASHTO type PC I-girders because most current design equations used in design specifications are based on small-scale test results. An assessment of the existing design methods found significant differences in the magnitude of the FRP shear contribution calculated by various design methods. This assessment revealed the deficiencies of the existing design methods in predicting the shear resistance of a wide range of girder and FRP reinforcement characteristics. Therefore, new design equations for predicting the shear contribution of externally bonded FRP systems were developed and calibrated.

Research Findings

The major findings of this research effort are summarized as follows:

- Externally bonded FRP can be used to enhance the shear resistance of concrete girders.
- The effectiveness of externally bonded FRP for shear strengthening depends on the failure mode (i.e., FRP rupture or debonding).
- The effectiveness of FRP shear strengthening is significantly affected by the cross-sectional shape of the girder.
- The use of a properly designed mechanical anchorage system delays and in some cases prevents debonding of the FRP, resulting in a more effective strengthening scheme.

- An interaction exists between the transverse steel reinforcement and externally bonded FRP; the effectiveness of externally bonded FRP for shear decreases as the transverse steel reinforcement ratio increases.
- The shear span-to-depth ratio (a/d) has a significant influence on the effectiveness of externally bonded FRP for shear.
- The size-effect has little influence on the effectiveness of externally bonded FRP and thus empirical design expressions calibrated from small-scale test results should provide reasonable accuracy.
- The presence of pre-existing cracks and slight damage due to corrosion of the internal transverse steel reinforcement prior to strengthening does not seem to impair the effectiveness of the external FRP shear reinforcement.
- Beam continuity does not seem to influence the effectiveness of the FRP strengthening system.
- The effective FRP strain used in evaluating the FRP shear contribution can be expressed by two separate design expressions to consider the two predominant failure modes (i.e., debonding and FRP rupture).
- Under severe fatigue loading conditions (e.g., stirrups yielding), externally bonded FRP shear reinforcement may experience debonding if proper anchorage is not provided. If stress in the stirrups can be maintained below the yield strength, the externally bonded FRP shear strengthening can help delay fatigue yielding of the stirrups and extend the fatigue life of the girder. If stirrups have already yielded prior to FRP application, the FRP may still help contain the stresses and prevent catastrophic failure but not necessarily extending the service life of the girder.

CHAPTER 1

Introduction

1.1 Background

Fiber-Reinforced Polymer (FRP) systems have shown potential for use in rehabilitating and retrofitting existing structures. They can be used to provide increased ductility as well as shear and flexural strength to structural elements such as columns, beams/girders, slabs/decks, and walls. Typical applications include compensation for increased traffic volumes on bridges, dampening of vibration, corrosion rehabilitation, correction of deficient design, etc. (Busel and Barno, 1995 and ACI 440.2R-08, 2008).

FRP systems have been used on a project-specific basis for the last two decades. They are now becoming a widely accepted method of strengthening concrete structures. FRP systems used for strengthening reinforced or prestressed concrete girders consist of externally bonded laminates or near-surface mounted bars. These systems may contain either carbon or glass fibers and thus carbon fiber reinforced polymer (CFRP) or glass fiber reinforced polymer (GFRP). The acceptance and use of these strengthening techniques depend on the availability of clear design guidelines, installation procedures, and construction specifications. Standard specifications exist for all materials commonly used in civil engineering structures. However, design specifications for FRP use are not readily available. Most research has focused on strengthening of axially loaded or flexural members with limited experimental and analytical data on the use of FRP systems for shear strengthening of girders. This research, performed under NCHRP Project 12-75, was initiated to address FRP-related shear design issues and related specifications and design methods.

1.2 Research Objectives

The objective of this project was to develop design methods, specifications, and examples for design of FRP systems for strengthening concrete girders in shear.

1.3 Research Plan and Methodology

The following tasks were performed to achieve the following project objectives:

1. Review of relevant practice, data, specifications, and research findings from both foreign and domestic sources on the strengthening of concrete girders in shear using FRP systems containing carbon or glass fibers and identification of FRP systems available for shear strengthening.
2. Identification of criteria that influence design of FRP shear strengthening systems.
3. Evaluation of existing design methods and the identification of appropriate shear design provisions that account for FRP and preparation of a work plan for further development of potential design methods.
4. Execution of the work plan and development of the design methods.
5. Preparation of recommended specifications and commentary for shear design of FRP-strengthened concrete girders together with design examples to illustrate the application of the recommended design methods and specifications.
6. Preparation of a report that documents the entire research.

Figure 1.1 shows the process used to determine the critical issues that were addressed in the project. Figure 1.2 illustrates the process used to develop the design methods and specifications.

1.4 Organization of the Report

This chapter presents the background, objectives, methodology, and scope of the project. Chapter 2 summarizes the findings of the research, including the literature review as well as experimental and analytical investigations. Chapter 3

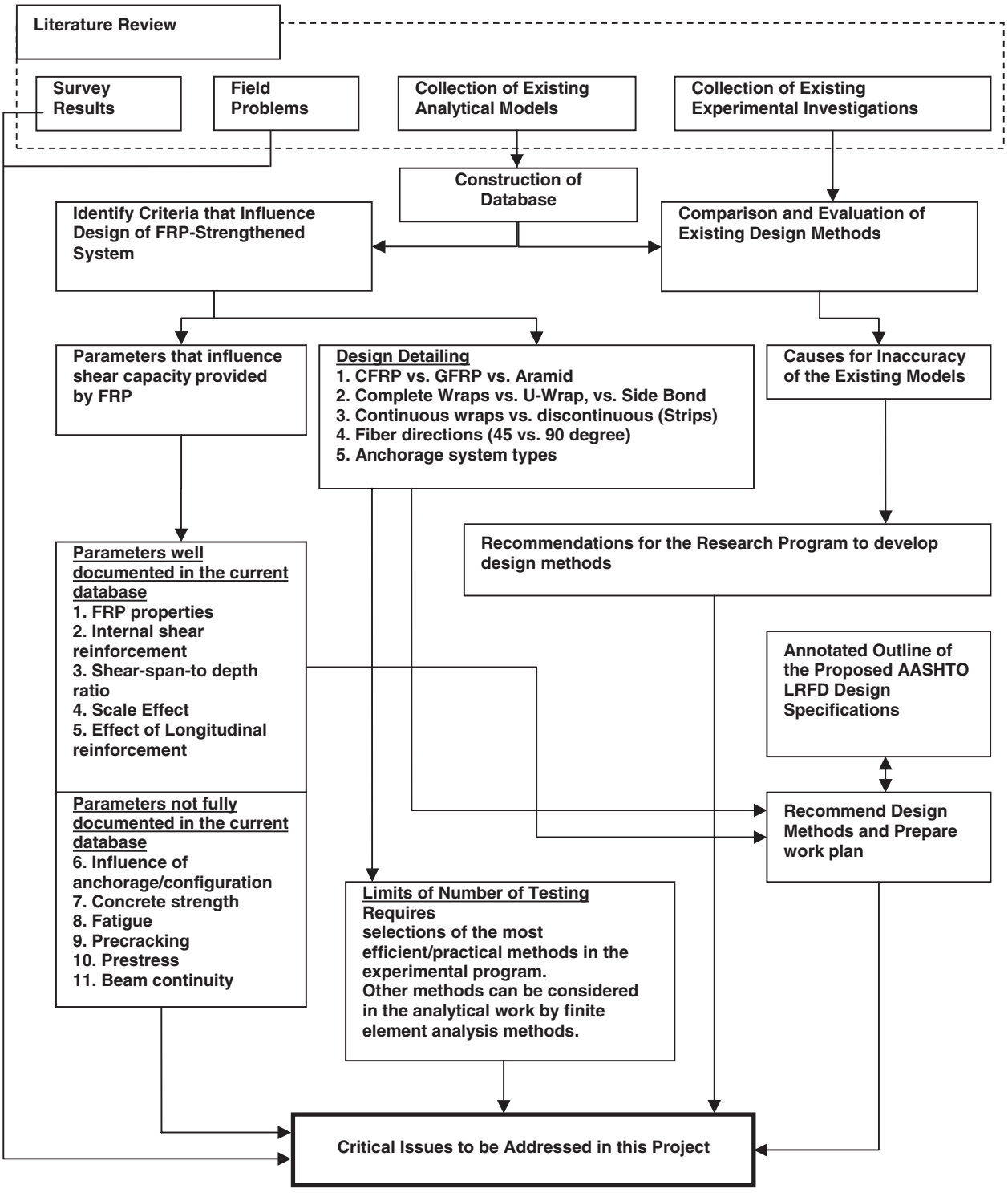

Figure 1.1. Process to determine potential critical issues.

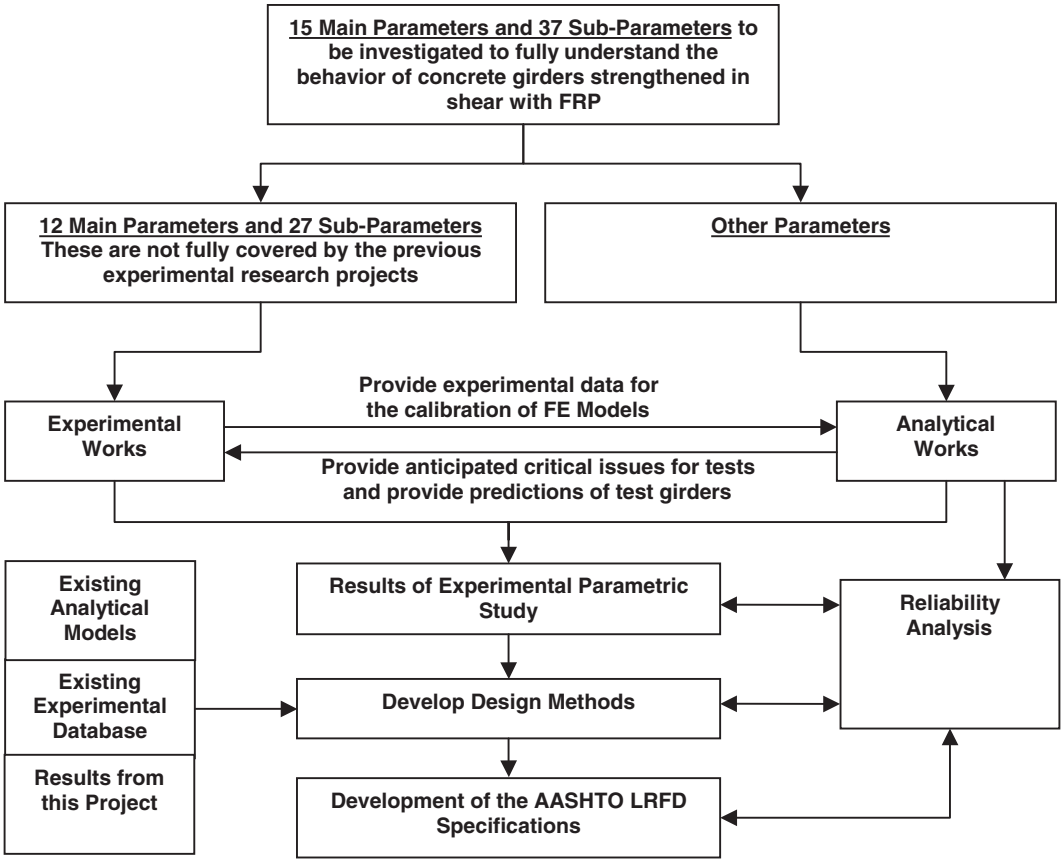

Figure 1.2. Process for developing design methods and specifications.

discusses the application and implementation of the recommended design method and specifications. Chapter 4 presents the conclusions and suggestions for future research. Attachments A and B present suggested changes to AASHTO LRFD Bridge Design Specifications (AASHTO, 2008) and recommended design guidelines, respectively. Appendix A provides more details on all aspects of the research including, the literature review, survey of state DOTs, existing analytical models, experimental investigations, and data analysis. Appendix A is not published herein but can be found on the *NCHRP Report 678* summary webpage at http://www.trb.org/Main/Blurbs/164622.aspx.

CHAPTER 2

Summary of Major Findings

2.1 Use of FRP for Shear Strengthening of Concrete Girders

A survey of state departments of transportation (DOTs), Washington, DC, and Puerto Rico, was conducted to determine the extent of using FRP for shear strengthening. This survey included a written questionnaire (followed by either a telephone briefing or a written response) aimed at determining the practices for designing concrete girders strengthened in shear using FRP and their perceived deficiencies.

The responses received from 39 agencies revealed that only 7 state DOTs used FRP for shear strengthening of concrete girders and 32 DOTs have never used FRP for shear strengthening of concrete girders. Fourteen DOTs indicated no need for shear strengthening of concrete girders, and 12 DOTs expressed a concern about the lack of proper design specifications or provisions for FRP shear strengthening. Some DOTs considered the use of FRPs less efficient when compared to other strengthening techniques.

The DOTs using FRP for shear strengthening follow the design methods contained in ACI 440.2R-02 (ACI 440, 2002) because it was the only design guidelines document available in the United States. Some DOTs (e.g., New York, Oregon, and Pennsylvania) have made slight modifications to ACI 440.2R-02 (ACI 440, 2002). Design guidelines and specifications provided by FRP manufacturers and course notes from a workshop provided by several organizations were used by some state DOTs. Most state DOTs identified provisions regarding properties of FRP composite materials and control of failure modes as the most important issues to be addressed in future design specifications. An in-depth explanation on FRP strengthening schemes and fatigue and durability issues were also noted as major issues to be addressed.

2.2 Field Applications

Although there are several field projects related to FRP strengthening systems, detailed information on these projects is not available and most of these projects were strengthened for flexural rehabilitation. The following six projects were identified as directly related to FRP shear strengthening of concrete bridge girders:

A single span, reinforced concrete T-beam bridge in New York State was strengthened in flexure and shear with externally bonded FRP laminates in November 1999 (Hag-Elsafi et al., 2001b).

The Gröndals Bridge in Sweden is a prestressed concrete box bridge approximately 1,300 feet in length and a free span of 394 feet. CFRP laminate strips were applied to the inside walls with steel plate anchorage system to increase the shear strength (Taljsten et al., 2007).

The Langevin Bridge in Calgary, Canada, is a six-span, four-cell, continuous box-girder bridge constructed in 1972. The internal webs were found to be deficient at the right end of span 2 where the internal prestressing tendons are horizontal and thus contribute nothing to the shear resistance. To correct these deficiencies, CFRP sheets were bonded to the inside face of the external webs and to both faces of the interior webs.

The John Hart Bridge in Prince George, British Columbia and the Maryland Bridge in Winnipeg, Manitoba, are two bridges in western Canada that have been strengthened in shear with externally bonded CFRP. The John Hart Bridge consists of seven simply supported spans with six I-shaped prestressed concrete AASHTO girders per span, and the Maryland Bridge consists of two sets of five continuous spans with seven I-shaped prestressed concrete AASHTO girders per span (Hutchinson et al., 2003).

The Willamette River Bridge located near Newberg, Oregon, was found to have significant diagonal cracking during an inspection conducted by the Oregon Department of Transportation (ODOT) in late summer of 2001. CFRP strips of 12 inch width were applied vertically in a U-shape wrapping scheme (Williams and Higgins, 2008).

The Ebay Island Viaduct Bridge is a 2¼ mile long section of westbound Washington State Route 2 that crosses over environmentally sensitive wetlands near the outflow of the Snohomish River into Puget Sound near Everett, Washington. The bridge was built during the late 1960s. In 1996, bridge condition inspectors noted that the bottoms of the existing precast concrete webs exhibited considerable concrete spalling accompanied with primary steel reinforcement corrosion. In 1999, carbon fiber sheets were bonded to the deteriorated elements for flexural strengthening and to compensate for steel reinforcement loss due to corrosion. In addition, carbon fiber sheets were applied with a U-wrap configuration to compensate for the shear capacity loss due to the cross-sectional loss of stirrups caused by corrosion. The carbon fiber repairs were inspected annually after the completion of the repair project with no debonding or deterioration of the carbon fiber plies being reported through spring 2007 (Dornsife, 2007).

2.3 Existing Analytical Models

This section summarizes the analytical models previously developed for determining the shear resistance of reinforced concrete members strengthened with externally bonded FRP. Seventeen models were found in the literature. These models have been divided into four groups based on their approaches and are presented in the same units as the original papers.

The first group of models is those relying on an empirically determined value of strain/stress associated with failure of the member for which the shear contribution of the FRP is determined; the principal equations of the analytical models in this group are listed in Table 2.1. The second group of models is those based on the determination of an effective FRP strain; the corresponding principal equations are listed in Table 2.2. The third group of models focuses on the non-uniformity of the strain distribution in externally bonded FRP reinforcements; the corresponding principal equations are listed in Table 2.3. The fourth group of models is mechanics-based theoretical approaches that do not rely on experimental results for regression or calibration; the principal equations of these models are listed in Table 2.4.

2.4 Experimental Investigations Reported in the Literature

A review was conducted of experimental investigations which included studies on (1) the behavior of concrete girders strengthened in shear with externally bonded FRP, (2) bond behavior of FRP-concrete interface, and (3) anchorage systems to enhance the effectiveness of FRP strengthening systems.

2.4.1 Studies on the Behavior of Concrete Girders Strengthened in Shear with Externally Bonded FRP

The review included 49 experimental studies, encompassing more than 500 test specimens. The review provides information on the objectives, the methodology, the experimental program, the test method, the FRP used and its orientation, as well as the strengthening scheme used (configuration).

Table 2.1. Models based on experimentally determined limiting value of FRP shear strain/stress.

Reference Author (Year)	Equations
Al-Sulaimani et al. (1994)	$V_P = \dfrac{2\left[\tau_{ave}\dfrac{t_s h_s}{2}\right]d}{S_P}$ (for shear strips) $V_P = 2\left[\tau_{ave}\left(\dfrac{dh_w}{2}\right)\right]$ (for shear wings) $V_P = 2\left[\tau_{ult}\left(\dfrac{dh_j}{2}\right)\right]$ (for U-jackets)
Chajes et al. (1995)	$V_f = A_f E_f \varepsilon v_{cu} d$ (for FRP oriented at 0/90 degree) $V_f = A_f E_f \varepsilon v_{cu} d\sqrt{2}$ (for FRP oriented at 45/135 degree)

* Terms are defined in notations section.

Table 2.2. Models based on an effective FRP strain.

Reference Author (Year)	Equations
Triantafillou (1998)	$V_{frp,d} = \frac{0.9}{\gamma_{frp}} \rho_{frp} E_{frp} \varepsilon_{frp,e} b_w d \left(1 + \cot\beta\right) \sin\beta$ $\varepsilon_{frp,e} = 0.0119 - 0.0205\left(\rho_{frp} E_{frp}\right) + 0.0104\left(\rho_{frp} E_{frp}\right)^2$ when $0 \le \rho_{frp} E_{frp} \le 1$ GPa $\varepsilon_{frp,e} = -0.00065\left(\rho_{frp} E_{frp}\right) + 0.00245$ when $\rho_{frp} E_{frp} > 1$ GPa
Khalifa et al. (1998)	$V_f = 0.9 \rho_{frp} E_{frp} \varepsilon_{fe} b_w d \left(1 + \cot\beta\right) \sin\beta$ (Eurocode format) $V_f = \frac{A_f f_{fe} \left(\sin\beta + \cos\beta\right) d_f}{s_f}$ (ACI format) $\varepsilon_{fe} = R \varepsilon_{fu} \qquad f_{fe} = R f_{fu}$ Based on the effective FRP stress: $R = 0.5622\left(\rho_{frp} E_{frp}\right)^2 - 1.2188\left(\rho_{frp} E_{frp}\right) + 0.778 \le 0.5$ when $\rho_{frp} E_{frp} < 1.1$ GPa Based on bond mechanism: $R = \frac{0.0042\left(f_c^{'}\right)^{2/3} w_{fe}}{\left(E_{frp} t_f\right)^{0.58} \varepsilon_{fu} d_f}$ Effective width: $w_{fe} = d_f$ (complete wrapping) $w_{fe} = d_f - L_e$ (U-wrap) $w_{fe} = d_f - 2L_e$ (side bonded) $s_{f,\max} = w_f + \frac{d}{4} \qquad V_s + V_f \le \frac{2\sqrt{f_c^{'}} b_w d}{3}$
Hutchinson and Rizkalla (1999)	$V_n = V_c + V_{se} + V_{f,\max}$ $V_{f,\max} = \varepsilon_{f,ave} E_f 2 n t_f w_f \frac{d_f \left(\cot\theta + \cot\alpha_f\right) \sin\alpha_f}{s_f}$ $\varepsilon_{f,ave} = \varepsilon_{f\max} \frac{\left[d/2 + 0.5\left(d_f - d/2\right)\right]}{d_f}$ $\varepsilon_{f\max} = L_{fe} C$ $L_{fe} = e^{6.134 - 0.580 \ln\left(t_f E_f\right)}$ and $C = constant\ strain\ rate\ of\ 110 \times 10^{-6}\, mm^{-1}$ $V_{se} = \varepsilon_{se} E_s A_v \frac{d \cot\theta}{s}$ where $\varepsilon_{se} = \varepsilon_{f,ave} \sin\alpha_f / \gamma_{fs} \le \varepsilon_{sy}$

(continued on next page)

Table 2.2. (Continued).

Khalifa and Nanni (2000)	$V_f = 0.9\rho_{frp}E_{frp}\varepsilon_{fe}b_w d\left(1+\cot\beta\right)\sin\beta$ (Eurocode format) $V_f = \dfrac{A_f f_{fe}\left(\sin\beta+\cos\beta\right)d_f}{s_f}$ (ACI format) $\varepsilon_{fe} = R\varepsilon_{fu} \qquad f_{fe} = Rf_{fu}$ R is the least of : $R = 0.5622\left(\rho_{frp}E_{frp}\right)^2 - 1.2188\left(\rho_{frp}E_{frp}\right) + 0.778 \le 0.5$ $R = \dfrac{\left(f_c^{'}\right)^{2/3} w_{fe}}{\varepsilon_{fu}d_f}\left[738.93 - 4.06(t_f E_{frp})\right]\times 10^{-6}$ $R = \dfrac{0.006}{\varepsilon_{fu}}$
Triantafillou and Antonopoulos (2000)	$V_{fd} = 0.9\dfrac{\varepsilon_{fk,e}}{\gamma_f}E_f\rho_f b_w d\left(1+\cot\beta\right)\sin\beta$ (Eurocode format) $\varepsilon_{fk,e} = \alpha\varepsilon_{f,e} \le \varepsilon_{\max} = 0.005 \qquad \alpha = 0.8$ (recommended) $\phi_f V_f = \phi_f \varepsilon_{f,e,A} E_f \rho_f \left(\sin\beta+\cos\beta\right)bd$ (ACI format) $\varepsilon_{f,e,A} = 0.9\varepsilon_{f,e} \le \varepsilon_{\max,A} = 0.006$ $\varepsilon_{f,e} = 0.65\left(\dfrac{f_c^{2/3}}{E_f\rho_f}\right)^{0.56}\times 10^{-3}$ (CFRP debonding failure mode) $\varepsilon_{f,e} = 0.17\left(\dfrac{f_c^{2/3}}{E_f\rho_f}\right)^{0.30}\varepsilon_{f,u}$ (shear failure combined with or followed by CFRP fracture) $\varepsilon_{f,e} = 0.048\left(\dfrac{f_c^{2/3}}{E_f\rho_f}\right)^{0.47}\varepsilon_{f,u}$ (shear failure combined with or followed by AFRP fracture) $\left(E_f\rho_f\right)_{\lim} = \left(\dfrac{0.65\times 10^{-3}\alpha}{\varepsilon_{\max}}\right)^{1/0.56} \qquad f_c^{2/3} = 0.018 f_c^{2/3}$
Chaallal et al. (2002)	$V_f = f\left(\dfrac{a}{d},\rho_{tot}\right)\left(\dfrac{A_f}{s_f}\right)E_f\varepsilon_{eff}d_f$ $\varepsilon_{eff} = 3\times 10^{-5}\times\rho_{tot}^{-0.6522}, \quad \rho_{tot} = n\rho_f + \rho_s$ New deep beam coefficient: $f\left(\dfrac{a}{d},\rho_{tot}\right) = \dfrac{1+2a/d}{12} + \left(1000\rho_{tot} - 0.6\right) \le 1$ but greater than $\dfrac{1+2a/d}{12}$

Table 2.2. (Continued).

Pellegrino and Modena (2002)	$V_f = 0.9\rho_{frp}E_{frp}\varepsilon_{fe}b_w d\left(1+\cot\beta\right)\sin\beta$ (Eurocode format) $V_f = \dfrac{A_f f_{fe}\left(\sin\beta+\cos\beta\right)d_f}{s_f}$ (ACI format) $\varepsilon_{fe} = R\varepsilon_{fu} \qquad f_{fe} = Rf_{fu}$ R is the least of : $R = 0.5622\left(\rho_{frp}E_{frp}\right)^2 - 1.2188\left(\rho_{frp}E_{frp}\right) + 0.778 \le 0.5$ $R = \dfrac{0.006}{\varepsilon_{fu}}$ $R = R^*\left\{0.0042\left(f_{cm}\right)^{2/3} w_{fe} / \left[\left(E_{frp}t_f\right)^{0.58}\varepsilon_{fu}d\right]\right\}$ $0 \le R^* = -0.53\ln\rho_{s,f} + 0.29 \le 1$ $\rho_{s,f} = E_s A_{sw} / E_f A_f$
Hsu et al. (2003)	for continuous fiber sheet: $V_f = w_{fe}t_f f_{fe}\sin^2\beta$ for FRP strips: $V_f = \dfrac{A_f f_{fe}\left(\sin\beta+\cos\beta\right)d_f}{s_f}$ $f_{fe} = Rf_{fu}$, $\varepsilon_{fe} = R\varepsilon_{fu}$ Based on model calibration: $R = 1.4871\left(\rho_f E_f / f_c^{'}\right)^{-0.7488}$ Based on bonding mechanism: $R = \dfrac{\tau_{\max}L_e}{2f_{fu}t_f} \le 1$ $\tau_{\max} = \left(5\times10^{-6}\times f_c^{'2}\right) - \left(2.73\times10^{-2}\times f_c^{'}\right) + 925.3 \quad (English)$ $\tau_{\max} = \left(7.64\times10^{-4}\times f_c^{'2}\right) - \left(2.73\times10^{-2}\times f_c^{'}\right) + 6.38 \quad (Metric)$

* Terms are defined in notations section.

Whenever necessary, the review provides comments or comparisons with other studies. The numerical data extracted from the experimental studies were assembled in a database.

The test parameters considered in these studies are listed in Table 2.5. The major test parameters are (a) the geometry of the beam used in the experiments, (b) beam type, (c) properties of concrete and steel reinforcement, (d) types of FRP, and (e) strengthening schemes. As seen from Table 2.5, most of these studies have focused on rectangular beams, although most RC bridge girders have a T-section with integrated deck slabs. The shape of the cross section is related also to the strengthening scheme. For example, rectangular beams are commonly strengthened by fully wrapping the member, an impractical solution for T-beams due to the presence of the flange. Therefore, more focus should be placed on T-beams with U-wrap and side-bonding configurations as well as on the use of mechanical anchorage systems to address the issue of debonding. Also, few tests have been conducted on members with spans comparable to those used for bridges, and fewer tests have investigated the influence of scale (i.e., model-scale versus large-scale) on the shear behavior of members strengthened with FRPs. Furthermore, because FRP is generally used to strengthen damaged structures, attention needs to be given to the effects of existing cracks on the behavior of the strengthened member.

The previously developed analytical models were based on the studies listed in Table 2.5, the majority of which considered only small-scale testing. Therefore, this research aimed at expanding the experimental database with results from tests on full-scale T-beams, which are more representative

Table 2.3. Models that account for non-uniform strain distribution in FRP.

Reference Author (Year)	Equations
Chen and Teng (2003a and 2003b)	$V_{frp} = 2\frac{f_{frp,ed}}{\gamma_{frp}} t_{frp} w_{frp} \frac{h_{frp,e}\left(\sin\beta + \cos\beta\right)}{s_{frp}}$ $f_{frp,ed} = D_{frp}\sigma_{frp,\max}$ Debonding model: $D_{frp} = \frac{\int_{zl}^{zb}\sigma_{frp,z}dz}{h_{frp,e}\sigma_{frp,\max d}} = \begin{cases} \frac{2}{\pi\lambda}\frac{1-\cos\frac{\pi}{2}\lambda}{\sin\frac{\pi}{2}\lambda} & if\ \ \lambda \le 1 \\ 1-\frac{\pi-2}{\pi\lambda} & if\ \ \lambda > 1 \end{cases}$ $\sigma_{frp,\max,d} = 0.315\beta_w\beta_L\sqrt{\frac{E_{frp}}{t_{frp}}\sqrt{f_c^{'}}} \le f_{frp}$ Rupture model: $D_{frp} = \frac{\int_{z_l}^{z_b}\bar{\varepsilon}_z dz}{h_{frp,e}\bar{\varepsilon}_{z,\max}} = \frac{1+\zeta}{2}$ $\sigma_{frp,\max} = \begin{cases} 0.8f_{frp} & \text{if} \quad \frac{f_{frp}}{E_{frp}} \le \varepsilon_{\max} \\ 0.8\varepsilon_{\max}E_{frp} & \text{if} \quad \frac{f_{frp}}{E_{frp}} > \varepsilon_{\max} \end{cases}$ Strip spacing limitation: $s_{frp} - \frac{w_{frp}}{\sin\beta} \le \min\begin{cases} \frac{h_{frp,e}\left(1+\cot\beta\right)}{2} \\ 300\ mm \end{cases}$
Carolin and Taljsten (2005b)	for complete wrap: $V_f = \eta\varepsilon_{cr}E_f t_f z\frac{\cos\theta}{\sin\alpha}$ for composite strips: $V_f = \eta\varepsilon_{cr}E_f t_f z\frac{b_f}{s_f\sin\beta}\frac{\cos\theta}{\sin\alpha}$ $\eta = \frac{\int_{-h/2}^{h/2}\varepsilon_f(y)dy}{\varepsilon_{\max}h}$ $\varepsilon_{cr} = \min\begin{cases} \varepsilon_{fu} \\ \varepsilon_{bond}\cos^2\theta \\ \varepsilon_{c\max}\cos^2\theta \end{cases}$

Table 2.3. (Continued).

Cao et al. (2005)	$V_{frp} = 2D_{f\theta} t_{frp} w_{frp} E_{frp} \varepsilon_{f,\max} \frac{h_{frp}}{s_{frp}}$ $D_{f\theta} = \left(1 - \frac{\pi - 2}{\lambda_{frp}\pi}\right) \times \begin{cases} 1 \quad for\ \lambda \le 1.4 \\ \frac{1}{1 - 0.2(\lambda - 1.4)^2} \quad for\ 1.4 < \lambda < 3 \\ 2.05 \quad for\ \lambda \ge 3 \end{cases}$ $\varepsilon_{f,\max} = \frac{0.427 \beta_w \sqrt[4]{f_c'}}{\sqrt{E_{frp} t_{frp}}}$

* Terms are defined in notations section.

Table 2.4. Models derived from mechanics-based approaches.

Reference Author (Year)	Equations
Malek and Saadatmanesh (1998)	$V_f = h t_p \left[\overline{Q_{13}} \varepsilon_2 + \overline{Q_{23}} \varepsilon_1 + \frac{\left(\overline{Q_{12}} \varepsilon_2 + \overline{Q_{22}} \varepsilon_1\right)}{\tan(\theta_c)} \right]$ $V_s = E_s \varepsilon_y A_v \frac{h_v}{\tan(\theta_c) s} \quad for \quad \varepsilon_y < \frac{F_y}{E_s}$ $V_s = F_y A_v \frac{h_v}{\tan(\theta_c) s} \quad for \quad \varepsilon_y \ge \frac{F_y}{E_s}$
Deniaud and Cheng (2001, 2004)	Discrete formulation: $V_r = 0.25 k^2 f_c' \left(A_{cf} \tan\theta_f + A_{cw} \tan\theta_w \right) + T_v n_s + T_{FRP}$ Continuous formulation: $V_r = k \sqrt{f_c' A_c \left(T_v + T_{FRP}\right) \frac{d_s}{s}} - T_v$ $k = 2.1 \left(f_c'\right)^{-0.4}$ $T_v = A_v f_{vy}$ $T_{FRP} = d_{FRP} t E_{frp} \varepsilon_{\max} R_L \left(\frac{w_{frp}}{s_{frp}} \right)^2 \left(\frac{\sin\alpha}{\tan\theta_w} + (n_s + 1)\cos\alpha \right) \sin\alpha$ $T_{FRP} = d_{FRP} t E_{frp} \varepsilon_{\max} R_L \left(\frac{w_{frp}}{s_{frp}} \right)^2 \left(\frac{s}{d_s} \sin\alpha + \cos\alpha \right) \sin\alpha$ Maximum allowable strain in FRP: $\varepsilon_{\max} = \frac{3\sqrt{f_c'} d_{FRP}^{0.16}}{\left(t E_{frp}\right)^{0.67} (k_a \sin\alpha)^{0.1}} (\%) \le \varepsilon_{ultFRP}$ Remaining bonded width over initial width ratio: $R_L = 1 - 1.2 \exp\left[-\left(\frac{d_{FRP}}{k_e L_{eff} \sin\alpha} \right)^{0.4} \right]$

(continued on next page)

Table 2.4. (Continued).

Monti and Liotta (2005)	Side bonding: $V_{Rd,f} = \frac{1}{\gamma_{Rd}} \cdot \min\{0.9d, h_w\} \cdot f_{fed} \cdot 2t_f \cdot \frac{\sin\beta}{\sin\theta} \cdot \frac{w_f}{p_f}$ design effective stress for side bonding: $f_{fed} = f_{fdd} \cdot \frac{z_{rid,eq}}{min\{0.9d, h_w\}} \cdot \left(1 - 0.6\sqrt{\frac{l_{eq}}{z_{rid,eq}}}\right)^2$ $z_{rid,eq} = \min\{0.9d, h_w\} - \left(l_e - \frac{s_f}{f_{fdd}/E_f}\right)\sin\beta$ U-wrap or complete wrapping: $V_{Rd,f} = \frac{1}{\gamma_{Rd}} \cdot 0.9d \cdot f_{fed} \cdot 2t_f \cdot (\cot\theta + \cot\beta) \cdot \frac{w_f}{p_f}$ design effective stress for U-wrapping: $f_{fed} = f_{fdd} \cdot \left[1 - \frac{1}{3}\frac{l_e \sin\beta}{min\{0.9d, h_w\}}\right]$ design effective stress for complete wrapping: $f_{fed} = f_{fdd} \cdot \left[1 - \frac{1}{6}\frac{l_e \sin\beta}{min\{0.9d, h_w\}}\right] + \frac{1}{2}(\phi_R f_{fd} - f_{fdd}) \cdot \left[1 - \frac{l_e \sin\beta}{min\{0.9d, h_w\}}\right]$ $l_e = \sqrt{\frac{E_f t_f}{2 f_{ctm}}}$ where: $f_{ctm} = 0.27 R_{ck}^{2/3}$ $f_{fdd} = \frac{0.80}{\gamma_{f,d}} \sqrt{\frac{2E_f \Gamma_{Fk}}{t_f}}$ where: $\Gamma_{Fk} = 0.03 k_b \sqrt{f_{ck} f_{ctm}}$ $k_b = \sqrt{\frac{2 - w_f/p_f}{1 + w_f/400}} \geq 1$ $w_f \leq \min(0.9d, h_w)\sin(\theta+\beta)/\sin\theta$ $f_{fdd}(l_b) = f_{fdd}\frac{l_b}{l_e}\left(2 - \frac{l_b}{l_e}\right)$ (for $l_b < l_e$) $\phi_R = 0.2 + 1.6\frac{r_c}{b_w}$ where $0 \leq \frac{r_c}{b_w} \leq 0.5$
Sim et al. (2005)	$\frac{\tau}{\nu\sigma_{cu}} = \frac{\sqrt{a^2+d^2} - (1-2\phi)a}{2d}$ *if* $\phi < \frac{\sqrt{(a^2+d^2)} - a}{2\sqrt{(a^2+d^2)}}$ $\frac{\tau}{\nu\sigma_{cu}} = \sqrt{\phi(1-\phi)}$ *if* $\frac{\sqrt{(a^2+d^2)} - a}{2\sqrt{(a^2+d^2)}} \leq \phi \leq \frac{1}{2}$ $\frac{\tau}{\nu\sigma_{cu}} = \frac{1}{2}$ *if* $\phi > \frac{1}{2}$ $\tau = \frac{V}{b \cdot h}$ and $\phi = \frac{A_v \cdot f_{sy}}{b \cdot e \cdot \nu\sigma_{cu}} + \alpha\left(\frac{A_p \cdot f_{py}}{b \cdot t \cdot \nu\sigma_{cu}}(\sin\beta + \cos\beta)\right)$

* Terms are defined in notations section.

Table 2.5. Summary of experimental studies.

Author	Year	Number of Tests	Properties and Parameters																						
			Geometry					Type of Beam				Concrete and Steel			Type of FRP			Strengthening Scheme						
			Rectangular Section	T-Section	Beam Spanning L< 7 ft	Beam Spanning 7 ft <L<13 ft	Beam Spanning L>13 ft	Regular Beams (a/d>2.5)	Deep Beams	Scale Effect	Precracking	Concrete Strength	Longitudinal Reinforcement	Transverse Reinforcement	Carbon	Aramid	Glass	Two-Side Bonding	U-Wrap	Complete Wrap	Continuous	Strips	Angle to Long. Axis=90 º	Angle to Long. Axis≠90 º
Berset	1992	2	■		■			■									■	■			■			■
Uji	1992	4	■		■			■							■			■		■	■		■	■
Al-Sulaimani et al.	1994	4	■		■			■			■						■	■			■	■	■	
Ohuchi et al.	1994	13	■		■				■					■	■					■			■	
Chajes et al.	1995	5		■	■			■							■	■	■		■		■		■	■
Sato et al.	1996	3	■			■		■							■			■	■		■	■	■	
Araki et al.	1997	8	■		■				■						■	■				■	■	■	■	
Funakawa et al.	1997	3	■				■	■							■					■	■		■	
Kamiharako et al.	1997	1	■			■		■	■							■				■			■	
Miyauchi et al.	1997	4	■		■			■	■						■					■		■	■	
Sato et al.	1997	2		■	■			■							■				■		■		■	
Taerwe et al.	1997	3	■				■	■							■				■	■		■	■	
Taljsten	1997	3	■				■	■			■				■			■			■	■		■
Umezu et al.	1997	15	■			■		■					■	■	■	■				■	■	■	■	
Chaallal et al.	1998	2	■		■			■							■			■				■	■	■
Mitsui et al.	1998	6	■			■			■		■				■					■	■		■	
Triantafillou	1998	9	■		■			■							■			■				■	■	■
Khalifa et al.	1999	6	■			■		■							■				■		■	■	■	
Kachlakev and Barnes	1999	3	■				■	■									■	■			■		■	
Khalifa et al.	2000	4		■		■		■							■				■		■	■	■	
Deniaud and Cheng	2001	5		■		■		■		■		■		■	■		■		■		■	■	■	■
Li et al.	2001a	5	■		■				■						■			■			■		■	
Li et al.	2001b	9	■			■		■					■		■			■				■		■
Park et al.	2001	2	■	■	■			■							■			■	■		■		■	
Chaallal et al.	2002	10		■			■		■					■	■				■		■		■	
Khalifa and Nanni	2002	4	■			■		■							■				■		■	■	■	
Li et al.	2002	9	■			■		■					■		■			■				■		■
Micelli et al.	2002	10		■		■			■						■	■			■				■	
Pellegrino and Modena	2002	9	■			■		■						■	■			■			■		■	
Beber	2003	28	■			■		■							■			■	■	■		■	■	■
Diagana et al.	2003	8	■			■			■						■				■	■		■	■	■
Hsu et al.	2003	3	■		■			■							■		■	■			■	■	■	■

(continued on next page)

Table 2.5. (Continued).

Author	Year	Number of Tests	Properties and Parameters																						
			Geometry					Type of Beam				Concrete and Steel			Type of FRP			Strengthening Scheme							
			Rectangular Section	T-Section	Beam Spanning L< 7 ft	Beam Spanning 7 ft <L<13 ft	Beam Spanning L>13 ft	Regular Beams (a/d>2.5)	Deep Beams	Scale Effect	Precracking	Concrete Strength	Longitudinal Reinforcement	Transverse Reinforcement	Carbon	Aramid	Glass	Two-Side Bonding	U-Wrap	Complete Wrap	Continuous	Strips	Angle to Long. Axis=90 º	Angle to Long. Axis≠90 º
Taljsten	2003	6	■				■	■							■				■		■		■	■
Adhikary et al.	2004	8	■			■		■							■	■			■	■	■	■	■	
Xue Song et al.	2004	12	■		■				■						■				■			■	■	
Cao et al.	2005	10	■		■			■	■					■	■		■			■		■	■	
Carolin and Taljsten	2005a	18	■					■			■	■			■				■	■			■	■
Miyajima et al.	2005	4	■			■		■							■					■	■	■	■	
Monti and Liotta	2005	16	■			■		■							■			■	■	■	■	■	■	■
Sim et al.	2005	9	■		■				■						■		■	■	■	■	■	■	■	■
Zhang and Hsu	2005	10		■			■	■						■	■				■					■
Barros and Dias	2006	5		■	■				■						■				■			■	■	
Bousselham and Chaallal	2006a	20		■			■	■	■					■	■				■		■		■	
Pellegrino and Modena	2006	8	■			■		■						■	■				■		■		■	
Lees and Kesse	2007	8	■		■			■							■				■				■	
Leung et al.	2007	12	■		■	■		■					■	■	■				■	■	■	■	■	
Alrousan et al.	2009	4	■				■	■	■						■				■	■	■	■	■	
Arteaga et al.	2009	15	■				■	■		■					■				■	■		■	■	■
Gamino et al.	2009	7		■	■			■							■								■	
Rizzo and De Lorenzis	2009	1	■		■			■							■				■		■		■	

Note: (1) Shaded cells denote considered parameters.
(2) Control specimens without FRP strengthening are not included in the table.

of bridge girders and consider the effects of other parameters such as pre-cracking and the amount of transverse reinforcement.

2.4.2 Bond Behavior of FRP-Concrete Interface

The performance of shear strengthening of concrete girders by using externally bonded FRP sheets depends on the interface bond behavior between the FRP sheets and the concrete substrates. Many analytical models attempted to consider the bond characteristics at the interface between FRP and concrete substrate to predict the shear contribution of FRP when the expected failure is caused by debonding of FRP. Consideration of the bond mechanism, the intermediate crack (IC) debonding, the bond stress-slip relationship, the effective bond length, and the bond strength is required for the development of improved shear design equations.

The most important role of the interface bond between the FRP sheets and concrete is to transfer shear stresses from existing concrete structures to externally bonded FRP sheets for both shear and flexural strengthening. The bond properties

of FRP sheet-concrete interfaces have been widely studied. Various test methods have been developed to evaluate the average interfacial bond strength. These methods include single-lap-type, double-lap-type, bending-type, and inserted-type tests, as shown in Figure 2.1. Among the interface parameters evaluated are average shear bond strength, effective bond length, maximum shear bond stress, interfacial fracture energy, and the local bond stress-slip relationship. Bond behavior is influenced by the mechanical and physical properties of the concrete, FRP composite, and adhesive; the influencing factors are listed in Table 2.6.

In evaluating FRP-concrete interface bond behavior, the bond stress-slip (τ-s) relationship is the most important factor. For FRP sheets bonded to concrete, this relationship

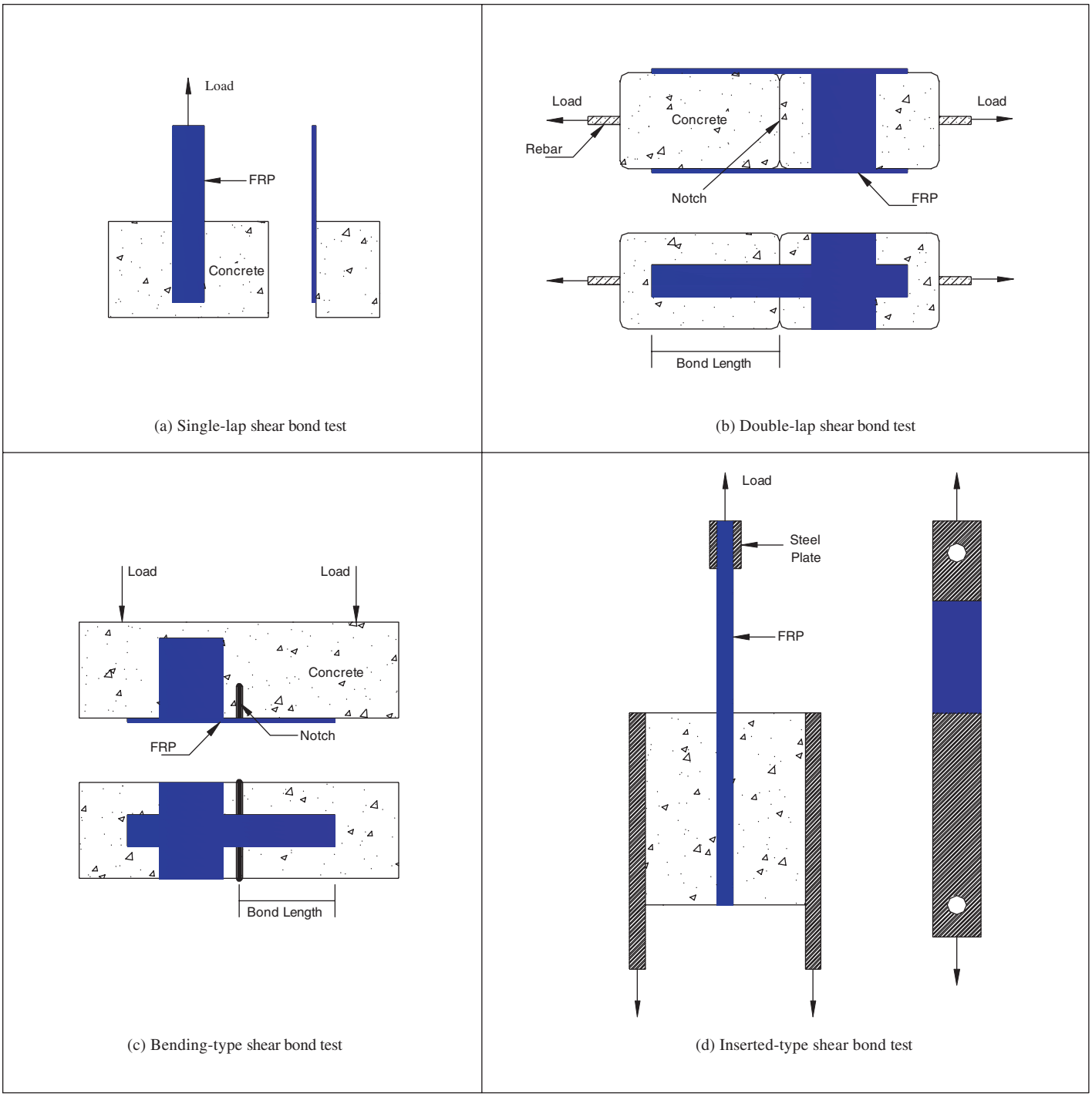

(a) Single-lap shear bond test

(b) Double-lap shear bond test

(c) Bending-type shear bond test

(d) Inserted-type shear bond test

Figure 2.1. Test methods to evaluate the bond strength.

Table 2.6. Factors influencing the bond behavior at FRP-concrete interface.

Elements		Influencing Factor
Concrete		Modulus of elasticity, thickness, surface condition, strength, drying shrinkage, water content
FRP application	Continuous Fiber Sheet	Modulus of elasticity, strength, thickness, stiffness, length/width of sheet, weave
	Bonding Resin	Modulus of elasticity, strength, glass transition temperature, spread
	Primer	
	Putty	
Loading condition		Bending, shearing, punching, cyclic
Environmental actions		Ambient temperature, moisture, sun light radiation, etc.

is determined by the strain distributions in the FRP, and the local bond stresses measured in the FRP sheets. Several empirical τ-s relationships have been proposed including a elasto-plastic model (Sato et al., 1997 and De Lorenzis et al., 2001); a bilinear model based on interfacial fracture energy (Yoshizawa et al., 2000); a model based on the Popovic's expression (Nakaba et al., 2001); and a shear softening model (Sato et al., 2000).

The experimental studies have shown that the bond shear stress at the FRP-to-concrete interface increases rapidly with increases in the interfacial slip until it reaches the peak stress (bond strength) as illustrated in Figure 2.2. After this point, interfacial softening (or micro-cracking) starts, together with a decrease in the interfacial shear stress and an increase in the interfacial slip.

There is no agreement among researchers on the shape of the model, however, use of fracture mechanics implicitly leads to a very simple generic expression that considers only the FRP stiffness and interfacial fracture energy (defined as the area beneath the bond stress-slip curve) for the determination of bond capacity. Debonding occurs first within the effective bond length (defined as a length over which the majority of the bond stress is maintained, see Figure 2.3) as a result of debonding of a very thin layer of concrete rather than debonding at the FRP/concrete interfaces. When the bonded length of FRP along the FRP-concrete interface exceeds the effective bond length, no further increase in failure load can be achieved. However, a longer bond length may delay complete debonding and thus improve the ductility.

Several studies have been performed to determine effective bond length. Figure 2.4 shows the effective bond lengths calculated by analytical models and equations stipulated in many current code and design guidelines versus the rigidity of FRP reinforcement ($E_f \rho_f$). As shown in the figure, most studies have reported that effective bond length increases as the stiffness of FRP sheets increases. However, two studies (Maeda et al., 1997 and ACI 440.2R-08) show a different trend, probably because these models were derived using a very limited experimental database.

The analytical models for effective bond length and bond strength were derived based on small-scale tests; the bond behavior of full-size beams may be different than that prescribed by these models. Thus, full-scale tests would provide data to calibrate/improve these models.

2.4.3 Anchorage Systems to Enhance the Effectiveness of FRP Strengthening Systems

When a proper anchorage system is not provided, failure of FRP-strengthened reinforced concrete members is commonly manifested by debonding of the FRP. Therefore, vari-

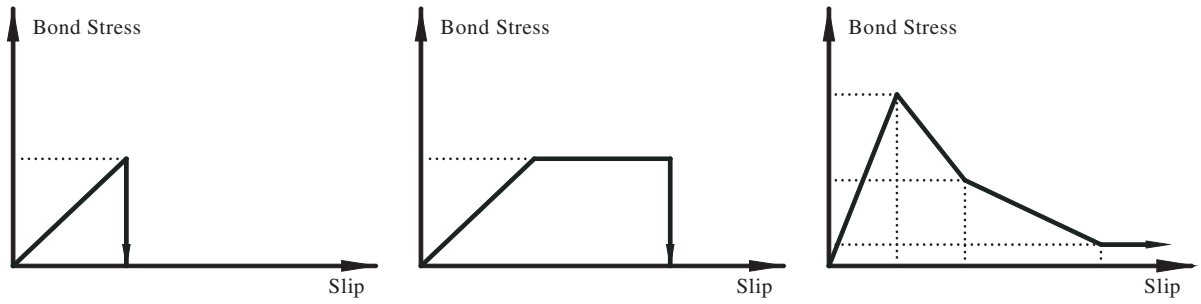

(a) Cutoff type (b) Bilinear type (c) Tensile softening type

Figure 2.2. Various bond stress-slip models.

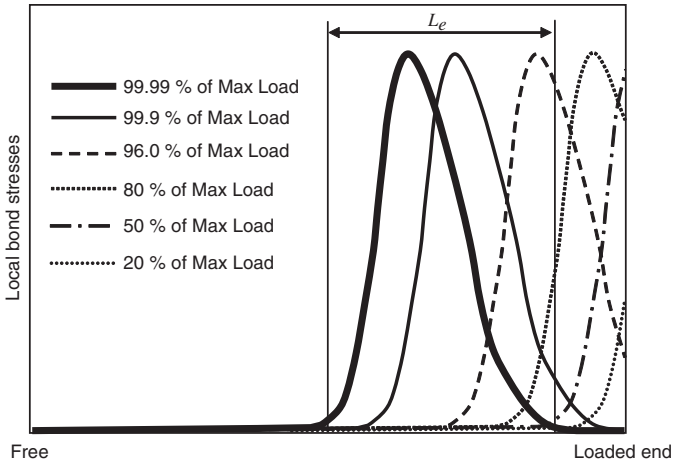

Figure 2.3. Concept of effective bond length based on stress distribution (Ueda and Dai, 2005).

ous types of anchorage systems, including the near surface mounted system (NSM), fiber reinforced polymer anchor spikes, additional horizontal strips, and various mechanical anchorage systems have been studied to evaluate their effect on FRP failure by debonding.

Many experimental studies have demonstrated the effectiveness of the NSM system (Khalifa and Nanni, 2000; De Lorenzis, 2002; Micelli et al., 2002). In this system, a bent portion of the end (or a region near the end) of the FRP reinforcement is embedded into the concrete, as shown in Figure 2.5. For fiber sheets, the bend is created during wet lay-up, and in the case of laminates, it is pre-formed. This technique requires no surface preparation work but considerable labor for cutting the grooves.

Another system used to prevent debonding of FRP is anchor spikes (Eshwar et al., 2003; Eshwar et al., 2008; Orton, 2007; Niemitz, 2008). Each anchor spike consists of a precured fiber portion and a dry fiber portion (see Figure 2.6). The anchor spikes may be constructed in situ. First, fibers are bundled together, and half of the fiber length is covered with plastic or duct tape. The uncovered bundled fibers are then impregnated and thoroughly saturated with resin. Finally, the saturated fibers are passed through a circular hole in a steel plate, or die, to obtain the desired diameter of the anchor spikes. The dry fibers are used for bonding purposes and trimmed to the appropriate length according to specific requirements. Following surface preparation of the concrete, holes of the desired diameter and depth are drilled and partially filled with saturant. The laminate is then applied, and while it is wet, the precured portion of each spike anchor is inserted into the holes. The dry fibers are spread around the layer in a circular fashion, and a layer of saturant is then applied (see Figure 2.6).

An additional horizontal FRP strip applied on top of the vertical FRP strips has also been used as an anchorage system (Hutchinson and Rizkalla, 1999; Schnerch, 2001). This technique is very easy to install and requires no more labor than other anchorage systems. However, different levels of effectiveness have been reported. Schnerch (2001) reported that the horizontal strip neither delays nor prevents debonding, and it does not increase the contribution of the FRP to the shear strength of the beam at failure. Test results reported by Hutchinson

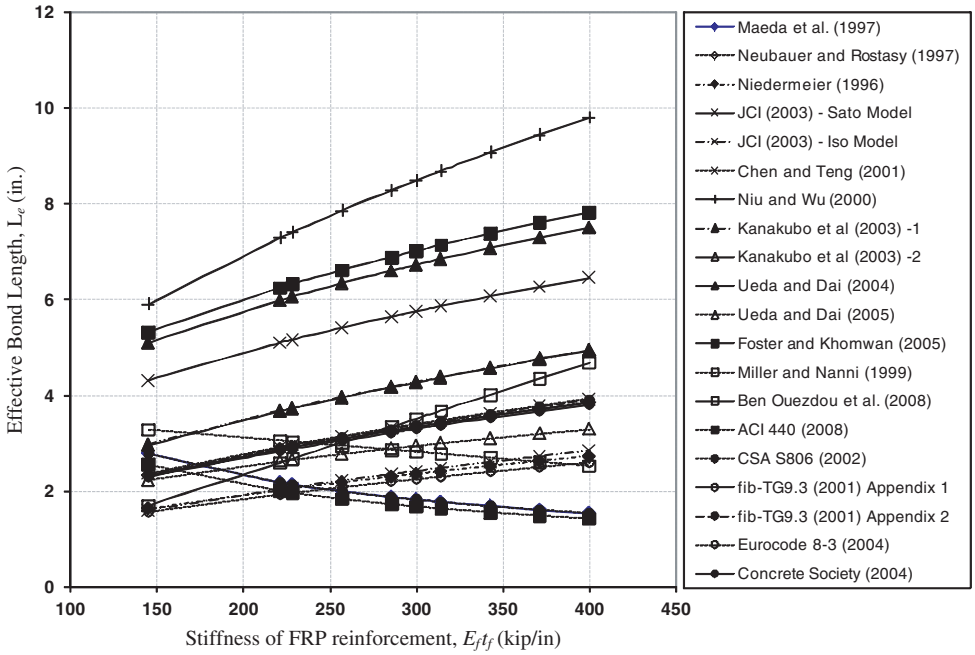

Figure 2.4. Effective bond length versus FRP rigidity.

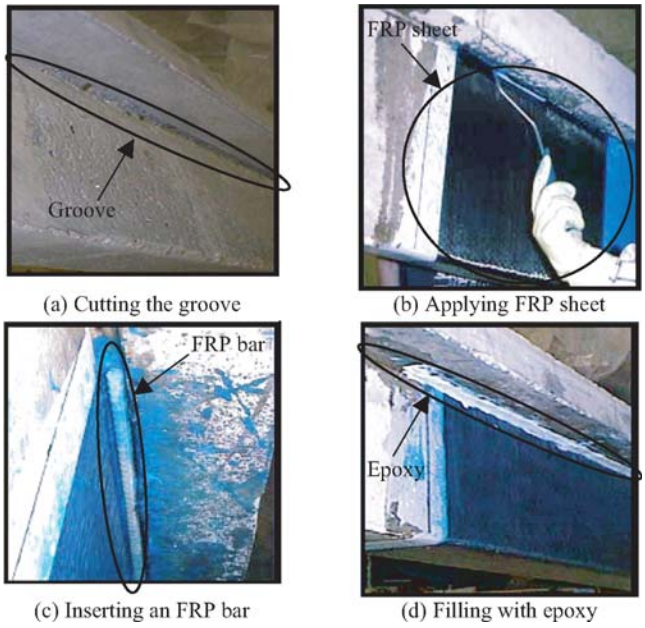

Figure 2.5. Construction of a NSM Anchorage System.

and Rizkalla (1999) indicated that using the horizontal strip increased the shear contribution of FRP by 16 percent.

Mechanical anchorage systems have been used widely to prevent premature FRP debonding. Steel angles, steel or FRP composite plates, and anchor bolts are examples of most commonly used mechanical anchorage systems.

Sato et al. (1997) conducted a series of tests using various anchoring methods to develop a shear strengthening technique for beams and a method of estimating their effectiveness. The test results showed that sufficient strength can be achieved only if the CFRP sheets are mechanically anchored.

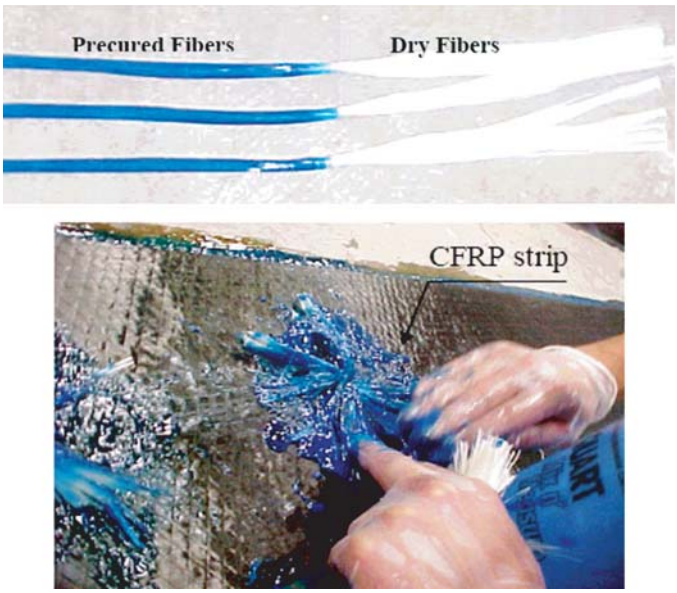

Figure 2.6. Anchor spikes.

The four methods used to anchor the FRP sheets as shown in Figure 2.7 are (a) nail type, (b) semi-closed type, (c) sub-variation of semi-closed type, and (d) closed type.

Sato et al. (1997) concluded that the shear strength of beams can be improved by transverse wrapping of FRP sheets if adequate anchoring is provided by steel plates and bolts and recommended the use of long anchor bolts that penetrate the full web. This anchorage system, however, creates stress concentrations where the anchors are placed, and the bolts lead to discontinuity of the FRP system.

Matthys (2000) conducted a project to strengthen four continuous reinforced concrete beams in shear and flexure, by supporting them with masonry columns. Bond/anchorage tests indicated a 44% increase in anchorage capacity with the use of steel bolted connections. Mechanical anchorage resulted in a less brittle failure mode due to the transition to an external tensioning system after debonding and to increased displacements resulting from CFRP slip.

Schuman (2004) conducted a comprehensive study on anchorage systems for shear strengthening of reinforced concrete (RC) beams. A mechanical anchorage system was applied to increase the shear contribution of CFRP systems by embedding anchor rods into the cross section with various bearing plates, (e.g., GFRP plate). The anchorage systems are possible, the four methods described by Schuman (2004) can be summarized as (1) complete wrapping through the flange (called complete wrap), (2) FRP laminate extended into the flange, (3) bonded steel anchors with bearing plates (called two-side bonding), and (4) GFRP plate anchors.

The two particularly important conclusions from Schuman's (2004) research are (1) the FRP composite alone provides the T-beam with little additional ultimate load and displacement capacity and creates a more brittle failure mode and (2) the use of properly embedded and sized anchors allows the vertical ties to remain intact during failure. These anchors then force a more ductile compression zone and ensure a shear/flexural failure mode.

Schuman (2004) also concluded that short anchors (Figure 2.8) lead to an increase in load carrying and displacement capacity and cause the CFRP reinforcement to be activated before the steel reinforcement yields but deeper anchors (Figure 2.8) allow the CFRP reinforcement to be activated earlier, thus delaying yielding in the steel stirrups.

For all mechanical anchorage systems configurations, the embedment length, diameter of the anchor, and the bearing strength of the plate are primary considerations. Regarding embedment length, longer anchors are more effective, but they increase the amount of labor required and present the risk of damaging the concrete and steel reinforcement. The diameter of the anchor must be chosen based on the failure modes of the connection (e.g., bearing of the plate, spalling of concrete, and yielding or rupture of the anchor).

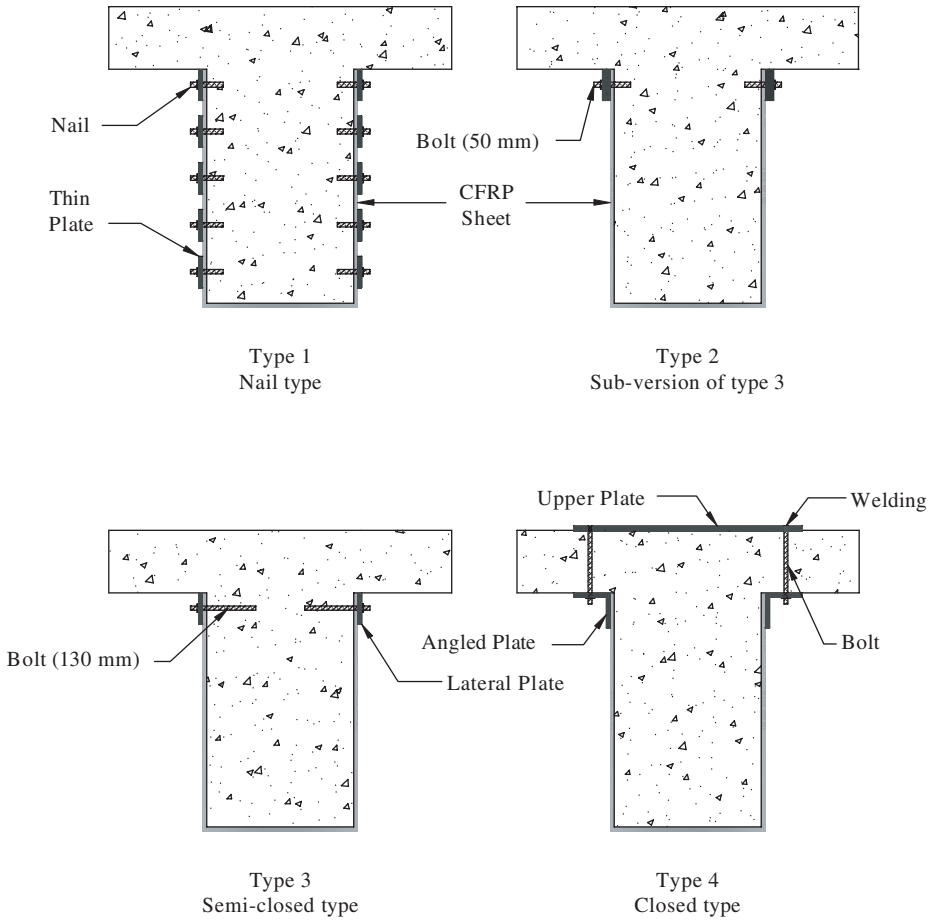

Figure 2.7. Anchoring methods of CFRP sheets.

2.5 Current Codes/Guidelines/ Specifications

Design procedures for shear strengthening of concrete structures with externally bonded FRP are available in various forms (e.g., codes, guidelines, and specifications).

The *Guide for the Design and Construction of Externally Bonded FRP Systems for Strengthening Concrete Structures* (ACI 440, 2008) was developed based on ACI 318-08 (ACI 318, 2008). This guide determines the shear contribution of externally bonded FRP based on failure modes. FRP rupture is the likely mode of failure for complete wrapping applications and the ultimate strain of the FRP can be used for calculation of the shear contribution of FRP, with the use of a strength reduction factor of 0.75. However, the ultimate strain is limited to 0.004 in order to maintain aggregate interlock. For U-wrap and side bonding applications, both FRP debonding and rupture are potential failure modes, and the shear contribution of the FRP should be investigated for each failure mode with the lesser value used for design. The analytical

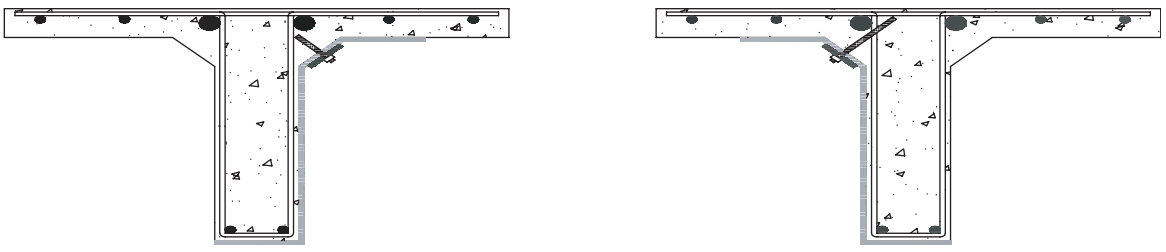

Figure 2.8. Specimen details (Schuman 2004).

model proposed by Khalifa et al. (1998) is adopted to predict the shear contribution of FRP for debonding of FRP.

The Canadian Design and Construction of Building Composites with Fiber Reinforced Polymers (CAN/CSA S806, 2002) is a design code that addresses externally bonded FRP reinforcement for concrete. The equations in this code are based on the simplified method for shear design used in the concrete design code (CAN/CSA A23.3, 1994), which is limited to the usual cases of shear reinforcement (including FRP) perpendicular to the longitudinal axis of beams. The shear contribution of the FRP is determined based on failure modes. The ultimate strain is limited to 0.004 for failure due to FRP rupture and 0.002 for bond critical applications.

The Canadian Highway Bridge Design Code (CAN/CSA S6-06, 2006) deals with the shear strengthening of concrete with externally-bonded FRPs. This code specifies that the FRP shear strengthening system should consist of U-wraps anchored in the compression zone or complete wrapping of the cross-section. This code specifies the same equations contained in ACI 440 (2002).

European fib bulletin 14 Design and Use of Externally Bonded Fiber Polymer Reinforcements (FRP EBR) for Reinforced Concrete Structures, (fib-TG9.3 2001) is a combination of guidelines and state-of-the-art reports and calculates the FRP contribution to shear capacity (V_{fd}) according to a model proposed by Triantafillou and Antonopoulos (2000), and the bulletin recognizes the difference in expected performance between FRP material types as well as between preformed and wet lay-up FRP systems, which is expressed in the form of various material safety factors. Delamination and debonding are addressed using a simplified bilinear bond model and by considering the effects of the loss of composite action between the FRP and concrete substrate. Durability is discussed but no design guidelines are provided.

Japan Society of Civil Engineering Recommendations for Upgrading of Concrete Structures with Use of Continuous Fiber Sheets (JSCE, 2001) employs a performance-based approach to the design of externally bonded FRP materials. In addition to verifying flexural and shear capacity, flexural crack width and protection of the concrete substrate from chloride ion penetration are also considered.

The Manual for Strengthening Reinforced Concrete Structures with Externally-Bonded Fiber Reinforced Polymers, prepared by the Canadian Intelligent Society of Innovative Structures (ISIS, 2001), provides guidance and design examples for the use of externally bonded FRP based on Canadian Codes (CAN/CSA S6-06, 2006 and CAN/CSA S806-02, 2002).

The British Concrete Society Technical Report 55, Design Guidelines on Strengthening Concrete Structures Using Fiber Composite Materials (Concrete Society, 2004) is similar to fib-Bulletin 14 (fib-TG9.3, 2001) in approach and scope; however, it addresses construction issues associated with the use of externally bonded FRP materials. Externally bonded FRP strips are treated using a 45-degree truss analogy. The strain in the FRP is limited to one half of the ultimate design strain for FRP rupture failure. For debonding failure, this report adopts an equation proposed by Neubauer and Rostasy (1997); the strain is limited to 0.004 for all cases.

2.6 Factors Affecting the Design of FRP Shear Strengthening

The factors affecting the design of FRP shear strengthening systems was investigated by (1) reviewing existing experimental databases, (2) conducting an experimental program to investigate the factors that had not been considered in prior research, and (3) performing an analysis using finite element method (FEM) to verify the experimental results.

2.6.1 Investigation on the Existing Experimental Database

A total of 49 published experimental studies containing more than 500 test results were reviewed. These studies covered all relevant, detailed and specific data from tests related to FRP shear strengthening (see Table 2.5). These data were examined for appropriateness and validity by reviewing the test set-up, failure modes reported, and material properties. The data was then compiled into a tabular format to facilitate identification of the parameters that influence design of externally bonded FRP systems. These data were also used to (1) develop an experimental program to be carried out as part of this project and (2) develop and calibrate shear design provisions for concrete girders retrofitted with externally bonded FRP. The following parameters and criteria were successively subjected to qualitative and quantitative analysis: (a) mechanical and geometric properties of the FRP, (b) transverse steel ratio, (c) longitudinal steel ratio, (d) shear span-to-depth ratio or type of beams (slender versus deep), and (e) scale factor or size effect of the specimens. Other parameters and criteria that were also qualitatively examined included the effects of (a) concrete strength, (b) fatigue, (c) anchorage details, (d) pre-cracking, and (e) prestress.

The effects of failure modes were also considered because the analysis was performed by discretization of the various failure modes. The failure modes considered were (a) shear failure due to debonding, including delamination and (b) shear failure due to rupture of the FRP. Other shear failure modes (due to diagonal concrete crushing or concrete splitting) were not considered in the analyses. Results of tests in which test beams failed in flexure were disregarded.

2.6.1.1 Influence of FRP Properties

Table 2.5 indicates that CFRP sheets have been used in almost all studies addressing performance of RC beams strengthened in shear with FRP. The effective strain concept was used to evaluate the effectiveness of FRP shear strengthening systems. Figure 2.9 shows the variation of the effective FRP strain (ε_{fe}) versus ($E_f\rho_f/f_c'^{2/3}$) a function of FRP rigidity ($E_f\rho_f$) and the compressive strength of concrete (f_c'). The effective FRP strain (ε_{fe}) was determined based on the traditional truss analogy using the following expression:

$$\varepsilon_{fe} = V_f / \left(b_w d_f E_f \rho_f \left(1 + \cot\beta\right)\right) \qquad \text{(Eq. 2.1)}$$

where: b_w = the width of the web
d_f = the effective depth of FRP reinforcement
β = the angle of inclination of the FRP with respect to the longitudinal axis of the beam.

The term ($E_f\rho_f/f_c'^{2/3}$) was used because it includes the effects of (1) the amount of FRP expressed in terms of the FRP ratio ($\rho_f = A_f/(b_w s_f)$), (2) the fiber type expressed in terms of the modulus of elasticity of FRP (E_f), and (3) the compressive strength of concrete (f_c') which is a major factor influencing the bond performance of FRP strengthening. The term ($E_f\rho_f/f_c'^{2/3}$) is particularly important for evaluating the contribution of FRP to shear resistance, as it was established in the European design guidelines (*fib*-TG 9.3, 2001). It includes all the factors affecting the behavior of the materials at the FRP-concrete interface. This term is also used in many design methods to calculate the contribution of FRP to shear resistance (ACI 440.2R-08, 2008; Chen and Teng, 2001; Khalifa and Nanni, 2000; and Deniaud and Cheng, 2004).

Figure 2.9 shows that the effective FRP strain decreases as FRP stiffness increases. It also shows that beams failing by FRP debonding are likely to exhibit smaller effective strains than beams failing by FRP rupture or other failure modes. Similar results were reported by other researchers (Bousselham and Chaallal, 2004; Khalifa and Nanni, 2000; and Triantafillou and Antonopoulos, 2000).

Figure 2.10 shows the variation in the ratio of the effective FRP strain to the ultimate FRP strain ($R = \varepsilon_{fe}/\varepsilon_{fu}$) an indicator of the effectiveness of the FRP strengthening system versus $E_f\rho_f/f_c'^{2/3}$. Figure 2.10 shows similar trends to those shown in Figure 2.9. In all cases, the effective strains are a modest fraction of the ultimate FRP strain. However, there is a high degree of scatter indicating an effect of other parameters on the shear resistance mechanism of FRP shear strengthening systems.

2.6.1.2 Effect of Internal Transverse Steel Reinforcement

Recent studies have shown that the contribution of externally bonded FRP to shear resistance is less for beams containing internal transverse steel than for beams without such reinforcement (Li et al., 2002; Pellegrino and Modena, 2002; Chaallal et al., 2002; Bousselham and Chaallal, 2004; and Czaderski, 2002). This interaction was observed in terms of resistance and strains (Bousselham and Chaallal, 2006a, b). This study also showed that for a given load, the stresses in transverse steel reinforcement of FRP-retrofitted beams were less than in beams that were not retrofitted.

2.6.1.3 Scale Effect

Although a T-section is generally used in practice, the majority of the experimental data were obtained for rectangular beams, and most tests were performed on small-scale specimens. Also, studies on the influence of the depth of an

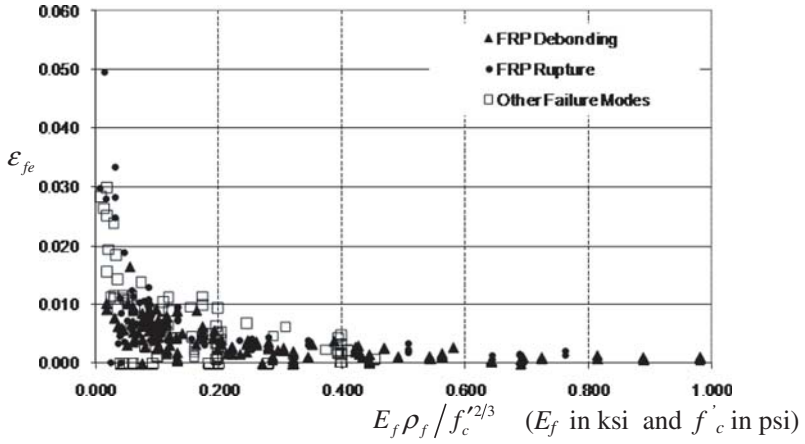

Figure 2.9. Effective strain of FRP versus $E_f\rho_f/f_c'^{2/3}$.

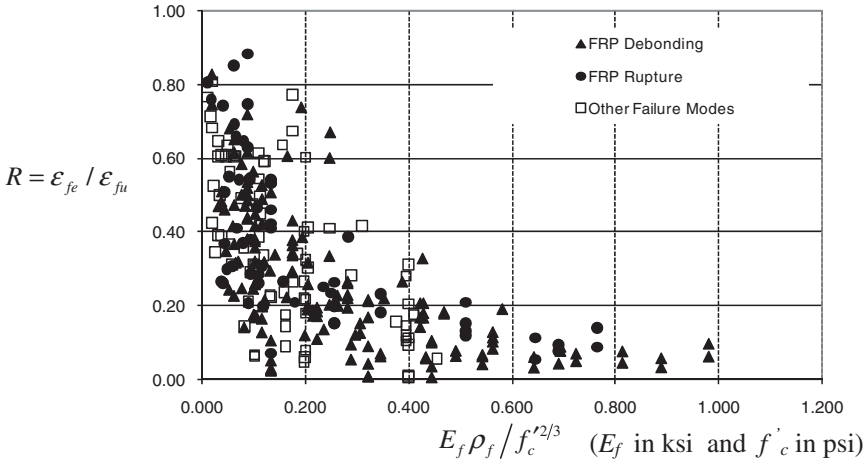

Figure 2.10. $\varepsilon_{fe}/\varepsilon_{fu}$ versus $E_f\rho_f/f_c'^{2/3}$.

RC beam on its shear behavior have shown that for beams without shear reinforcement the shear resistance decreases as the beam size increases (ACI-ASCE, 1998). This scale effect is considered one of the major factors affecting shear data. For this reason, most concrete standards (except those in North America) have introduced correction factors for size to adjust for the contribution of the concrete to shear resistance. It is also desirable to determine if there is a scale effect on the results of tests on RC beams strengthened in shear with externally bonded FRP as shown in a preliminary investigation (Bousselham and Chaallal, 2004). Analysis of the test results reported in the literature on shear strengthening showed a tendency for a decrease in the gain of shear resistance due to FRP as the height of the specimen increased (Bousselham and Chaallal, 2004; Leung et al., 2007). The predictive models for the contribution of FRP to shear strength proposed in the literature are largely based on test results from small-scale testing and, therefore, may yield higher than actual strength values.

2.6.1.4 Effect of Shear Span-to-Depth Ratio (Slender versus Deep Beam)

The majority of the available experimental data were derived from tests on slender beams. However, the shear behavior of RC beams depends largely on the shear span-to-depth ratio [defined as the shear length (a) divided by the effective beam depth (d)]. This ratio (a/d) is used to distinguish between slender and deep beams. It is important to determine whether slender and deep beams strengthened in sheer with externally applied FRP exhibits the same shear behavior. Bousselham and Chaallal (2006b) studied the influence of the a/d ratio by considering both slender beams ($a/d = 3.0$) and deep beams ($a/d = 1.5$). The results of this study indicated a larger gain in shear resistance due to FRP for slender beams than for deep beams, probably because of the arch action exhibited by deep beams. Thus, the shear contribution of externally bonded FRP is less for deep beams than for slender beams.

2.6.1.5 Influence of FRP Configuration and Anchorage

The frequency of each mode of failure occurrence for different FRP configurations (side bonding, U-wrap, or complete wrap), as determined from examination of the database information, is illustrated in Figure 2.11. The figure indicates that (a) debonding is the dominant mode of failure for beams strengthened with FRP and bonded on the sides only, (b) FRP debonding almost never occurs in beams retrofitted with complete FRP wrap and U-wraps with anchorage systems, and (c) failure of beams retrofitted with U-wraps occurs by debonding (65%) or by other failure modes (35%), such as diagonal tension failure in the web, shear compression failure in the compression zone, and flexural failure.

2.6.1.6 Influence of Concrete Strength

Concrete strength influences the performance of shear strengthening with FRP because it influences the bonding performance at the FRP-concrete interface and the failure mode. A higher concrete strength will delay, or even inhibit, failure by debonding. A low concrete strength will inhibit early crushing of concrete in the compression zone or in the diagonal struts (Bousselham and Chaallal, 2006a) but it will decrease the bond strength at the FRP-concrete interface. The guidelines for the design of RC structures strengthened with externally applied FRP take into account the concrete strength when calculating the contribution of FRP to shear resistance (ACI 440.2R, 2008; and *fib*-TG 9.3, 2001), either for the determination of the effective FRP strain or to prevent premature

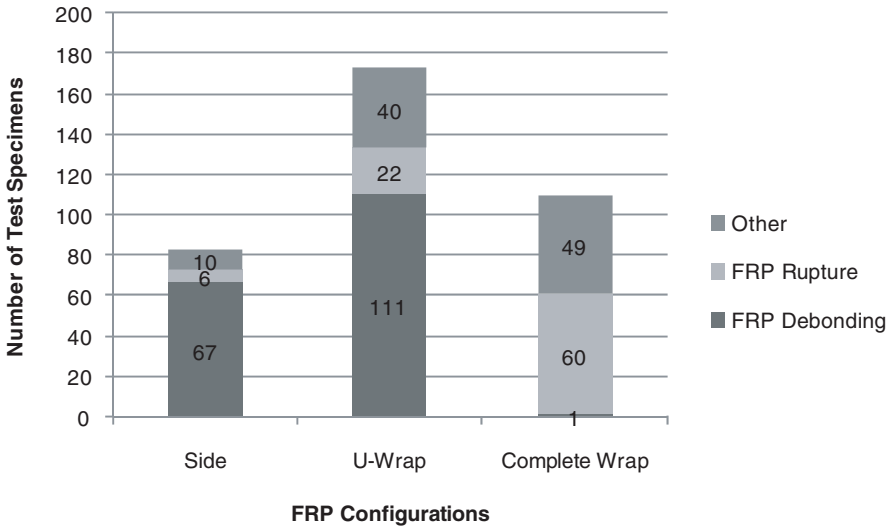

Figure 2.11. Modes of failure related to strengthening scheme.

crushing of concrete. Therefore, the range in concrete strengths used in tests should be representative of the strength prevailing in practice for existing bridge structures.

2.6.1.7 Influence of Fatigue

Limited research has dealt with fatigue behavior of concrete structures strengthened with externally bonded FRP laminates; most of the research have focused on flexural strengthening (Muszynski and Sierakowski, 1996; Papakonstantinou et al., 2001; Senthilnath et al., 2001; Lopez-Anido et al., 2003; Breña and Gussenhoven, 2005; Ekenel and Myers, 2005).

Williams and Higgins (2008) reported on repeated load tests conducted on three full-size girder specimens repaired with bonded carbon fiber laminate for shear strengthening and static tests conducted on two similar specimens. The specimens were 1,219 mm high with a 356 mm wide stem and a deck portion 914 mm wide by 152 mm thick. The fatigue loading resulted in localized debonding along the FRP termination locations at the stem-deck interface but did not significantly alter the ultimate shear capacity of the specimens.

Chaallal et al., (2009) tested six specimens under fatigue loading that varied between 35% and 65% of the respective static capacity of the specimen. Three of the beams had no internal shear reinforcement, and the other three had internal transverse steel reinforcement. The specimens of each group were tested with none, one, and two layers of continuously wrapped CFRP for up to 5 million cycles at a frequency of 2 Hz. However, the predicted capacities differed by as much as 50% from the measured values.

2.6.1.8 Influence of Pre-Cracking

Almost all reported experimental investigations that dealt with the shear performance of strengthened RC beams were performed on beams that had not been loaded (or cracked) prior to their retrofit. However, external strengthening with FRP is often performed on pre-cracked, or slightly-damaged, structures. The few investigations carried out on RC beams that were pre-cracked prior to strengthening indicated that pre-cracking does not affect the shear performance of retrofitted beams (Czaderski, 2002; Carolin and Taljsten, 2005a, and Hassan Dirar et al., 2006).

2.6.1.9 Influence of Prestress

According to a *fib* report (*fib*-T.G 9.3, 2001), less than 10% of the bridges that have been strengthened with FRP are prestressed. The literature review revealed only one study dealing with PC beams strengthened in shear with FRP (Hutchinson and Rizkalla, 1999). In this study, the authors proposed shear equations based on ACI 318 (ACI 318, 1999) and reported predictions in good agreement with the test results of seven prestressed concrete beams strengthened with CFRP strips.

2.6.1.10 Influence of Structural Continuity

The ACI 440 Committee (ACI 440, 2008) reported that the methodology for determining the bond reduction coefficient κ_v described in this guide has been validated for members in regions of high shear and low moment, such as monotonically-loaded, simply supported beams. However, no reference was made to the shear response for areas subjected to a combination of high flexural and shear stresses. The literature reports on very few tests performed on continuous beams (Khalifa et al., 1999; Mitsui et al., 1998; and Miyauchi et al., 1997) but provides no information on the behavior of the web under this condition.

2.6.1.11 Factors Recommended for Further Investigation

Based on the review of the factors affecting the design of FRP shear strengthening, the effects of (a) internal transverse steel reinforcement, (b) scale, (c) FRP configuration and anchorage, (d) fatigue (e) pre-cracking (f) prestressing, and (g) structural continuity were selected for further investigation.

2.6.2 Results of Experimental Investigation

An experimental investigation was designed to address the factors and designs that affect the shear behavior of FRP strengthened girders but have not been fully investigated in earlier studies. These factors include the effects of: (1) pre-cracking, (2) negative moments, (3) long-term conditions such as fatigue loading and corrosion of internal steel reinforcement, and (4) prestressing. The experimental program included full-scale RC T-beams and AASHTO type prestressed I-girders. The results of this experimental program, together with the existing experimental database were used to develop design equations for predicting the contribution of externally bonded FRP to shear strength.

2.6.2.1 RC T-Beams

The experimental program was conducted to investigate the shear performance of full-scale RC T-beams strengthened with externally bonded FRP sheets. Tests were performed on eight full-scale RC beams, seven of which were designed to provide two distinct test regions and one beam was designated for fatigue testing. Thus a total of 15 tests were performed to investigate the effects of (1) transverse steel reinforcement, (2) pre-cracking, (3) mechanical anchorage systems, (4) fiber orientations (45 and 90 relative to the longitudinal axis of the beam), (5) negative moment, (6) environmental conditioning (corrosion damage), and (7) fatigue loading.

The test beams were designed to mimic the geometry of beams used in a bridge located in Troy, New York (Hag-Elsafi et al., 2001a), that were strengthened with externally bonded FRP in 1999. This bridge is a 42-feet long by 120-feet wide RC structure consisting of 26 simply-supported T-beams spaced at 4.5 feet on center with an integral concrete deck. The bridge was built in 1932 and exhibited severe corrosion damage. The RC T-beams of the bridge have been strengthened in shear and flexure with externally bonded CFRP laminates. The cross section of the test beams is shown in Figure 2.12. The transverse reinforcement was designed to ensure shear failure prior to flexural failure and thus required the use of #3 stirrups at moderate (8 in.) and large (12 in.) spacing. Grade 40 steel (similar to that used in the Troy Bridge) was used for the transverse reinforcement. The test set-up, shown

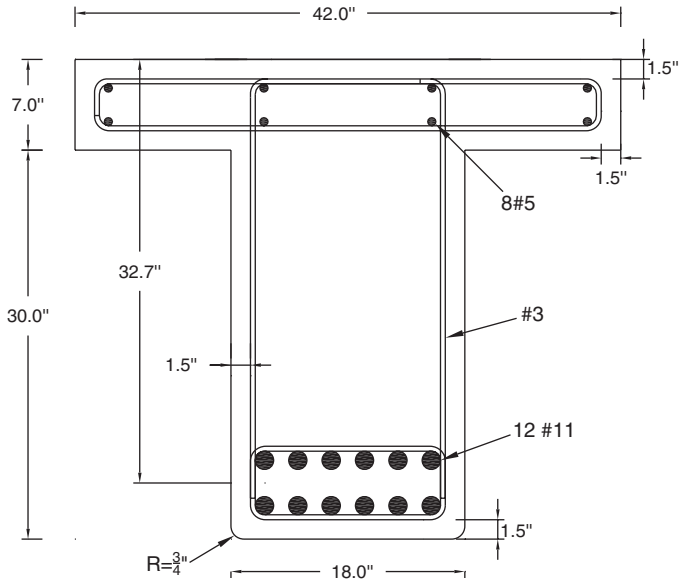

Figure 2.12. Cross-section of test beams.

in Figure 2.13, was designed to provide a shear-span-to-depth ratio of 3.3.

Table 2.3 summarizes the test results. The specimen designations indicate the stirrup spacing in inches (8 or 12), the strengthening configuration (S90 = strips at 90 to the longitudinal axis, and S45 = strips at 45), the presence and type of mechanical anchorage (NA = no anchorage, DMA = discontinuous mechanical anchorage, SDMA = sandwich discontinuous mechanical anchorage, and HA = additional horizontal strips), the presence of pre-existing cracks (PC), testing under negative moment conditions (HM), and fatigue loading conditions (Ftg).

The shear contributions of stirrups (V_s) and FRP (V_f) listed in Table 2.7, were determined from the measured strains in the stirrups and FRP sheets bridging the critical cracks. The shear contribution of the concrete was calculated by subtracting the contributions of the stirrups and FRP from the total shear resistance ($V_{n,test}$). A direct comparison of the shear strengths of the test beams could not be made because of the differences in concrete strength. Thus, the concrete strength and shear strength were normalized and listed in the table.

The test results showed that the differences in the amount of internal transverse steel reinforcement (stirrups) used in the RC-8 and RC-12-Series beams did not significantly influence the shear strength gain. However, a shear component analysis revealed an interaction between the contribution of FRP and the contribution of stirrups. Of the different anchorage systems, the sandwich discontinuous mechanical anchorage (SDMA) systems provided the best performance leading to rupture of FRP sheets. The specimens with discontinuous mechanical anchorage (DMA) systems and horizontal additional (HA) FRP strips provided higher shear strength than

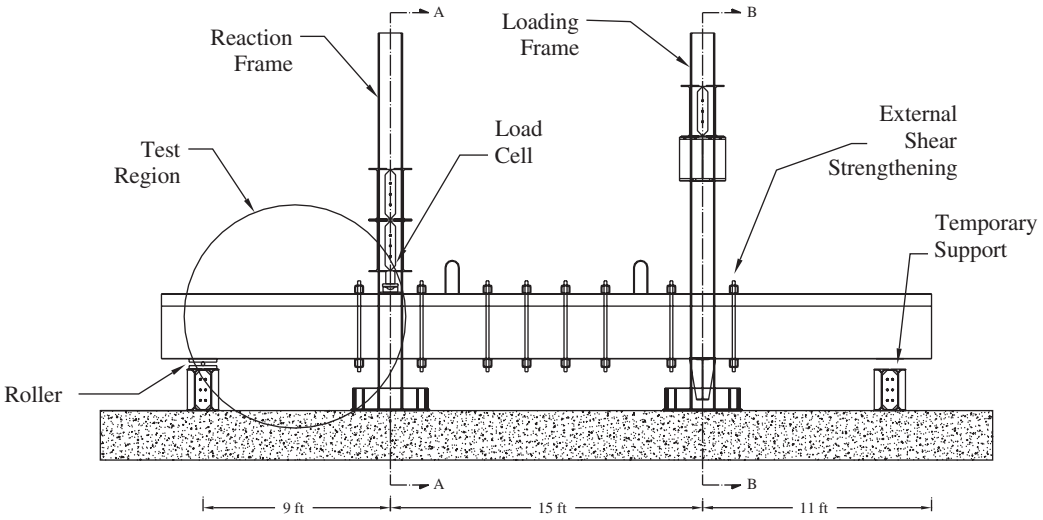

Figure 2.13. Details of test set-up.

those with no anchorage systems. The fibers oriented at 45 with respect to the longitudinal axis of the beams appeared to be more effective than those oriented at 90 . However, such orientation is less practical because of the difficulty of installation. Specimens tested under negative moment condition exhibited similar behavior to that of the specimens tested under positive moment conditions. Test results showed that beams with slight corrosion damage can be effectively repaired in shear by externally bonded FRP sheets since cracks due to corrosion do not influence the effectiveness of FRP shear strengthening. The stirrups in the beams with pre-existing cracks yielded at a lower shear force than those in the beams without pre-existing cracks. However, the presence of pre-existing cracks did not influence the ultimate failure modes of the beams. Thus, pre-existing cracks do not seem to have a negative impact on the effectiveness of FRP shear strengthening.

The fatigue test performed in this study and other tests reported in the literature indicate that (a) if stresses in the shear stirrups are below the yield strength, the FRP strengthening can help delay the yielding and prevent fatigue failure of the girder in shear; and (b) if the stirrups have already yielded under existing service loads, it is unlikely that adding

Table 2.7. Nominal shear strength and shear gain calculations based on normalized concrete strength.

Specimen Designation	f'_c (psi)	$V_{n,test}$ (kips)	V_c (kips)	V_s (kips)	V_f (kips)	$V_{n,norm}$ (kips)	Actual Shear Gain (kips)	Shear Gain (%)
RC-8-Control	2,800	153	72	81	-	153	-	-
RC-12-Control	2,880	124	65	59	-	124	-	-
RC-8-S90-NA	3,000	191	87	64	41	189	**36**	**23.2**
RC-8-S90-DMA	3,450	212	133	56	24	199	**47**	**30.9**
RC-12-S90-NA	4,190	172	92	41	40	156	**33**	**26.3**
RC-12-S90-DMA	4,420	205	112	38	55	183	**60**	**48.1**
RC-12-S90-SDMA-PC	2,780	214	118	37	59	216	**92**	**74.6**
RC-12-S90-HA-PC	2,650	188	88	38	61	191	**67**	**54.5**
RC-12-S90-SDMA-Cor	6,180	268	98	64	106	237	**113**	**91.1**
RC-12-S45-NA	6,050	217	79	44	95	191	**67**	**54.0**
RC-12-S45-HA	3,850	181	53	41	86	174	**50**	**40.2**
RC-12-S45-SDMA	4,230	203	37	42	124	196	**73**	**58.6**
RC-12-S90-NA-HM	3,710	186	28	103	55	182	**59**	**47.3**
RC-12-S90-SDMA-HM	4,060	229	44	87	84	222	**99**	**80.4**
RC-12-S90-NA-Ftg	4,730	-	-	-	-	-	-	-

f'_c : Concrete strength at the time of testing
$V_{n,test}$: Measured Shear Strength
V_c: Shear contribution of concrete
V_s: Shear contribution of stirrups
V_f: Shear contribution of FRP
$V_{n,norm}$: Normalized Shear Strength

an FRP strengthening system will reduce stresses considerably, but it would help contain the stresses and prevent catastrophic failure of the girder.

Therefore, it is important to consider shear strengthening of a concrete girder using FRP within an overall strengthening plan that also considers the flexural capacity. Strengthening a girder that is deficient in shear may be required to raise the shear resistance to an acceptable level without the need to increase flexural capacity. In addition, limiting the stress in the stirrups to the yield strength will eliminate that fatigue failure of the girder in shear.

2.6.2.2 PC Girders

Tests were conducted on full-scale AASHTO type PC girders to investigate the effects of FRP shear strengthening. Table 2.8 lists the test parameters for the PC girders. The parameters investigated included (a) size of test girders (Type 4 and

Table 2.8. PC girder test parameters.

MoDOT Standard	Girder	Test I.D.	Test Parameters							
			Cross-Section Type	Pre-Existing Cracks	Strengthening Scheme	Anchorage Type	Steel Shear Reinforcement	FRP Shear Reinforcement	Shear Span (ft)	Shear Span-to-Depth Ratio (a/d)
Type 4	1	T4-12-Control	I	No	None	None	#3 @ 12" (ρ_v = 0.0031)	ρ_f = 0	9	2.9
		T4-18-Control	I	No	None	None	#3 @ 18" (ρ_v = 0.0020)	ρ_f = 0	9	2.9
	2	T4-18-S90-NA	I	No	Strips/90	None	#3 @ 18" (ρ_v = 0.0020)	ρ_f = 0.0014	9	2.9
		T4-18-S90-CMA	II	No	Strips/90	Continuous CFRP Plates	#3 @ 18" (ρ_v = 0.0020)	ρ_f = 0.0014	12	2.9
	3	T4-18-S90-DMA	II	No	Strips/90	Discontinuous CFRP Plates	#3 @ 18" (ρ_v = 0.0020)	ρ_f = 0.0014	12	2.9
		T4-18-S45-DMA	II	No	Strips/45	Discontinuous CFRP Plates	#3 @ 18" (ρ_v = 0.0020)	ρ_f = 0.0010	12	2.9
	4	T4-12-Control-Deck	II	No	None	None	#3 @ 12" (ρ_v = 0.0031)	ρ_f = 0	12	2.9
		T4-12-S90-SDMA	II	No	Strips/90	Discontinuous Sandwich CFRP Plates	#3 @ 12" (ρ_v = 0.0031)	ρ_f = 0.0014	12	2.9
Type 3	5	T3-12-Control	III	No	None	None	#3 @ 12" (ρ_v = 0.0031)	ρ_f = 0	12	3.4
		T3-12-S90-NA	III	No	Strips/90	None	#3 @ 12" (ρ_v = 0.0031)	ρ_f = 0.0014	12	3.4
	6	T3-12-S90-NA-PC	III	Yes	Strips/90	None	#3 @ 12" (ρ_v = 0.0031)	ρ_f = 0.0014	12	3.4
		T3-12-S90-DMA	III	No	Strips/90	Discontinuous CFRP Plates	#3 @ 12" (ρ_v = 0.0031)	ρ_f = 0.0014	12	3.4
	7	T3-18-Control	IV	No	None	None	#3 @ 18" (ρ_v = 0.0020)	ρ_f = 0	12	3.4
		T3-18-S90-NA	IV	No	Strips/90	None	#3 @ 18" (ρ_v = 0.0020)	ρ_f = 0.0014	12	3.4
	8	T3-18-S90-HS	IV	No	Strips/90	Horizontal FRP Strips	#3 @ 18" (ρ_v = 0.0020)	ρ_f = 0.0014	12	3.4
		T3-18-S90-SDMA	IV	No	Strips/90	Discontinuous Sandwich CFRP Plates	#3 @ 18" (ρ_v = 0.0020)	ρ_f = 0.0014	12	3.4

Type 3), (b) stiffness of top and bottom flanges (cross-sectional type), (c) effects of pre-existing damage (pre-cracking), (f) FRP strengthening scheme (fibers oriented at 90 versus 45), (g) types of mechanical anchorage, and (h) transverse steel reinforcement (stirrups) ratio.

All PC girders were designed with consideration for the AASHTO LRFD design guidelines (AASHTO, 2008). Girder geometry and strand patterns were based on standard I-girders used by the Missouri Department of Transportation (MoDOT). The girders were designed to fail in shear, with moderate and low levels of shear reinforcement, to investigate the influence of the transverse reinforcement on the shear behavior. Girders with the four cross-sectional designs shown in Figure 2.14 were constructed and tested.

The PC girders were tested in a three point loading configuration with each girder being designed to have two test regions: one on each end of the girder. Electric resistance strain gages, confinement bars, and longitudinal reinforcement to monitor local strains were installed on the stirrups within the test regions. Strain gages were also installed on the mechanical anchorage systems and at various locations along the FRP strips to monitor strain variation along the width and height of the FRP strips. These gages were also used to monitor the progression of delamination/debonding of the FRP. A strain rosette consisting of 21 LVDTs was anchored to the web of each test girder to measure shear strains within the test region for the purpose of determining the principal strains and their orientation. A similar system consisting of Demec gages glued to the opposite side of the web was used as a secondary measure for evaluating the principal strains and their orientations. Additional string transducers and LVDTs were also used to monitor deformations at critical points along the test girders.

The results of the PC girder testing were inconclusive as to the effectiveness of the FRP shear strengthening because of the variety of failure modes observed during the testing. In many cases, no shear gain was observed for the FRP strengthened specimens. Failure modes included (1) horizontal failure along the top flange, (2) debonding of FRP, (3) localized rupture of FRP, (4) diagonal shear tension, (5) web crushing, (6) mechanical anchorage failure, and (7) failure due to high stress concentrations localized at the reaction point. Some test specimens exhibited multiple failure modes either at the same time or in a sequential manner.

For the MoDOT Type 4 girders [Figures 2.14 (a) and (b)], shear cracks in the web propagated toward the top flange at which point they turned and ran horizontally along the longitudinal compression reinforcement located at the interface between the web and top flange. The maximum shear force carried by all MoDOT Type 4 girders was ultimately governed by a failure plane created by the horizontal cracks along the top flange (failure mode—TF). For the MoDOT Type 4 girders strengthened in shear with FRP, the horizontal top flange failure was generally preceded by debonding of the FRP (failure mode—D). In two extreme cases, ultimate failure was accompanied by failure of the mechanical anchorage (T4-18-S90-CMA) (failure mode—MA) and localized rupture of the FRP (T4-18-S90-DMA) (failure mode—LR). For the MoDOT Type 3 girders, failure due to web crushing (failure mode—WC) or high stress concentrations near the reaction point (failure mode—SC) were observed when a moderate level of transverse steel reinforcement was provided (stirrups spaced at 12 inches). For the MoDOT Type 3 girders with low transverse steel reinforcement conditions (stirrups spaced at 18 inches), ultimate failure was always characterized by diagonal shear-tension failure (failure mode—DT) preceded by some level of debonding (failure mode—D) when FRP reinforcement was present. The diminished effectiveness of the FRP shear strengthening is probably related to the thin web and stiff flange geometry of the PC girders and the adverse effect of FRP debonding when it is accompanied by peeling off of the concrete cover. In extreme cases, web crushing failure can occur, which is a failure mode that cannot benefit from FRP strengthening. The use of properly anchored FRP systems (e.g., with mechanical anchorage) will minimize the extent of debonding and improve performance.

To better understand the shear resistance mechanisms and quantify the FRP contribution to the ultimate shear capacity, it is necessary to examine the effects of the individual components contributing to the total shear resistance. The primary components contributing to the shear resistance are those provided by the concrete (V_c), steel stirrups (V_s), and externally bonded FRP (V_f). A shear component analysis was conducted on the experimental data to identify the contribution of each component throughout the loading history of the test girders. The three individual components (V_c, V_s, and V_f) were evaluated from crack-based free-body diagrams of a portion of the test girders along the critical shear cracks. V_s and V_f were determined from strain gage measurements along the stirrups and FRP strips within the test regions. Only strain measurements closest to the critical shear crack were used for such analysis. V_c was estimated as the difference between the applied shear force (V_n) and the contributions of the stirrups and FRP (i.e., $V_s + V_f$). A shear component analysis showed that externally bonded FRP provides a significant contribution to the total shear resistance of a PC girder. The results of this analysis are summarized in Table 2.9 at the stages corresponding to yielding of the steel stirrups and ultimate load.

2.6.3 Results of Finite Element Method (FEM) Analysis

Nonlinear finite element analyses were carried out using the commercial FE program DIANA (DIsplacement ANAlyzer) to (1) predict the behavior of the test girders prior to testing, (2) investigate the effects of additional parameters not

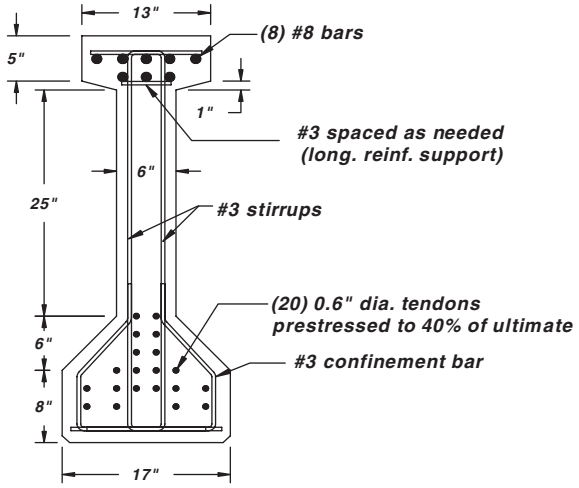

(a) Cross-Section Type I

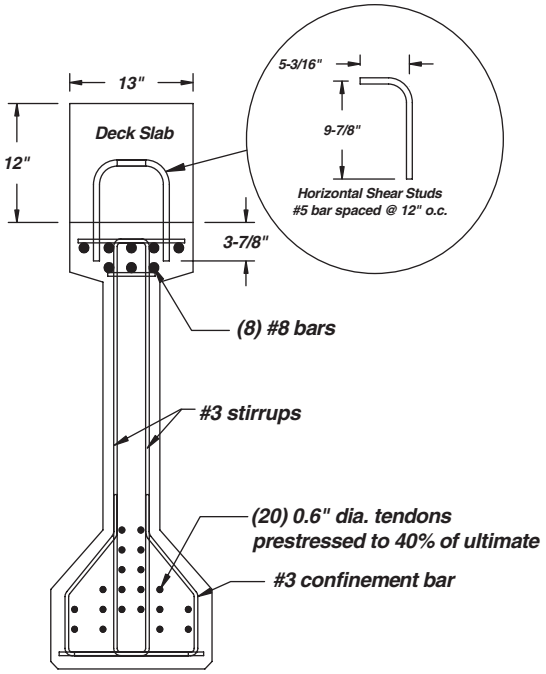

(b) Cross-Section Type II

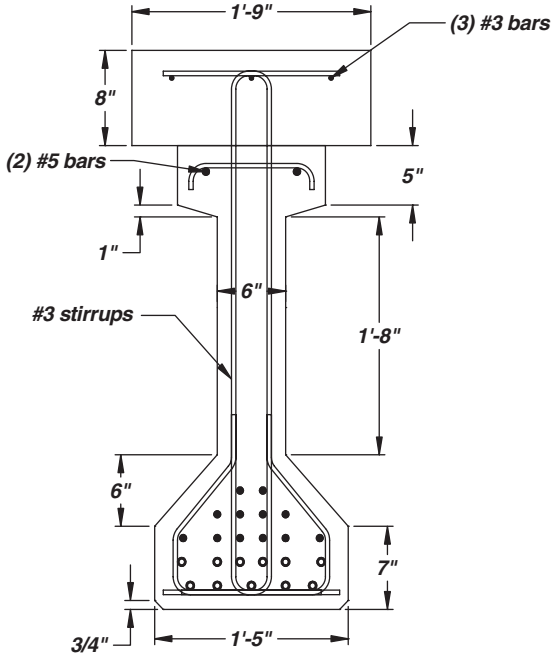

- (12) 0.6" dia. tendons prestressed to 70% of ultimate
- (11) #6 bars

(c) Cross-Section Type III

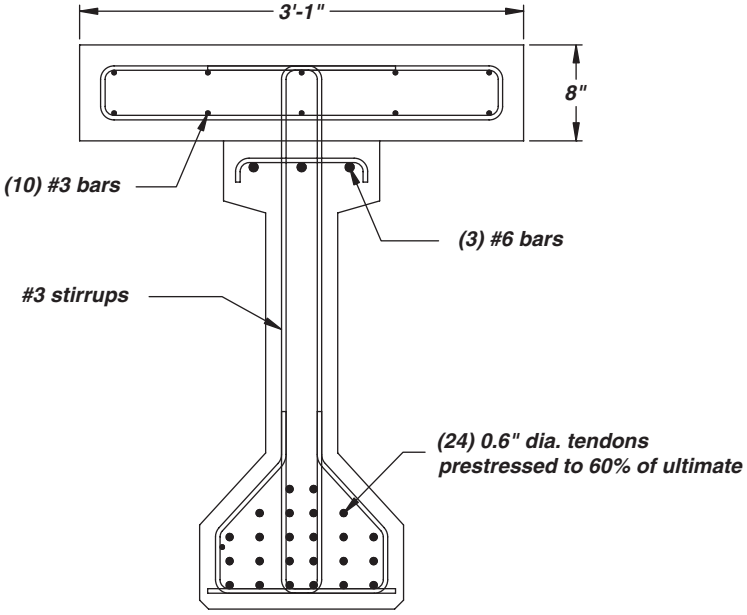

(d) Cross-Section Type IV

Figure 2.14. Specimen cross sections.

Table 2.9. Summary of shear contributions.

Test I.D.	f'_c (psi)	Cross Section Type	Shear Crack Angle (deg.)	Failure Mode	At Yielding of Steel Stirrups			At Ultimate Load		
					V_{cy} (kips)	V_{sy} (kips)	V_{fy} (kips)	V_{cu} (kips)	V_{su} (kips)	V_{fu} (kips)
T4-12-Control	9,970	I	32.0	TF	N/A	N/A	N/A	131	71	N/A
T4-18-Control	9,930	I	26.0	TF	127	57	N/A	149	57	N/A
T4-18-S90-NA	10,020	I	21.0	D + TF	83	43	67	83	43	67
T4-18-S90-CMA	10,120	II	25.0	D + MA + TF	N/A	N/A	N/A	95	47	87
T4-18-S90-DMA	10,160	II	24.0	D + LR + TF	N/A	N/A	N/A	161	39	44
T4-18-S45-DMA	10,190	II	32.0	D + TF	N/A	N/A	N/A	144	34	77
T4-12-Control-Deck	10,660	II	26.0	TF	142	86	N/A	159	86	N/A
T4-12-S90-SDMA	10,330	II	30.0	TF	113	57	35	134	57	67
T3-12-Control	8,890	III	23.0	SC	133	100	N/A	153	100	N/A
T3-12-S90-NA	8,910	III	22.0	D + WC	120	86	23	143	90	38
T3-12-S90-NA-PC	9,470	III	21.0	D + WC	110	86	41	115	86	39
T3-12-S90-DMA	10,380	III	25.0	SC	N/A	N/A	N/A	158	60	31
T3-18-Control	9,590	IV	21.0	DT	108	59	N/A	192	60	N/A
T3-18-S90-NA	10,120	IV	15.0	D + DT	52	86	26	112	86	18
T3-18-S90-HS	10,190	IV	26.0	D + DT	82	43	38	140	51	31
T3-18-S90-SDMA	10,430	IV	33.0	D + DT	48	77	110	48	77	110

considered in the experimental test program, and (3) identify the global and local behaviors of girders that were not monitored in the tests such as the interface behavior between concrete and FRP sheets. DIANA is a program with its own library of structural elements and constitutive material models and includes a user-defined option for adding specific elements and constitutive models to provide flexibility for FE modeling. Subsequently, an FE model capable of simulating the global and local behavior of the RC and PC girders strengthened with FRP in shear was developed. The progression of the FE model development was as follows: (i) Preliminary analyses, focused on the modeling aspects of the FE model, were carried out at the initial state of the FE analysis using two- and three-dimensional FE models. Another finite element program, FEAP, was used to confirm the results of DIANA; (ii) The results of the two-dimensional FE analysis were used to refine the input parameters of the three-dimensional model and improve accuracy; (iii) Other modeling techniques (e.g., phase analysis, modeling of the interface region between concrete and FRP, use of different elements, and refinement of mesh size) were introduced in the developed FE models to better reflect the processes observed in the experimental girders; (iv) Because results of FE models are strongly dependent on the material models chosen for each material, several material models for concrete, steel, FRP, and interface were examined, and optimized material models were incorporated in the FE model (special consideration was given to concrete and interface models because of their inherent complex properties and effects on the shear behavior).

The results obtained from the FE models were compared to the experimental results with respect to global behavior (i.e., shear force-displacement relationships and final failure modes) and local behavior (i.e., stress and strain variations for each component). The shear force-displacement relationships obtained from the FE model showed somewhat stiffer behavior than that obtained from the tests on RC and PC girders regardless of FRP strengthening (see Figure 2.15). This phenomenon is attributed to the configuration considered in the FE model that differed from the test. For example, the FE simulation did not consider external configurations such as strengthening of the specimens with the Dywidag bars. Also, the smeared crack model used for concrete in the FE simulation does not precisely replicate the behavior of the test specimens that were mostly governed by a few primary discrete diagonal cracks. However, accurate prediction of cracking and ultimate loads, similar crack patterns, consistent ductility, and similar strain/stress variations in each component are indications of the developed FE model's efficiency.

In terms of failure strength, the average ratio of experimental shear strength to analytically evaluated shear strength of the PC girders (V_{exp}/V_{FE}) was 1.04 with a maximum ratio of 1.22 and a minimum ratio of 0.95. The variance (VAR), standard deviation (STDEV), and coefficient of variance

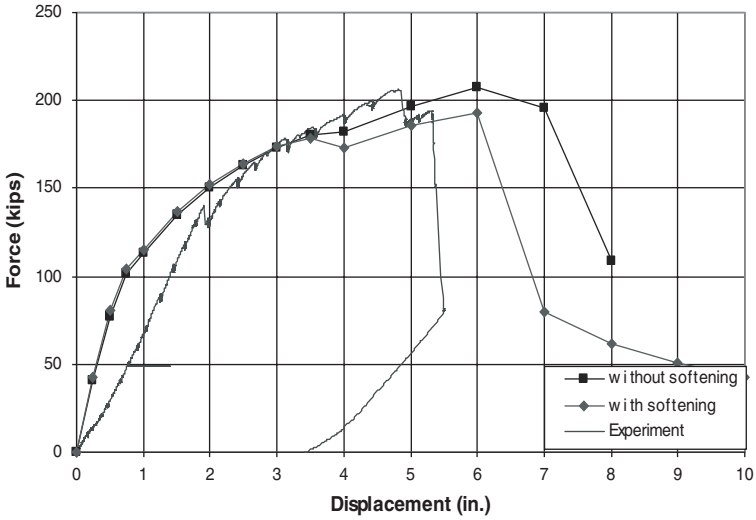

(a) PC girders

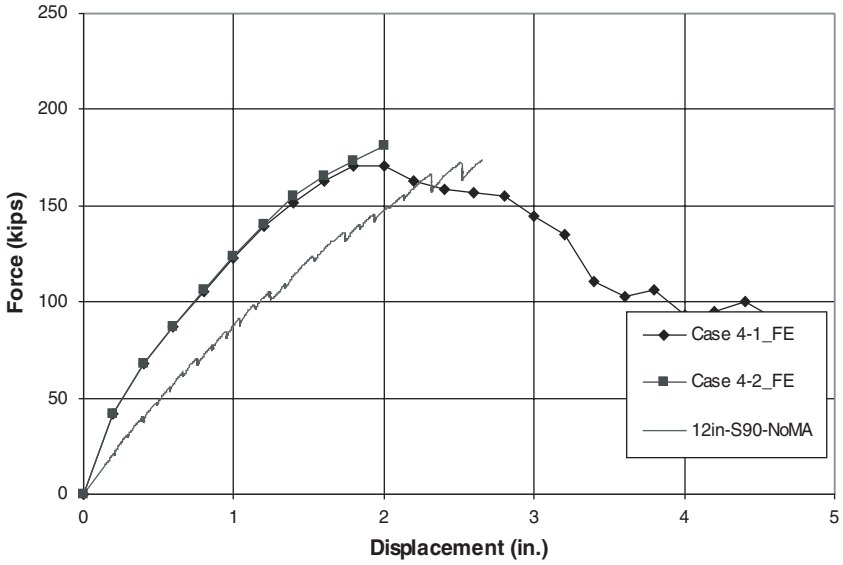

(b) RC girders

Figure 2.15. Representative shear force-displacement relationship.

(COV) are calculated as 0.01, 0.07, and 0.07, respectively. For RC girders, the average shear strength ratio was 0.98 with a maximum ratio of 1.11 and a minimum ratio of 0.90, and VAR, STDEV, and COV are calculated as 0.00, 0.07, and 0.07, respectively. The FE analyses showed a good agreement with test results for the ultimate strength suggesting that the developed FE models appropriately predict the ultimate strength of both PC and RC girders.

The FE analysis allowed investigation of local behaviors that could not be examined through experiments such as the interface behavior between concrete and FRP sheets. The FE analysis also provides the stress and strain variations for concrete, steel, FRP, and interface regions that were used to investigate each component contribution to the shear transfer mechanism. In particular, strain variations along the principal direction of FRP sheets are valuable inputs for designing FRP strengthening for shear. Figure 2.16 illustrates the strain distribution determined from FE analysis along the principal direction of a critical FRP sheet for a series of increasing load stages. As shown in the figure, when the test beam reached the ultimate state (i.e., a loading state of 250 kips), the maximum strain in the FRP was only 0.0091 which is 54% of the rupture strain (0.017).

2.7 Performance Evaluation of Existing Design Methods

This section presents a summary of the performance evaluation conducted for existing models and relationships for Vf. Table 2.10 presents a summary of the performance of 21 different relationships (i.e., 17 models presented in research papers and four models included in code and guideline docu-

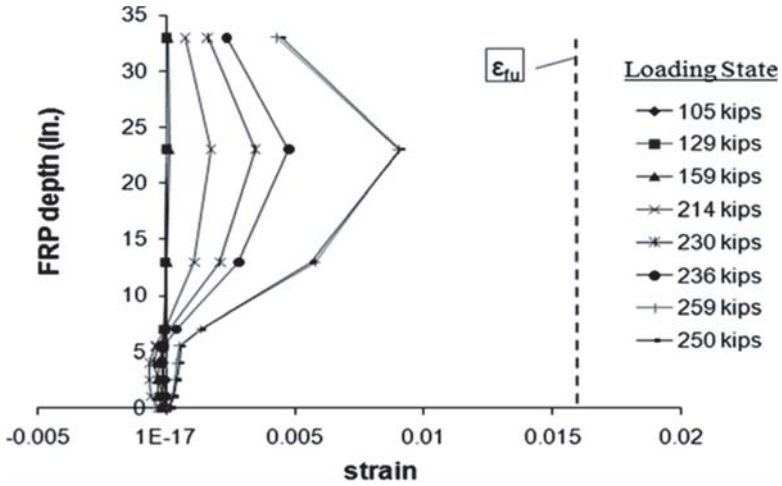

Figure 2.16. Strain variations along principal direction of critical FRP sheet.

ments) for calculating Vf based on the comparisons of the FRP contributions predicted by each model to the experimentally measured FRP contributions as reported in the database. Table 2.10 presents the average ratio of the shear strength provided by FRP reinforcement ($V_{f,test}/V_f$), the COV, and the number of beams used in calculating this average for 13 segments of the experimental dataset. $V_{f,test}$ is the experimentally measured strength of a test beam with FRP reinforcement minus the experimentally measured strength of the corresponding (control) beam without FRP reinforcement, and V_f is the strength calculated from each model. The first segment is the entire dataset of "all beams;" the second set contains only those test results considered appropriate for calibrating provisions to be used in codes of practice including the AASHTO LRFD Bridge Design Specifications (AASHTO, 2008). This action reduced the potential number of available test results from 324 to 251. These results were further separated into segments according to the Mode of Failure (MoF), the use of steel shear reinforcement (No Av or With Av), and by combinations of these two. It was apparent that within each segment, there was a large variation in the average strength ratio, and generally, the COVs are large because the models were derived to provide a best fit with a relatively small number of tests, and there is a very wide range in types and effectiveness of FRP including stiffness (E_f), ultimate strength (f_{fu}), means of application, anchorage, orientation, and other factors. Therefore, the individual models would perform better (reasonable strength ratio and lower COV) for some segments of the test data than others. For example, the model by Khalifa et al., (1998) shows COV of 1.47 and 0.48 for members with observed rupture failures without and with steel shear reinforcement, respectively. Relationships for V_f in codes and guidelines are expected to consider a wide range of test results with a uniform average strength ratio and COV across all segments of the test data. Model (fib-TG9.3, 2001) exhibited the most uniform performance. Models 3, 9, 13, and 14 also demonstrated similar performance across a broad range in categories.

2.8 Suggestions for Improved Design Methods

The statistical assessment of the performance of models for V_f determined that the following five models provide the lowest COV across a wide range of segments of the database:

Model 3 (Triantafillou and Antonopoulos, 2000)
Model 9 (Chen and Teng, 2003a and 2003b)
Model 13, (Cao et al., 2005)
Model 14, (Zhang and Hsu, 2005)
Model 18 (fib-TG 9.3, 2001 and Triantafillou and Antonopoulos, 2000)

Based on the review of these models, a V_f model that includes the following features would be appropriate for incorporation into the LRFD specifications (AASHTO, 2008):

axial stiffness of FRP reinforcement ($\rho_f E_f$)
compressive strength of concrete (f_c)
mode of failure (debonding or rupture)
type of FRP application (full wrap, side bonding, or U-wrap)
development length available for FRP (L_e)
bond strength between FRP and concrete (τ_{max})

For use in design the V_f model must also consider the following:

1. **Complexity of Relationship for Evaluation.** The majority of available models for V_f are much more complex than

Table 2.10. Statistical evaluation of strength ratios $V_{f,test}/V_{f,model}$ by test beam type.

Model Affiliation	Al-Sulaimani et al.	Chajes et al.	Triantafillou and Antonopoulos	Malek and Saadatmanesh	Khalifa et al.	Khalifa and Nanni	Hutchinson and Rizkalla	Chaallal et al.	Chen and Teng	Pellegrino and Modena	Hsu et al.	Deniaud and Cheng	Cao et al.	Zhang and Hsu	Carolin and Taljsten	Monti and Liotta	Pellegrino and Modena	fib-TG9.3	JSCE	CSA S806	ACI 440
Year	1994	1995	2000	1998	1998	2000	1999	2002	2003a,b	2002	2003	2001	2005	2005	2005b	2005	2006	2001	2001	2002	2008
Model #	1	2	3	4	5	6	7	8	9	10	11	12	13	14	15	16	17	18	19	20	21
1.) All Beams																					
Mean	0.23	1.10	0.84	0.34	1.46	1.49	1.90	1.16	1.68	3.56	1.30	8.39	0.75	1.19	1.15	1.67	0.41	1.24	0.52	1.46	1.65
COV	0.67	1.05	1.10	0.81	1.05	1.03	1.01	0.77	0.64	2.29	0.89	1.71	0.71	0.59	0.81	0.75	0.73	0.60	0.76	0.99	0.96
Num	324	324	324	324	315	317	324	324	324	244	244	324	324	324	324	324	324	317	324	324	317
2.) All "Valid" Beams (those used in LRFD Vf Model Calibration)																					
Mean	0.25	1.23	0.98	0.38	1.53	1.57	2.10	1.18	1.83	3.24	1.39	9.30	0.78	1.30	1.25	1.84	0.44	1.35	0.57	1.61	1.78
COV	0.62	0.94	0.56	0.73	0.97	0.95	0.91	0.60	7.57	1.34	0.89	1.71	0.57	0.53	0.73	0.66	0.67	0.50	0.66	0.89	0.88
Num	251	251	251	251	244	244	251	251	251	187	187	251	251	251	251	251	251	244	251	251	244
3.) "Valid" Beams: MoF = Rupture																					
Mean	0.24	0.88	0.81	0.32	1.25	1.32	1.53	1.07	1.48	2.73	1.35	8.85	0.62	1.22	1.08	1.58	0.38	1.17	0.48	1.18	1.35
COV	0.69	0.70	0.38	0.69	0.57	0.69	0.68	0.62	0.45	1.16	0.79	1.33	0.52	0.44	0.69	0.51	0.63	0.43	0.59	0.67	0.61
Num	126	126	126	126	125	125	126	126	126	94	94	126	126	126	126	126	126	125	126	126	125
4.) "Valid" Beams: MoF = Debonding																					
Mean	0.22	1.60	1.19	0.49	2.14	2.07	2.73	1.43	2.23	4.85	1.92	15.70	1.01	1.64	1.65	2.31	0.56	1.58	0.73	2.09	2.36
COV	0.45	1.00	0.62	0.77	1.18	1.18	0.96	0.67	0.57	1.31	1.03	1.63	0.49	0.56	0.77	0.73	0.73	0.48	0.72	0.94	1.00
Num	61	61	61	61	58	58	61	61	61	40	40	61	61	61	61	61	61	58	61	61	58
5.) "Valid" Beams: MoF = Other																					
Mean	0.30	1.55	1.12	0.37	1.51	1.62	2.63	1.18	2.12	2.91	1.05	4.08	0.89	1.15	1.23	1.89	0.42	1.52	0.58	2.00	2.10
COV	0.53	0.82	0.53	0.56	0.72	0.66	0.80	0.66	0.54	1.35	0.35	1.29	0.53	0.52	0.56	0.64	0.50	0.50	0.55	0.78	0.73
Num	64	64	64	64	61	61	64	64	64	53	53	64	64	64	64	64	64	61	64	64	61
6.) "Valid" Beams: No Av																					
Mean	0.30	1.48	1.14	0.41	1.74	1.92	2.54	1.01	2.06	1.89	1.22	4.31	0.83	1.23	1.36	1.89	0.47	1.49	0.62	1.94	2.15
COV	0.61	1.00	0.59	0.77	1.16	1.04	0.97	0.53	0.58	1.08	0.76	1.21	0.56	0.41	0.77	0.68	0.70	0.44	0.69	0.95	0.96
Num	114	114	114	114	108	108	114	114	114	108	108	114	114	114	114	114	114	108	114	114	108
7.) "Valid" Beam: With Av																					
Mean	0.21	1.01	0.85	0.35	1.36	1.30	1.74	1.33	1.63	5.08	1.62	13.45	0.74	1.37	1.16	1.80	0.41	1.25	0.52	1.33	1.48
COV	0.54	0.71	0.44	0.67	0.58	0.62	0.68	0.70	0.51	1.13	0.96	1.49	0.56	0.59	0.67	0.64	0.63	0.53	0.61	0.67	0.62
Num	137	137	137	137	136	136	137	137	137	79	79	137	137	137	137	137	137	136	137	137	136
8.) "Valid" Beams: MoF = Debonding: No Av																					
Mean	0.31	0.82	0.87	0.30	1.38	1.62	1.43	0.91	1.53	1.42	1.18	5.21	0.63	1.22	1.00	1.62	0.39	1.27	0.47	1.10	1.42
COV	0.71	0.77	0.40	0.73	0.65	0.74	0.75	0.47	0.49	0.65	0.52	0.77	0.57	0.40	0.73	0.55	0.71	0.42	0.60	0.75	0.67
Num	47	47	47	47	46	46	47	47	47	46	46	47	47	47	47	47	47	46	47	47	46
9.) "Valid" Beams: MoF = Rupture: No Av																					
Mean	0.22	1.95	1.36	0.57	2.45	2.55	3.33	1.10	2.37	2.67	1.53	5.62	0.94	1.34	1.90	2.08	0.62	1.61	0.79	2.55	2.88
COV	0.39	1.09	0.73	0.86	1.47	1.35	1.05	0.61	0.67	1.34	1.06	1.50	0.60	0.43	0.86	0.90	0.78	0.54	0.84	1.03	1.13
Num	29	29	29	29	26	26	29	29	29	26	26	29	29	29	29	29	29	26	29	29	26
10.) "Valid" Beams: MoF = Other: No Av																					
Mean	0.33	1.96	1.30	0.42	1.68	1.84	3.31	1.05	2.48	1.93	1.05	2.20	1.01	1.16	1.40	2.07	0.45	1.69	0.66	2.51	2.56
COV	0.50	0.67	0.43	0.33	0.69	0.60	0.65	0.48	0.42	0.64	0.30	0.48	0.41	0.38	0.33	0.51	0.36	0.32	0.37	0.64	0.64
Num	38	38	38	38	36	36	38	38	38	36	36	38	38	38	38	38	38	36	38	38	36
11.) "Valid" Beams: MoF = Debonding: With Av																					
Mean	0.19	0.92	0.77	0.34	1.17	1.14	1.59	1.16	1.44	3.99	1.52	11.02	0.61	1.22	1.12	1.56	0.38	1.11	0.48	1.22	1.31
COV	0.50	0.65	0.36	0.66	0.49	0.55	0.64	0.65	0.42	0.99	0.89	1.28	0.48	0.46	0.66	0.48	0.57	0.43	0.58	0.63	0.55
Num	79	79	79	79	79	79	79	79	79	48	48	79	79	79	79	79	79	79	79	79	79
12.) "Valid" Beams: MoF = Rupture: With Av																					
Mean	0.22	1.28	1.03	0.43	1.89	1.68	2.19	1.72	2.11	8.91	2.64	24.84	1.07	1.91	1.42	2.51	0.51	1.56	0.66	1.68	1.94
COV	0.50	0.57	0.32	0.53	0.48	0.57	0.54	0.62	0.42	0.92	0.89	1.27	0.39	0.56	0.53	0.59	0.62	0.43	0.48	0.52	0.53
Num	32	32	32	32	32	32	32	32	32	14	14	32	32	32	32	32	32	32	32	32	32
13.) "Valid" Beams: MoF = Other: With Av																					
Mean	0.27	0.96	0.86	0.29	1.26	1.30	1.63	1.36	1.60	5.00	1.07	6.82	0.72	1.13	0.97	1.63	0.38	1.28	0.47	1.25	1.44
COV	0.56	0.97	0.64	0.89	0.73	0.73	0.93	0.76	0.69	1.24	0.44	1.07	0.69	0.69	0.89	0.83	0.67	0.74	0.80	0.90	0.77
Num	26	26	26	26	25	25	26	26	26	17	17	26	26	26	26	26	26	25	26	26	25

most formulas in codes of practice and therefore, not suitable for use in practice.

2. **Availability and Reliability of Model Parameter Data.** The models proposed by most researchers require knowledge of the measurable features of the test beam and FRP application, such as the development length of the FRP reinforcement. While such requirements improve accuracy, design provisions must include items that are available or can be appropriately assumed. The parameters proposed in a V_f relationship for use in the LRFD specifications should recognize that FRP shear reinforcement is most likely to be used for strengthening of an existing old structure for which full design details may not be available.
3. **Calibration with Full Shear Strength Ratio Considering Specific V_c and V_s Relationships.** A comparative evaluation of V_f models, can be conducted using the strength ratios of $V_{f,test}/V_f$. However, to include in a code of practice, the relationship for V_f must be calibrated based on the bias (strength ratio) and COV of the $V_{n,test}/V_n$ ratio ($V_n = V_c + V_s + V_f$).

2.9 Reliability Assessment

A study was conducted to assess the reliability of the proposed design equations using procedures similar to those used in the calibration of AASHTO-LRFD specifications (AASHTO, 2008). The First Order Reliability Method (FORM) was used for calculating the reliability index (β_r) of 36 bridges that were designed for such purposes. These bridges covered three span lengths, interior and exterior girders, and three shear deficiency levels that were strengthened with FRP shear reinforcement (i.e., a set of $3 \times 2 \times 3 = 18$ bridges). One set used anchored FRP reinforcement where FRP rupture is the dominating mode of failure, and another set used non-anchored FRP reinforcement where debonding is to be expected. Table 2.11 lists the nominal properties of these bridges, illustrating the wide range in the ratio of FRP contribution (V_f) to the nominal strength of the existing structure. The live-to-dead load shear demand ratio for these bridges ranges from 0.83 to 2.32.

The nominal values of the bridge properties were used to obtain random variables for each of the main parameters in the design equation. This step required knowledge of the statistical characteristics of the random variables. Some of the required information was obtained from the literature, and other information specific to this study had to be determined by estimating the random variables' bias (ratio of random variable's mean value to its nominal value) and COV (ratio of random variable's standard deviation to its mean value). For example, the statistical characteristics of the analysis model uncertainty, ξ_P, were obtained by comparing the predicted shear strength using the proposed equations to the experimentally, measured values as reported in the database. The effect of material and fabrication tolerances on the resistance model was determined using Monte Carlo simulations and some recently published data (Nowak and Szerszen, 2003). The statistical characteristics of load-related random variables were taken from *NCHRP Report 368* (Nowak, 1999). Table 2.12 shows the bias and coefficient of variation for the main parameters used in the limit state function (Z) that

Table 2.11. Shear resistance components.

Bridge		Case	$A_v d_v/s$	w_f	s_f	t_f (in)		V_c	V_s	V_f	$\frac{V_f}{V_c+V_s}$
Span Length	Girder		(in^2)	(in)	(in)	Rupture	Debond	(kips)	(kips)	(kips)	
45 ft	Interior	L45F1I	0.847	4.0	12.0	0.00774	0.01863	73.57	50.82	33.88	0.272
		L45F2I	0.730		10.0	0.01142	0.02749		43.79	40.91	0.349
		L45F3I	0.613		8.0	0.01477	0.03556		36.76	47.94	0.435
	Exterior	L45F1E	0.697		12.0	0.01461	0.03519		41.79	41.79	0.362
		L45F2E	0.532		10.0	0.02315	0.05575		31.92	51.66	0.490
		L45F3E	0.368		8.0	0.03146	0.07576		22.05	61.53	0.643
60 ft	Interior	L60F1I	0.696		14.0	0.00644	0.01023	111.24	41.77	41.77	0.273
		L60F2I	0.580		12.0	0.00644	0.01402		34.78	48.76	0.334
		L60F3I	0.463		10.0	0.00728	0.01753		27.79	55.76	0.401
	Exterior	L60F1E	0.565		14.0	0.01461	0.01855		33.89	50.84	0.350
		L60F2E	0.468		12.0	0.02315	0.02210		28.06	56.67	0.407
		L60F3E	0.371		10.0	0.03146	0.02477		22.23	62.49	0.468
75 ft	Interior	L75F1I	0.501		16.0	0.00596	0.00596	163.81	30.06	45.09	0.233
		L75F2I	0.319		14.0	0.00648	0.00776		19.12	56.03	0.306
		L75F3I	0.136		12.0	0.00664	0.01142		8.18	66.97	0.389
	Exterior	L75F1E	0.394		16.0	0.00730	0.00849		23.67	55.23	0.295
		L75F2E	0.214		14.0	0.00764	0.01277		12.86	66.04	0.374
		L75F3E	0.034		12.0	0.00762	0.01734		2.05	76.85	0.463

Table 2.12. Summary of bias and COV values used in calibration study.

Random Variable		Bias	COV
Material and Fabrication Tolerances, α_{MF}		Varies (see Appendix)	
Analysis Model, ξ_P	FRP Rupture	1.680	0.330
	Other	1.410	0.269
Wearing Surface DL, ζ_{WS}		1.000	0.250
Component DL, ζ_{DC}		1.050	0.100
Highway LL (including impact), ζ_{LL+IM}	L=45 ft	1.041	0.180
	L=60 ft	1.046	0.180
	L=75 ft	1.071	0.180
LRFD Girder Distribution Factor, η_{GDF}	Interior	1.134	0.157
	Exterior	1.307	0.239

accounts for variabilities and uncertainties in material and fabrication tolerances (α_{MF}), analysis model accuracy (ξ_p), and girder distribution factors (η_{GDF}) as well as the different loading types (wearing surface, dead load, and live load).

The simplified approximate expressions used in previous AASHTO calibration studies were not used because of the high COV for the analysis model, which exceed the limits of the applicability of the simplified approximated expressions. A detailed iterative FORM analysis was performed; the results were validated using Monte Carlo simulations for one bridge. After several trials, the proposed design expression was adjusted to achieve β_r values close to the level targeted by most AASHTO calibration studies (i.e., $\beta_{r,target} = 3.50$).

The performance of the proposed expression is illustrated in Figure 2.17 for a range of girder span lengths and spacings. The figure shows that the reliability index is nearly the same for all girder spacings and is about 3.50 for shorter span lengths but decreases for longer span lengths.

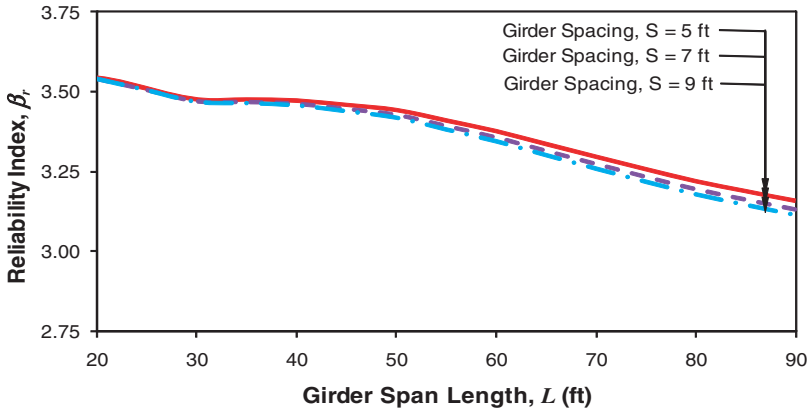

Figure 2.17. Reliability index (β_r) versus span lengths for different girder spacings.

CHAPTER 3

Application and Implementation

3.1 Approaches for Relevant Changes to AASHTO LRFD Bridge Design Specifications

The models for V_f were selected to provide best fit empirical expressions incorporating the variables that were found to influence V_f. These models were formulated and calibrated to achieve a β_r value around 3.5 as characterized by the AASHTO LRFD Bridge Design Specifications (AASHTO, 2008). For the evaluation of the bias and COV of strength ratios V_{test}/V_n, it was necessary to evaluate $V_c + V_s$. The AASHTO LRFD Bridge Design Specifications (AASHTO, 2008) provide six different means of evaluating shear resistance, however, only the simplified procedure was selected to calibrate the model for V_f to achieve the target reliability of, β_r, 3.5. The simplified procedure for evaluating V_c and V_s is given by the following equations:

$$V_c = 0.0316\beta\sqrt{f_c'}\,b_v d_v \qquad (5.8.3.3\text{-}1)$$

For: $\beta = 2 \quad V_c = 0.0632\sqrt{f_c'}\,b_v d_v \quad (f_c' \text{ in ksi})$

or $V_c = 2\sqrt{f_c'}\,b_v d_v \quad (f_c' \text{ in psi})$

While this method is not applicable to members greater than 16 inches in depth that do not contain shear reinforcement, the relationship provided for V_c is identical to that in the General Procedure (AASHTO, 2008) which is applicable to such members when distributed horizontal reinforcement is placed on 12-in. centers, and the strain in the longitudinal reinforcement (ε_s) is less than 0.00187. For $\varepsilon_s = 0.00187$:

$$\beta = \frac{4.8}{(1+750\varepsilon_s)}\frac{51}{(39+s_{xe})} = \frac{4.8}{(1+750(0.00187))}\frac{51}{(39+12)} = 2.00$$

The contribution of the steel reinforcement is given by:

$$V_s = \frac{A_v f_y d_v (\cot\theta + \cot\alpha)\sin\alpha}{s} \qquad (5.8.3.3\text{-}4)$$

where: θ = the angle of diagonal compression and α = the angle of the transverse reinforcement relative to the longitudinal axis of the member

If $\theta = 45$ and $\alpha = 90$ then: $V_s = \dfrac{A_v f_y d_v}{s}$

The contribution of the FRP reinforcement can be evaluated using the truss model used for evaluating the contribution of the steel shear reinforcement. In this case:

$$V_f = \frac{A_f f_{fe} d_f}{s_f}(\cot\theta + \cot\alpha)\sin\alpha$$

If $\theta = 45$ and $\alpha = 90$ then: $V_f = \dfrac{A_f f_{fe} d_f}{s_f}$

Since $f_{fe} = E_f \varepsilon_{fe}$, the contribution of the FRP to shear resistance may be controlled by ε_{fe} as done in most existing models for V_f.

Based on the results of statistical assessments (including the reliability study) and for simplicity, the following expressions are proposed for determining the effective strain (ε_{fe}) and use in the *AASHTO LRFD Bridge Design Specifications* (AASHTO, 2008).

When "full-anchorage" is provided such that the shear resistance at shear failure is controlled by FRP rupture:

$$\varepsilon_{fe} = R\,\varepsilon_{fu} \quad \textit{where} \quad \varepsilon_{fu} = f_{fu}/E_f \quad \textit{and}$$
$$R = 4(\rho_f E_f)^{-.67} \le 1.0$$

where $\rho_f E_f$ is in ksi units and limited to 300 ksi.

Comparison of this expression with the test data yields an average strength ratio (bias) of 1.68 and a corresponding COV of 0.33.

When "full-anchorage" is not provided, it is likely that the shear capacity will be controlled by FRP debonding or another mode of failure before FRP rupture can be achieved:

$$\varepsilon_{fe} = R\,\varepsilon_{fu} \le 0.012 \quad \text{where} \quad \varepsilon_{fu} = f_{fu}/E_f \quad \text{and}$$
$$R = 3(\rho_f E_f)^{-.67} \le 1.0$$

where $\rho_f E_f$ is in ksi units and limited to 300 ksi.

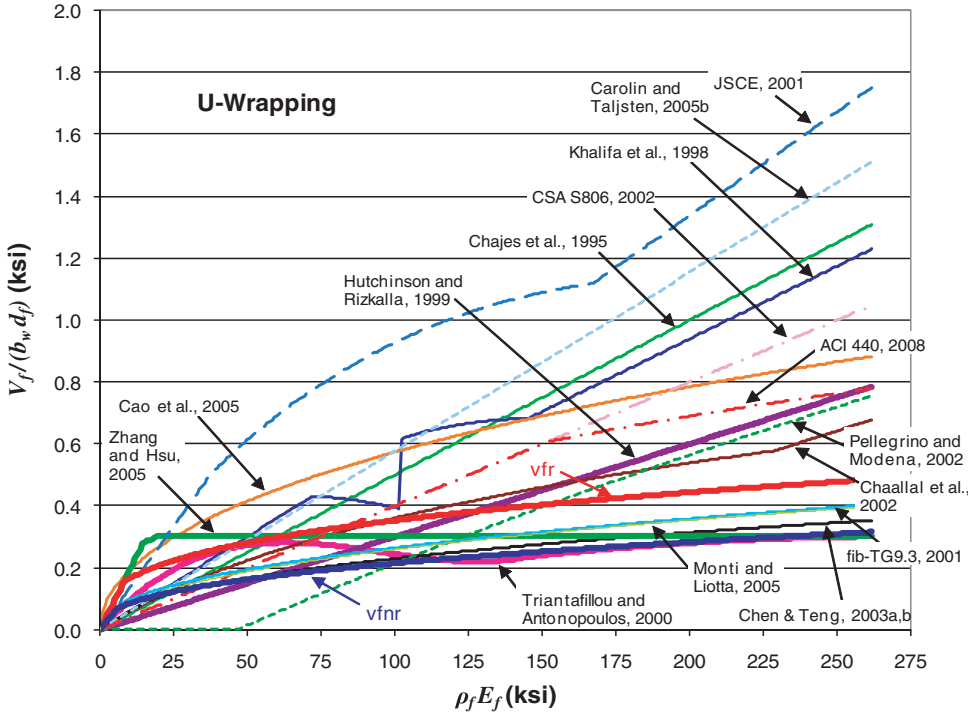

Figure 3.1. Influence of FRP axial rigidity on FRP shear stress resistance.

Comparison of this expression with the test data yields an average strength ratio (bias) of 1.44, and a corresponding COV of 0.25.

These expressions are only applicable for RC and PC members in which $d_v/b_v < 4.0$, and the calculated R value should not be taken greater than one (i.e., $R \leq 1.0$).

Figure 3.1 shows the calculated shear stress capacity provided by the FRP reinforcement ($V_f/b_w\, d_f$) *as a function of the axial rigidity of the FRP reinforcement* ($\rho_f E_f$) for 15 models and the two relationships identified in this study for a member having a rectangular cross-section and the following properties:

Dimensions: 7.09 inches wide, 19.69 inches high, and a shear span-to-depth ratio of 3.5
FRP reinforcement: CFRP sheets externally bonded with fibers oriented at 90 in a U-wrap configuration over a height of 17.32 inches
Concrete compressive strength: 8,557 psi
Modulus of elasticity of the CFRP sheets: 33,939 ksi
Ultimate tensile strength of the CFRP sheet: 653 ksi

The case of full anchorage for which FRP rupture failure is expected is labeled by *vfr*, and the case of less than full anchorage for which debonding or other non-rupture failure modes are expected is labeled *vfnr*. Figure 3.1 shows that the strength when full anchorage is not provided is less than when full anchorage is provided. In addition, the two relationships (Chen and Teng, 2003a,b; Zhang and Hsu, 2005) provide values similar to those obtained from the models that provide the best estimates of FRP shear contribution (i.e., Triantafillou and Antonopoulos, 2000; and fib-TG9.3, 2001).

3.2 Design Guidelines

Recommended design guidelines for concrete girders strengthened in shear with FRP were developed based on the findings of this research. The guidelines, provided as Attachment B, were drafted in LRFD format to facilitate incorporation into the *AASHTO LRFD Bridge Design Specifications* (AASHTO, 2008).

3.3 Design Examples

Six design examples were prepared to illustrate the use of the proposed design. Four of the design examples consider RC T-beams (i.e., two with transverse steel reinforcement and two without transverse steel reinforcement) with a U-wrap FRP strengthening scheme with and without anchorage (i.e., two with mechanical anchorage and two without any anchorage). The other two design examples consider PC I-girders with transverse steel reinforcement and U-wrap FRP strengthening scheme with and without anchorage (i.e., one with mechanical anchorage and one without any anchorage).

CHAPTER 4

Summary of Findings and Recommendations for Future Research

This section summarizes the findings of this research effort and provides suggestions for future research.

4.1 Summary of Findings

This research effort has produced recommended design methods and specifications for strengthening concrete girders in shear using externally bonded FRP systems. The findings of this research regarding use of FRP systems for strengthening concrete girders in shear are as follows:

- Externally bonded FRP can be used to enhance the shear resistance of concrete girders.
- Externally bonded FRP systems can be applied in a variety of configurations and molded to any geometrical shape to provide side bonding, U-wrap, or complete wrapping of the girder web and as continuous sheets or discrete strips. The fibers of the composite may be oriented in any direction. Fibers oriented perpendicular to the longitudinal axis of the girder provide the most practical application, but fibers oriented orthogonal to the shear crack provide the most effective application.
- There is an interaction between transverse steel reinforcement and externally bonded FRP shear reinforcement. The effectiveness of externally bonded FRP for shear strengthening decreases as the transverse steel reinforcement ratio increases.
- The shear span-to-depth ratio (a/d) influences the effectiveness of externally bonded FRP for shear. Shear span-to-depth ratios (a/d) less than 2.0 develop arch action resistance mechanisms (deep beam behavior) that reduce the effectiveness of FRP shear strengthening.
- Tests on large scale RC T-beams showed that the size-effect has little influence on the effectiveness of externally bonded FRP (effective strains in the FRP of the large-scale specimens were found to be similar to those reported for small-scale tests).
- Tests on beams with pre-existing cracks prior to strengthening showed that stirrups yield at a lower shear force than for beams without cracks. However, the existence of cracks seemed not to change the failure modes of the beams suggesting that the existence of cracks does not adversely influence the effectiveness of FRP shear strengthening.
- Beam continuity (negative moment) did not appear to influence the behavior of the beams strengthened with FRP (similar behavior to beams tested under positive moment conditions).
- The effectiveness of externally bonded FRP for shear strengthening depends on the failure mode (i.e., FRP rupture or debonding). Debonding occurs when girders are strengthened in shear by side bonding and occasionally in cases of U-wrapping due to insufficient bond length. FRP rupture can be reached through use of proper anchorage such as that provided by complete wrapping, adequate bond length, or by some form of mechanical anchorage. Girders strengthened in shear with a U-wrapping configuration fail by either debonding or FRP rupture, depending on the bond characteristics.
- The use of mechanical anchorage delays and, in some cases, prevents debonding of the FRP, resulting in a greater increase of the ultimate shear resistance. Use of horizontal strips of FRP as mechanical anchorage does not provide much additional shear capacity. Continuous CFRP plates with anchorage bolts are not very effective in anchoring the CFRP sheets. Discontinuous CFRP plates attached with concrete wedge anchors or bolts through the web provide the most effective mechanical anchorage. The effectiveness of this method can be further improved by the use of a sandwich application that prevents slippage of the FRP sheet from beneath the anchorage plate. For PC girders with very thin webs, the embedment length of anchor bolts may not be sufficient to avoid premature failure due to the anchor bolts pulling out. In such cases, the use of a thru-bolt systems are more practical and provide better performance.

- The effectiveness of FRP for shear strengthening is significantly affected by the cross-sectional shape of the girder. Debonding of FRP accompanied by peeling of the concrete cover can result in a web crushing failure.
- If the stresses in the stirrups are less than the yield strength, the FRP strengthening can help delay yielding and prevent fatigue failure of the girder in shear. However, if the stirrups have already yielded, the FRP strengthening system would not reduce the stresses but could help restrain steel stress increases and prevent catastrophic failure of the girder.
- In the absence of a proper anchorage system, the externally bonded FRP sheets for shear strengthening could become debonded and result in no shear strengthening.
- Limiting the stress in the stirrups to the yield strength will assure that shear fatigue failure of the girder will not occur.
- The effective FRP strain used in evaluating the FRP shear contribution can be expressed by two separate design expressions to consider the two predominant failure modes (i.e., debonding and FRP rupture). One expression is for members in which sufficient anchorage is provided (FRP rupture failure mode), and the other is for members in which insufficient anchorage is provided (FRP debonding failure mode).

4.2 Suggestions for Future Research

Based on the work performed in this research, the following research efforts are needed to enhance understanding of the mechanisms associated with the use of externally bonded FRP for shear.

- An interaction exists between the internal transverse steel reinforcement and externally bonded FRP shear reinforcement, but there are insufficient data to quantify this interaction. Further investigations are needed to better quantify the mechanisms involved in this interaction and incorporate it into an enhanced model for the shear resistance of RC beams strengthened with externally-bonded FRP.
- The use of mechanical anchorage involving discontinuous CFRP plates attached with steel concrete wedge anchors or bolts through the web was found to delay or, in some cases, prevent debonding of FRP. However, because these anchors and bolts are susceptible to corrosion, research is needed to explore alternative mechanical anchorage techniques that are not susceptible to such corrosion.
- The cross-sectional geometry of PC girders influences the effectiveness of externally bonded FRP. Also thin web and stiff flange geometry reduce the effectiveness of the FRP shear strengthening. However, limited results are available to fully understand the mechanisms involved in such behavior. Further research is needed to examine the effect of cross-sectional geometry of PC girders.
- The effective strain concept was adopted for design guidelines and codes to provide a simple and practical method for estimating the shear contribution of FRP. Research is needed to investigate the non-uniform FRP distribution and develop more reliable design equations.
- Research is needed to investigate the long-term fatigue performance of FRP systems for shear strengthening, particularly the effects of cracks on bond characteristics.

Notations

a	Shear span length
a/d	Shear span-to-depth ratio
A_c	Concrete area
A_{cf}	Effective flange concrete area
A_{cw}	Web concrete area = $b_w h$
A_f	Cross-sectional area of FRP
A_p	Cross-sectional area of strengthening material [Sim et al., 2005]
A_{sw}, A_v	Area of transverse steel reinforcement
b, b_v, b_w	Minimum width of cross-section over effective depth
b_f	Width of FRP strip [Carolin and Taljsten, 2005]
C	Constant strain rate = 110×10^{-6} mm^{-1}
d, d_v	Effective depth of cross-section
d_f	Effective depth of FRP reinforcement
D_{frp}	Stress distribution factor for FRP intersected by the shear crack [Chen and Teng, 2003 a and b]
d_{FRP}	FRP sheet height along side of beam web [Deniaud and Cheng, 2001, 2004]
$D_{f\theta}$	Modified FRP strain distribution factor = D_{frp}/θ [Cao et al., 2005]
d_S	Stirrup height
e	spacing of stirrups [Sim et al., 2005]
E_f, E_{frp}	Elastic modulus of FRP
$(E_f\rho_f)_{\lim}$	Limiting value of FRP rigidity separating debonding and FRP rupture failure modes
E_s	Elastic modulus of steel reinforcement
f_c, f'_c	Concrete compressive strength
f_{ck}	Concrete characteristic cubic strength
f_{cm}	Mean cylindrical compressive strength of concrete
f_{ctm}	Concrete mean tensile strength
f_{fd}	Design ultimate strength of FRP
f_{fdd}	Debonding FRP strength

f_{fe}	Effective tensile stress in FRP sheet/strip in the direction of the principal fibers
f_{fed}	Design effective strength of the FRP shear strengthening
f_{frp}	Tensile strength of FRP in the main fiber direction [Chen and Teng, 2003 a and b]
$f_{frp,\,ed}$	Average/effective design stress of FRP intersected by shear crack at beam failure
f_{fu}	FRP ultimate tensile strength
f_{py}	Yield strength of strengthening material [Sim et al., 2005]
f_y, f_{vy}, F_y, f_{sy}	Yield strength of steel reinforcement
h	Height of RC/PC member
h_{frp}, $h_{frp,e}$	Effective FRP height
h_j	Depth of U-jacket strengthening [Al-Sulaimani et al., 1994]
h_s	Depth of each FRP strip [Al-Sulaimani et al., 1994]
h_v	Effective depth of the concrete beam [Malek and Saadatmanesh, 1998]
h_w	Height of web [Monti and Liotta, 2005]
h_w	Height of shear wing strengthening [Al-Sulaimani et al., 1994]
k	Experimentally determined factor [Deniaud and Cheng, 2001, 2004]
k_a	Coefficient describing anchorage considerations [Deniaud and Cheng, 2001, 2004]
k_b	Covering/scale coefficient
k_e	Integer describing number of debonding ends
L	Girder span length
l_b	Available bond length of FRP
L_e, L_{eff}, L_{fe}, l_e	Effective bond length
l_{eq}	Bonded length projected vertically that would be necessary if the fabric strain was uniform
$L_{\max}$	Maximum bond length
n	Number of FRP plies
n	Ratio of elastic modulus of FRP to elastic modulus of transverse steel (E_f/E_s) [Chaallal et al., 2002]
n	Number of spaces between stirrups [Deniaud and Cheng, 2001, 2004]
n_s	Total number of stirrups crossing concrete shear plane
p_f	FRP spacing measured orthogonal to the FRP orientation [Monti and Liotta, 2005]
$\overline{Q}_{12}$, $\overline{Q}_{13}$, $\overline{Q}_{22}$, $\overline{Q}_{23}$	Stiffness elements of FRP
R	Ratio of effective stress/strain in the FRP sheet to its ultimate strength/strain
R^*	Additional reduction factor for debonding failures of beams with steel web reinforcement [Pellegrino and Modena, 2002]
r_c	Corner rounding radius of concrete section for which FRP is wrapped
R_{ck}	Concrete characteristic cubic strength
R_L	Remaining bonded width over initial width ratio [Deniaud and Cheng, 2001, 2004]

S	Girder spacing
s	Spacing of stirrups
s_f, s_{frp}	Spacing of FRP strips
s_f	FRP slip at debonding [Monti and Liotta, 2005]
$s_{f,\max}$	Maximum spacing limitation for FRP strips
s_{xe}	Crack spacing parameter
t, t_f, t_{frp}	FRP thickness
t	Spacing of strengthening material [Sim et al., 2005]
T_{FRP}	Tension force in FRP
t_p	Nominal thickness of FRP sheet or bonded plate
t_s	Width of each FRP strip
T_v	Tension force in stirrups
V	Shear force
V_c	Shear contribution of concrete
V_{cy}	Concrete contribution to shear resistance corresponding with yielding of the stirrups along the primary shear crack
V_{cu}	Concrete contribution to shear resistance corresponding with the ultimate (maximum) load carried by the girder
$V_{\exp}$	Experimentally measured ultimate shear strength
V_f, V_{fd}, $V_{f,\max}$, $V_{f,\max}$, V_{frp}	Shear contribution of FRP
V_{FE}	Analytically (Finite Element) predicted ultimate shear strength
$V_{f,model}$	FRP contribution to shear resistance predicted by analytical models
vfnr	Relationship developed for the case of less than full anchorage such that debonding or other non-rupture failures are expected
vfr	Relationship developed for the case of full anchorage such that FRP rupture failure is expected
$V_{frp,d}$	Contribution of external FRP reinforcement (design value) [Triantafillou, 1998]
$V_{f,test}$	Experimentally measured shear strength of a test beam with FRP reinforcement minus the experimentally measured shear strength of the corresponding control beam without FRP reinforcement
V_{fy}	FRP contribution to shear resistance corresponding with yielding of the stirrups along the primary shear crack
V_{fu}	FRP contribution to shear resistance corresponding with the ultimate (maximum) load carried by the girder
V_n	Total shear capacity
$V_{n,norm}$	Normalized shear strength
$V_{n,test}$	Experimentally measured shear strength of a beam
V_P	Fiber glass plate component of shear capacity [Al-Sulaimani et al., 1994]
V_r	Total shear resistance [Deniaud and Cheng, 2001, 2004]
$V_{Rd,f}$	Shear carried by FRP [Monti and Liotta, 2005]
V_s, V_{se}	Shear contribution of stirrups
V_{sy}	Transverse steel (stirrup) contribution to shear resistance corresponding with yielding of the stirrups along the primary shear crack

V_{su}	Transverse steel (stirrup) contribution to shear resistance corresponding with the ultimate (maximum) load carried by the girder
w_f, w_{frp}	Width of FRP strip
w_{fe}	Effective width of FRP strip
Z	Limit state function
z	Length of a vertical tension tie
z_b	Co-ordinate of lower edge of effective FRP bonded to the sides of a beam
$z_{rid,eq}$	Vertically projected length of the FRP strip, minus the effective bond length where bond is building up, plus a bonded length that would be necessary if the FRP stress was uniform under the debonding slip
z_t	Co-ordinate of upper edge of effective FRP bonded to the sides of a beam
α	Angle of inclination of transverse steel reinforcement to longitudinal axis of beam
α	Reduction factor [Triantafillou and Antonopoulos, 2000]
α	Crack inclination angle [Carolin and Taljsten, 2005]
α	Angle between principal direction of FRP sheets and the longitudinal axis of the beam [Deniaud and Cheng, 2001, 2004]
α	Strength efficiency factor [Sim et al., 2005]
α_f	Angle between principal direction of FRP sheets and the longitudinal axis of the beam [Hutchinson and Rizkalla, 1999]
α_{MF}	Random variable for uncertainties in material and fabrication tolerances
β	Angle of inclination of FRP fibers to longitudinal axis of member
β	Factor relating effect of longitudinal strain on the shear capacity of concrete, as indicated by the ability of diagonally cracked concrete to transmit tension [AASHTO LRFD, 2008]
β_L	Bond length coefficient
β_r	Reliability index
$\beta_{r,target}$	Reliability index targeted by most AASHTO calibration studies
β_w	FRP strip width coefficient
ε_1, ε_2	Strains in the principal 1–2 directions
ε_{bond}	Maximum allowable strain without achieving anchor failure [Carolin and Taljsten, 2005]
$\varepsilon_{c\ max}$	Maximum allowable strain to achieve concrete contribution
ε_{cr}	Critical FRP strain
$\varepsilon_{f,ave}$	Average strain in FRP at failure [Hutchinson and Rizkalla, 1999]
ε_{fe}, $\varepsilon_{f,e}$, $\varepsilon_{frp,e}$, ε_{eff}	Effective tensile strain of FRP
$\varepsilon_{fk,e}$	Characteristic effective FRP strain in principal fiber direction [Triantafillou and Antonopoulos, 2000]
$\varepsilon_{f,e,A}$	Effective FRP strain in principal fiber direction—ACI code format [Triantafillou and Antonopoulos, 2000]
$\varepsilon_{f\ \max}$, $\varepsilon_{f,\ \max}$	Maximum strain in FRP sheet
ε_{fu}	Ultimate tensile strain of FRP
$\varepsilon_f(y)$	Strain in FRP fibers at height y [Carolin and Taljsten, 2005]

ε_{max}	Maximum or limiting value of FRP strain
ε_{max}	Maximum FRP strain over remaining bonded width [Deniaud and Cheng, 2001, 2004]
$\varepsilon_{max,A}$	Limiting value of effective FRP strain—ACI code format [Triantafillou and Antonopoulos, 2000]
ε_s	Tensile strain in cracked concrete in direction of tension tie
ε_{se}	Effective stirrup strain at failure [Hutchinson and Rizkalla, 1999]
ε_{sy}, ε_y	Yield strain of steel stirrups
ε_{ultFRP}	Ultimate FRP strain [Deniaud and Cheng, 2001, 2004]
$\varepsilon\nu_{cu}$	Ultimate vertical tensile strain of the concrete taken as 0.005 [Chajes et al., 1995]
$\overline{\varepsilon}_z$	Normalized strain in FRP [Chen and Teng, 2003b]
$\overline{\varepsilon}_{z,max}$	Maximum normalized strain in FRP [Chen and Teng, 2003 b]
ϕ_f	Shear strength reduction factor for FRP
ϕ_R	Coefficient accounting for the effects of sheets wrapped around a corner
γ_f, γ_{frp}, γ_{Rd}	Partial safety factor for FRP
γ_{fs}	The ratio of the vertical component of average strain in the FRP sheets to the average strain in the steel stirrups
$\gamma_{f,d}$	Partial safety factor depending on the FRP application accuracy
Γ_{Fk}	Specific fracture energy of the FRP-concrete bond interface
η	Average fiber utilization (effectiveness) factor
η_{GDF}	Random variable for girder distribution factor
λ	Shear span-to-effective depth ratio
λ	Normalized maximum bond length of FRP = L_{max}/L_e [Chen and Teng, 2003a]
λ_{frp}	Normalized FRP bond length = L_{max}/L_e [Cao et al., 2005]
ν	Constant that represents the contribution of compressive strength of concrete
θ, θ_c	Shear crack angle or angle of diagonal compression
θ	Angle between the principal tensile stress and the fiber direction [Carolin and Taljsten, 2005]
θ_f	Shear plane angle in flange
θ_w	Shear plane angle in web
ξ_P	Random variable for analysis model accuracy
ρ_f, ρ_{frp}	FRP reinforcement ratio = $\dfrac{A_f}{b_v s_f} = \dfrac{2n_f t_f w_f}{b_v s_f}$ ($w_f = s_f = 1.0$ for continuous wraps)
ρ_f	FRP reinforcement ratio = (A_f per unit length/bd) = $2t_f/bd$ [Chaallal et al., 2002]
ρ_s	Shear steel reinforcement ratio = (A_v per unit length/bd) = A_v/sbd [Chaallal et al., 2002]
$\rho_{s,f}$	Stiffness ratio between the transverse steel shear reinforcement and FRP shear reinforcement [Pellegrino and Modena, 2002]

ρ_{tot}	Total shear reinforcement ratio [Chaallal et al., 2002]
ρ_v	Transverse steel reinforcement ratio $= \frac{A_v}{b_v s}$
σ_{cu}	Concrete compressive strength
$\sigma_{frp,\max}$	Maximum stress in FRP intersected by shear crack [Chen and Teng, 2003b]
$\sigma_{frp,\max,d}$	Maximum stress in FRP intersected by shear crack for design [Chen and Teng, 2003a]
$\sigma_{frp,z}$	Stress in the FRP at the ultimate limit state at the location where the intersecting critical shear crack is at a coordinate z [Chen and Teng, 2003a]
τ	Shear stress
τ_{ave}	Average shear stress
$\tau_{\max}$	Ultimate direct bond shear strength between FRP and concrete
τ_{ult}	Interface shear strength between concrete and fiberglass plates [Al-Sulaimani et al., 1994]
ζ	Coordinate ratio of the upper edge to the lower edge of the effective FRP = z_t/z_b
ζ_{DC}	Random variable for component dead load
ζ_{LL+IM}	Random variable for highway live load including impact loads
ζ_{WS}	Random variable for wearing surface dead load

References

AASHTO (2008), *AASHTO LRFD Bridge Design Specifications,* 4th edition, Washington, DC.

ACI-ASCE Committee 445 (1998), "Recent Approaches to Shear Design of Structural Concrete," *Journal of Structural Engineering,* Vol. 124, No. 12, pp. 1375–1417.

ACI Committee 318 (1999), *Building Code Requirements for Structural Concrete and Commentary (ACI 318-99),* Farmington Hills, MI.

ACI Committee 318 (2008), *Building Code Requirements for Structural Concrete and Commentary (ACI 318-08),* Farmington Hills, MI.

ACI Committee 440 (2002), *Guide for the Design and Construction of Externally Bonded FRP Systems for Strengthening Concrete Structures (ACI 440.2R-02),* Farmington Hills, MI.

ACI Committee 440 (2008), *Guide for the Design and Construction of Externally Bonded FRP Systems for Strengthening Concrete Structures (ACI 440.2R-08),* Farmington Hills, MI.

Adhikary, B. B., Mutsuyoshi, H., and Ashraf, M. (2004), "Shear Strengthening of Reinforced Concrete Beams Using Fiber-Reinforced Polymer Sheets with Bonded Anchorage," *ACI Structural Journal,* Vol. 101, No. 5, pp. 660–668.

Al-Sulaimani, G. J., Shariff, A., Basanbul, I. A., Baluch, M. H, and Ghaleb, B. N. (1994), "Shear Repair of Reinforced Concrete by Fiber Glass Plate Bonding," *ACI Structural Journal,* Vol. 91, No. 4, pp. 458–464.

Alrousan, R. Z., Issa, M. A. (2009), "Size Effect of Reinforced Concrete Beams on Shear Contribution of CFRP Composites," *Proceedings,* 9th International RILEM Symposium on Non-Metallic (FRP) Reinforcement for Concrete Structures (FRPRCS-9), Sidney, Australia, 4 pp.

Araki, N., Matsuzaki, Y., Nakano, K., Kataoka, T., and Fukuyama, H. (1997), "Shear Capacity of Retrofitted RC Members with Continuous Fiber Sheets," *Proceedings,* 3rd International RILEM Symposium on Non-Metallic (FRP) Reinforcement for Concrete Structures (FRPRCS-3), Sapporo, Japan, pp. 515–522.

Arteaga, A., Alzate, A., De Diego, A., Gutierrez, J. P., Lopez, C., Perera, R., and Barchin, M. (2009), "Experimental Study on FRP Shear Strengthened Full-Scale Concrete Beams," *Proceedings,* 9th International RILEM Symposium on Non-Metalic (FRP) Reinforcement for Concrete Structures (FRPRCS-9), Sidney, Australia, 4 pp.

Barros, J. A. O., and Dias, S. J. E. (2006), "Near Surface Mounted CFRP Laminates for Shear Strengthening of Concrete Beams," *Cement & Concrete Composites,* Vol. 28, No. 3, pp. 276–292.

Beber, A. J. (2003), "Comportamento Estrutural de Vigas de Concreto Armado Reforcadas com Compositos de Fibra de Carbono," Ph.D. Thesis, Universidade Federal do Rio Grande do Sul, Porto Alegre, Brasil.

Ben Ouezdou, M., Bae, S., and Belarbi, A. (2008), "Effective Bond Length of Externally Bonded FRP Sheets," *Proceedings,* 4th International Conference on FRP Composites in Civil Engineering (CICE-2008), Zurich, Switzerland.

Berset, J. D. (1992), "Strengthening of Reinforced Concrete Beams for Shear Using FRP Composites," M.S. Thesis, Department of Civil and Environmental Engineering, MIT, Boston, MA, USA.

Bousselham, A., and Chaallal, O. (2004), "Shear Strengthening Reinforced Concrete Beams with Fiber-Reinforced Polymer: Assessment of Influencing Parameters and Required Research," *ACI Structural Journal,* Vol. 101, No. 2, pp. 219–227.

Bousselham, A., and Chaallal, O. (2006a), "Behavior of Reinforced Concrete T-Beams Strengthened in Shear with Carbon Fiber-Reinforced Polymer—An Experimental Study," *ACI Structural Journal,* Vol. 103, No. 3, pp. 339–347.

Bousselham, A., and Chaallal, O. (2006b), "Effect of Transverse Steel and Shear Span on the Performance of RC Beams Strengthened in Shear with CFRP," *Composites Part B: Engineering,* Vol. 37, No. 1, pp. 37–46.

Breña, S. F., and Gussenhoven, R. (2005), "Fatigue Behaviour of Reinforced Concrete Beams Strengthened with Different FRP Laminate Configurations," *Proceedings,* 7th International RILEM Symposium on Non-Metallic (FRP) Reinforcement for Concrete Structures (FRPRCS-7), Kansas City, Missouri.

Busel, J., and Barno, D. S. (1995), "FRP Composites in Construction Application: A Profile in Progress," Report, SPI Composites Institute, New York, NY.

CAN/CSA A23.3-94 (1994), *Design of Concrete Structures for Buildings,* Canadian Standards Association, Rexdale, Ontario, Canada.

CAN/CSA S6-06 (2006), *Canadian Highway Bridge Design Code,* Canadian Standard Association, Rexdale, Ontario, Canada.

CAN/CSA S806-02 (2002), *Design and Construction of Building Components with Fiber-Reinforced Polymer,* Canadian Standard Association, Rexdale, Ontario, Canada.

Cao, S. Y., Chen, J. F., Teng, J. G., Hao, Z., and Chen, J. (2005), "Debonding in RC Beams Strengthened with Complete FRP Wraps," *Journal of Composites for Construction,* Vol. 9, No. 5, pp. 417–428.

Carolin, A., and Taljsten, B. (2005a), "Experimental Study of Strengthening for Increased Shear Bearing Capacity," *Journal of Composites for Construction,* Vol. 9, No. 6, pp. 488–496.

Carolin, A., and Taljsten, B. (2005b), "Theoretical Study of Strengthening for Increased Shear Bearing Capacity," *Journal of Composites for Construction,* Vol. 9, No. 6, pp. 497–506.

Chaallal, O., Nollet, M. J., and Perraton, D. (1998), "Shear Strengthening of RC Beams by Externally Bonded Side CFRP Strips," *Journal of Composites for Construction,* Vol. 2, No. 2, pp. 111–113.

Chaallal, O., Shahawy, M., and Hassan, M. (2002), "Performance of Reinforced Concrete T-Girders Strengthened in Shear with Carbon Fiber Reinforced Polymer Fabrics," *ACI Structural Journal,* Vol. 99, No. 3, pp. 335–343.

Chaallal, O., Boussaha, F., Bousselham, A., Nollet, M. J., Masmoudi, R., and Benmokrane, B. (2009), "Fatigue Behaviour of Reinforced Concrete Beams Strengthened in Shear with Advanced Composite," *Proceedings,* 9th International RILEM Symposium on Non-Metalic (FRP) Reinforcement for Concrete Structures (FRPRCS-9), Sidney, Australia, 4 pp.

Chajes, M. J., Jansuska, T. F., Mertz, D. R., Thomson, T. A., and Finch, W. W. (1995), "Shear Strength of RC Beams using Externally Applied Composite Fabrics," *ACI Structural Journal,* Vol. 92, No. 3, pp. 295–303.

Chen, J. F., and Teng, J. G. (2001), "Anchorage Strength Models for FRP and Steel Plates Bonded to Concrete," *Journal of Structural Engineering,* Vol. 127, No. 7, pp. 784–791.

Chen, J. F., and Teng, J. G. (2003a), "Shear Capacity of FRP Strengthened RC Beams: FRP Debonding," *Construction Building Materials,* Vol. 17, No. 1, pp. 27–41.

Chen, J. F., and Teng, J. G. (2003b), "Shear Capacity of Fiber-Reinforced Polymer-Strengthened Reinforced Concrete Beams: Fiber Reinforced Polymer Rupture," *Journal of Structural Engineering,* Vol. 129, No. 5, pp. 615–625.

Concrete Society (2004), *Design Guidance on Strengthening Concrete Structures using Fibre Composite Materials: Technical Report 55,* Second Edition, The Concrete Society, London, UK.

Czaderski, C. (2002), "Shear Strengthening with Prefabricated CFRP L-Shaped plates. Test Beams S1 to S6," EMPA. Report No. 116/7, Switzerland.

De Lorenzis, Miller, B., and Nanni, A. (2001), "Bond of Fiber-Reinforced Polymer Laminates to Concrete," *ACI Materials Journal,* Vol. 98, No. 3, pp. 256–264.

De Lorenzis, L. (2002), "Strengthening of RC Structures with Near-Surface Mounted FRP Rods," Ph.D. Thesis, Department of Innovation Engineering, University of Lecce, Lecce, Italy, 2002.

Deniaud, C., and Cheng, J. J. R. (2001), "Shear Behavior of Reinforced Concrete T-Beams with Externally Bonded Fiber-Reinforced Polymer Sheets," *ACI Structural Journal,* Vol. 98, No. 3, pp. 386–394.

Deniaud, C., and Cheng, J. J. R. (2004), "Simplified Shear Design Method for Concrete Beams Strengthened with Fiber Reinforced Polymer Sheets," *Journal of Composites for Construction,* Vol. 8, No. 5, pp. 425–433.

Diagana, C., Li, A., Gedalia, B., and Delmas, Y. (2003), "Shear Strengthening Effectiveness with CFF Strips," *Engineering Structures,* Elsevier, Vol. 25, No. 4, pp. 507–516.

Dornsife, R. (2007), "Ebey Island Viaduct Bridge: Pilot Project to Comprehensive Carbon Fiber Rehabilitation," *Proceedings,* 24th International Bridge Conference, Pittsburgh, Pennsylvania, 6 pp.

Ekenel, M., and Myers, J. J. (2005), "Effect of Environmental Conditioning & Sustained Loading on the Fatigue Performance of RC Beams Strengthened with Bonded CFRP Fabrics," *Proceedings,* 7th International RILEM Symposium on Non-Metallic (FRP) Reinforcement for Concrete Structures (FRPRCS-7), Kansas City, Missouri, USA, pp. 1571–1592.

Eshwar, N., Nanni, A., and Ibell, T. (2003), "CFRP Strengthening of Concrete Bridges with Curved Soffits," *Proceedings,* Proceedings of the International Conference on Structural Faults and Repairs, Montreal, Quebec.

Eshwar, N., Nanni, A., and Ibell, T. J. (2008), "Performance of Two Anchor Systems of Externally Bonded Fiber-Reinforced Polymer Laminates," *ACI Materials Journal,* Vol. 105, No. 1, pp. 72–80.

Eurocode 8-3 (2004), "Design of Structures for Earthquake Resistance; Part 3: Assessment and Retrofitting of Buildings," *European Standard,* EN 1998-3m Brussels, Belgium.

fib-TG9.3 (2001), "Design and Use of Externally Bonded Fiber Polymer Reinforcement (FRP EBR) for Reinforced Concrete Structures," Technical Report Prepared by EBR Task Group 9.3, Bulletin 14, Lausanne, Swiss.

Foster, S. J., and Khomwan, N. (2005), "Determination of Bond Stress versus Slip for Externally Bonded FRP from Standardized Bond Strength Tests," *Proceedings,* International Symposium on Bond Behavior of FRP Structures, Hong Kong, China, pp. 85–90.

Funakawa, I., Shimono, K., Watanabe, T., Asada, S., and Ushijima, S. (1997), "Experimental Study on Shear Strengthening with Continuous Fiber Reinforcement Sheet and Methyl Methacrylate Resin," *Proceedings,* 3rd International RILEM Symposium on Non-Metallic (FRP) Reinforcement for Concrete Structures (FRPRCS-3), Sapporo, Japan, pp. 491–498.

Gamino, A. L., Sousa, J. L. A. O., and Bittencourt, T. N. (2009), "Application of Carbon Fiber Reinforced Polymer in Strengthening to Shear R/C T Beams," *Proceedings,* 9th International RILEM Symposium on Non-Metalic (FRP) Reinforcement for Concrete Structures (FRPRCS-9), Sidney, Australia, 4 pp.

Hag-Elsafi, O., Kunin, J., Alampalli, S., and Conway, T. (2001a), "Strengthening of Route 378 Bridge Over Wynantskill Creek in New York Using FRP Laminates," New York State Department of Transportation, Special Report 135.

Hag-Elsafi, O., Kunin, J., and Alampalli, S. (2001b), "In-Service Evaluation of a Concrete Bridge FRP Strengthening System," New York State Department of Transportation, Special Report 139.

Hassan Dirar, S. M. O., Hoult, N. A., Morley, C. T., and Lees, J. M. (2006), "Shear Strengthening of Pre-cracked Reinforced Concrete Beams Using CFRP Straps," *Proceedings,* 2nd International Congress, Fédération Internationale de Béton (FIB), Naples, Italy, ID 10-70.

Hsu, C. T. T., Punurai, W., and Zhang, Z. (2003), "Flexural and Shear Strengthening of RC Beams using Carbon Fiber Reinforced Polymer Laminate," *ACI SP-211-5,* Farmington Hills, MI, pp. 89–113.

Hutchinson, R. L., and Rizkalla, S. H. (1999), "Shear Strengthening of AASHTO Bridge Girders Using Carbon Fiber Reinforced Polymer Sheets," *ACI Special Publications (SP-188),* Vol. 188, pp. 945–958.

Hutchinson, R., Tadros, G., Kroman, J., Rizkalla, S. (2003), "Use of Externally Bonded FRP Systems for Rehabilitation of Bridges in Western Canada. In: Field Applications of FRP Reinforcement: Case Studies," ACI Special Publication (SP-215-13), pp. 239–248.

ISIS Design Manual 4 (2001), *Strengthening Reinforced Concrete Structures with Externally-Bonded Fiber Reinforced Polymers,* Intelligent Sensing for Innovative Structures, Winnipeg, Canada, 2001.

JCI (2003), "International Symposium on Latest Achievement of Technology and Research on Retrofitting Concrete Structures," *Proceedings,* Proceedings and Technical Report on JCI Technical Committee, Sapporo, Japan.

JSCE (2001), *Recommendations for Upgrading of Concrete Structures with Use of Continuous Fiber Sheets,* Concrete Engineering Series 41, Japan Society of Civil Engineers, Tokyo, Japan.

Kachlakev, D. I, and Barnes, W. A. (1999), "Flexural and Shear Performance of Concrete Beams Strengthened with Fiber Reinforced Polymer Laminates," *Proceedings,* 4th International RILEM Symposium on Non-Metallic (FRP) Reinforcement for Concrete Structures (FRPRCS-4), Baltimore, Maryland, pp. 959–972.

Kamiharako, A., Maruyama, K., Takada, K., and Shimomura, T. (1997), "Evaluation of Shear Contribution of FRP Sheets Attached to Concrete Beams," *Non-Metallic (FRP) Reinforcement for Concrete Structures,* Vol. 1, pp. 467–474.

Kanakubo, T., Furuta, T., and Fukuyama, H. (2003), "Bond Strength between Fiber-Reinforced Polymer Laminates and Concrete," *Proceedings,* 6th International RILEM Symposium on Non-Metallic (FRP) Reinforcement for Concrete Structures (FRPRCS-6), World Scientific, Singapore, pp. 134–143.

Khalifa, A., Gold, W., Nanni, A., and Abdel Aziz, M. I. (1998), "Contribution of Externally Bonded FRP to Shear Capacity of RC Flexural Members," *Journal of Composites for Construction,* Vol. 2, No. 4, pp. 195–202.

Khalifa, A., Tumialan, G., Nanni, A., and Belarbi, A. (1999), "Shear Strengthening of Continuous Reinforced Concrete Beams using Externally Bonded Carbon Fiber Reinforced Polymer Sheets," *Proceedings,* 4th International RILEM Symposium on Non-Metallic (FRP) Reinforcement for Concrete Structures (FRPRCS-4), Baltimore, Maryland, pp. 995–1008.

Khalifa, A., Belarbi, A., and Nanni, A. (2000), "Shear Performance of RC Members Strengthened with Externally Bonded FRP Wraps," *Proceedings,* 12th World Conference on Earthquake Engineering, Auckland, New Zealand.

Khalifa, A., and Nanni, A. (2000), "Improving Shear Capacity of Existing RC T-Section Beams using CFRP Composites," *Cement & Concrete Composites,* Vol. 22, pp. 165–174.

Khalifa, A., and Nanni, A. (2002), "Rehabilitation of Rectangular Simply Supported RC Beams using CFRP Composites," *Construction and Building Materials,* Vol. 16, No. 3, pp. 135–146.

Lees, J. M., and Kesse, G. (2007), "Experimental Behavior of Reinforced Concrete Beams Strengthened with Prestressed CFRP Shear Straps," *Journal of Composites for Construction,* Vol. 11, No. 4, pp. 375–383.

Leung, C., Chen, Z., Lee, S., Mandy, N., Ming, X., and Tang, J. (2007), "Effect of Size on the Failure of Geometrically Similar Concrete Beams Strengthened in Shear with FRP Strips," *Journal of Composites for Construction,* Vol. 11, No. 5, pp. 487–496.

Li, A., Assih, J., and Delmas, Y. (2001a), "Shear Strengthening of RC Beams with Externally Bonded CFRP Sheets," *Journal of Structural Engineering,* Vol. 127, No. 4, pp. 374–380.

Li, A., Diagana, C., and Delmas, Y. (2001b), "CFRP Contribution to Shear Capacity of Strengthened RC Beams," *Engineering Structures,* Vol. 23, pp. 1212–1220.

Li, A., Diagana, C., and Delmas Y. (2002), "Shear Strengthening Effect by Bonded Composite Fabrics on RC Beams," *Composites Part B: Engineering,* Vol. 33, No. 3, pp. 225–239.

Lopez-Anido, R., Kwon, S. C., Dutta, P. K., and Kim, Y. H. (2003), "Comparison of the Fatigue Behaviors of FRP Bridge Decks and Reinforced Concrete Conventional Decks under Extreme Environmental Conditions," *KSME International Journal,* Vol. 17, No. 1, pp. 1–10.

Maeda, T., Asano, Y., and Sato, Y. (1997), "A Study on Bond Mechanism of Carbon Fiber Sheet," *Proceedings,* 3rd International RILEM Symposium on Non-Metallic (FRP) Reinforcement for Concrete Structures (FRPRCS-3), Sapporo, Japan, pp. 279–286.

Malek, A. M., and Saadatmanesh, H. (1998), "Ultimate Shear Capacity of Reinforced Concrete Beams Strengthened with Web-Bonded Fiber-Reinforced Plastic Plates," *ACI Structural Journal,* Vol. 95, No. 4, pp. 391–399.

Matthys, S. (2000), "Structural Behavior and Design of Concrete Members Strengthened with Externally Bonded FRP Reinforcement," Ph.D. Thesis, Department of Structural Engineering, University of Ghent, Belgium.

Micelli, F., Annaiah, R., and Nanni, A. (2002), "Strengthening of Short Shear Span RC-T Joists with FRP Composites," *Journal of Composites for Construction,* Vol. 6, No. 4, pp. 264–271.

Miller, B., and Nanni, A. (1999), "Bond between CFRP Sheets and Concrete," *Proceedings,* ASCE 5th Materials Congress, Cincinnati, OH, USA, pp 240–247.

Mitsui, Y., Murakami, K., Takeda, K., and Sakai, H. (1998), "A Study on Shear Reinforcement of Reinforced Concrete Beams Externally Bonded with Carbon Fiber Sheets," *Composites Interfaces,* Vol. 5, No. 4, pp. 285–295.

Miyajima, H., Kosa, K., Tasaki, K., and Matsumoto, S. (2005), "Shear Strengthening of RC Beams Using Carbon Fiber Sheets and its Resistance Mechanism," *Proceedings,* 5th Workshop on Safety and Stability of Infrastructures against Environmental Impacts, Manila, Philippines, pp. 114–125.

Miyauchi, K., Inoue, S., Nishibayashi, S., and Tanka, Y. (1997), "Shear Behavior of Reinforced Concrete Beam Strengthened with CFRP Sheet," *Transactions of the Japan Concrete Institute,* Vol. 19, pp. 97–104.

Monti, G., and Liotta, M. A. (2005), "FRP-Strengthening in Shear: Tests and Design Equations," *Proceedings,* 7th International RILEM Symposium on Non-Metallic (FRP) Reinforcement for Concrete Structures (FRPRCS-7), Kansas City, Missouri, pp. 543–562.

Muszynski, L. C., and Sierakowski, R. L. (1996), "Fatigue Strength of Externally Reinforced Concrete Beams," *Proceedings,* Materials for the New Millennium, Materials Engineering Conference, Washington, DC, Vol. 2, pp. 648–656.

Nakaba, K., Kanakubo, T., Furuta, T., and Yoshizawa, H. (2001), "Bond Behavior between Fiber-Reinforced Polymer Laminates and Concrete," *ACI Structural Journal,* Vol. 98, No. 3, pp. 359–367.

Neubauer, U., and Rostasy, F. S. (1997), "Design Aspects of Concrete Structures Strengthened with Externally Bonded CFRP Plates," *Proceedings,* 7th International Conference on Structural Faults and Repairs, pp. 109–118.

Niedermeier, R. (1996), "Stellungnahme zur Richtlinie fur das Verkleben von Beton-Bauteilen durch Ankleben von Stahllaschen—Entwurf Marz 1996," Schreiben Nr 1390 vom 30.10.1996 des Lehrstuhls fur Massivbau, TU Munchen, Germany.

Niemitz, C. W. (2008), "Anchorage of Carbon Fiber Reinforced Polymers to Reinforced Concrete in Shear Applications," M.S. Thesis, Department of Civil and Environmental Engineering, University of Massachusetts-Amherst.

Niu, H., and Wu, Z. S. (2000), "Study on Debonding Failure Load of RC Beams Strengthened with FRP Sheets," *Journal of Structural Engineering,* Vol. 46A, pp. 1431–1441.

Nowak, A. S. (1999), "Calibration of LRFD Bridge Design Code," NCHRP Report No. 368, Transportation Research Board, Washington, DC.

Nowak, A. S., and Szerszen, M. M. (2003), "Calibration of Design Code for Buildings (ACI 318): Part 1—Statistical Models for Resistance," *ACI Structural Journal,* Vol. 100, No. 3, pp. 377–382.

Ohuchi, H., Ohno, S., Katsumata, H., Kobatake, Y., Meta, T., Yamagata, K., Inokuma, Y., and Ogata, N. (1994), "Seismic Strengthening Design Technique for Existing Bridge Columns with CFRP," *Proceedings,* Proceedings of the 2nd International Workshop on Seismic Design and Retrofitting of Reinforced Concrete Bridges, Queenstown, New Zealand, pp. 495–514.

Orton, S. L. (2007), "Development of a CFRP System to Provide Continuity in Existing Reinforced Concrete Buildings Vulnerable to Progressive Collapse," Dissertation, Department of Civil, Architectural, and Environmental Engineering, University of Austin—Texas, Austin, Texas.

Papakonstantinou, C. G., Petrou, M. F. and Harries, K. A. (2001), "Fatigue of Reinforced Concrete Beams Strengthened with GFRP Sheets," *ASCE Journal of Composites in Construction,* Vol. 5, No. 4, pp. 246–253.

Park, S. Y., Naaman, A. E., Lopez, M. M., and Till, R. D. (2001), "Shear strengthening effect of R/C beams using glued CFRP sheets," *Proceedings,* International Conference on FRP Composites in Civil Engineering, Hong Kong, China, pp. 669–676.

Pellegrino, C., and Modena, C. (2002), "Fiber Reinforced Polymer Shear Strengthening of Reinforced Concrete Beams with Transverse Steel Reinforcement," *Journal of Composites for Construction,* Vol. 6, No. 2, pp. 104–111.

Pellegrino, C., and Modena, C. (2006), "Fiber-Reinforced Polymer Shear Strengthening of Reinforced Concrete Beams: Experimental Study and Analytical Modeling," *ACI Structural Journal,* Vol. 103, No. 5, pp. 720–728.

Rizzo, A., and De Lorenzis, L. (2009), "Behavior and capacity of RC beams strengthened in shear with NSM FRP reinforcement," *Construction and Building Materials,* Vol. 23, pp. 1555–1567.

Sato, Y., Ueda, T., Kakuta, Y., and Tanaka, T. (1996), "Shear Reinforcing Effect of Carbon Fiber Sheet Attached to the Side of Reinforced Concrete Beams," *Proceedings,* 3rd International Conference on Advanced Composite Materials in Bridges and Structures, Montreal, Canada, pp. 621–628.

Sato, Y., Ueda, T., Kakuta, Y., and Ono, S. (1997), "Ultimate Shear Capacity of Reinforced Concrete Beams with Carbon Fiber Sheet," *Proceedings,* 3rd International RILEM Symposium on Non-Metallic (FRP) Reinforcement for Concrete Structures (FRPRCS-3), Sapporo, Japan, pp. 499–506.

Sato, Y., Asano, Y., and Ueda, T. (2000), "Fundamental Study on Bond Mechanism of Carbon Fiber Sheet," *JSCE Journal of Material, Concrete Structures, and Pavements,* Vol. 47, No. 648, pp. 71–87.

Schnerch, A. (2001), "Shear Behavior of Large-Scale Concrete Beams Strengthened with Fibre Reinforced Polymer (FRP) Sheets," M.S. Thesis, Department of Civil Engineering, University of Manitoba.

Schuman, P. M. (2004), "Mechanical Anchorage for Shear Rehabilitation of Reinforced Concrete Structures with FRP: An Appropriate Design Approach," Ph.D. Thesis, Department of Structural Engineering, University of California, UCSD, San Diego, CA.

Senthilnath, P., Belarbi, A., and Myers, J. J. (2001), "Performance of CFRP Strengthened Reinforced Concrete (RC) Beams in the Presence of Delaminations and Lap Splices Under Fatigue Loading," *Proceedings,* International Conference on Composites in Construction (CCC-2001), Porto, Portugal, pp. 323–328.

Sim, J., Kim, G., Park, C., and Ju, M. (2005), "Shear Strengthening Effects with Varying Types of FRP Materials and Strengthening Methods," *Proceedings,* 7th International RILEM Symposium on Non-Metallic (FRP) Reinforcement for Concrete Structures (FRPRCS-7), Kansas City, Missouri, USA, pp. 1665–1680.

Taerwe, L., Khalil, H., and Matthys, S. (1997), "Behavior of RC Beams Strengthened in Shear by External CFRP Sheets," *Proceedings,* 3rd International RILEM Symposium on Non-Metallic (FRP) Reinforcement for Concrete Structures (FRPRCS-3), Sapporo, Japan, pp. 483–490.

Taljsten, B. (1997), "Strengthening of Concrete Structures for Shear with Bonded CFRP Fabrics," *Proceedings,* US-Canada-Europe Workshop on Bridge Engineering, Zurich, Switzerland, pp. 67–74.

Taljsten, B. (2003), "Strengthening for Concrete Beam for Shear with CFRP Sheets," *Construction and Building Materials,* Vol. 17, No. 1, pp. 15–26.

Taljsten, B., Hejll, A., and James, G. (2007), "Carbon Fiber-Reinforced Polymer Strengthening and Monitoring of the Gröndals Bridge in Sweden," *Journal of Composites of Construction,* Vol. 11, No. 2, pp. 227–235.

Triantafillou, T. C. (1998), "Shear Strengthening of Reinforced Concrete Beams Using Epoxy-Bonded FRP Composites," *ACI Structural Journal,* Vol. 95, No. 2, pp. 107–115.

Triantafillou, T. C., and Antonopoulos, C. P. (2000), "Design of Concrete Flexural Members Strengthened in Shear with FRP," *Journal of Composites for Construction,* Vol. 4, No. 4, pp. 198–205.

Ueda, T., and Dai, J. G. (2004), "New Shear Bond Model for FRP-Concrete Interface-from Modeling to Application," *Proceedings,* 2nd International Conference on FRP Composites in Civil Engineering-CICE 2004, Adelaide, Australia, pp. 69–81.

Ueda, T., and Dai, J. (2005), "Interface Bond between FRP Sheets and Concrete Substrates: Properties, Numerical Modeling and Roles in Member Behavior," *Progress in Structural Engineering and Materials,* John Wiley & Sons Ltd., Vol. 7, No. 1, pp. 27–43.

Uji, K. (1992), "Improving the Shear Capacity of Existing Reinforced Concrete Members by Applying Carbon Sheets," *Transactions of the Japan Concrete Institute,* Vol. 14, pp. 253–266.

Umezu, K., Fujita, M., Nakai, H., and Tamaki, K. (1997), "Shear Behavior of RC Beams with Aramid Fiber Sheet," *Proceedings,* 3rd International RILEM Symposium on Non-Metallic (FRP) Reinforcement for Concrete Structures (FRPRCS-3), Sapporo, Japan, pp. 491–498.

Williams, G., and Higgins, C. (2008), "Fatigue of Diagonally Cracked RC Girders Repaired with CFRP," *Journal of Bridge Engineering,* Vol. 13, No. 1, pp. 24–33.

Xue Song, F., Jie, L., and Zhong Fan, C. (2004), "Experimental Research on Shear Strengthening of Reinforced Concrete Beams with Externally Bonded CFRP Sheets."

Yoshizawa, H., Wu, Z. S., and Yuan, H. (2000), "Study on FRP-Concrete Interface Bond Performance," *Journal of Materials, Concrete Structures and Pavements,* Vol. 49, No. 662, pp. 105–119.

Zhang, Z., and Hsu, C. T. (2005), "Shear Strengthening of Reinforced Concrete Beams Using Carbon-Fiber-Reinforced Polymer Laminates," *Journal of Composites for Construction,* Vol. 9, No. 2, pp. 158–169.

ATTACHMENT A

Recommended Changes to AASHTO LRFD Bridge Design Specifications

These proposed changes to AASHTO LRFD Bridge Design Specifications are the recommendations of the NCHRP Project 12-75 Research Team at the Missouri University of Science and Technology. These changes have not been approved by NCHRP or any AASHTO committee nor formally accepted for the AASHTO specifications.

5.2 Definitions – (only additions are shown in this section)

FRP – fiber-reinforced polymer laminate consisting of fibers (carbon, aramid, or glass) and an epoxy matrix.

5.3 Notation – (only additions and particularly relevant notations are shown)

d_v = effective shear depth as determined in Article 5.8.2.9 (in.)
d_f = effective depth of FRP shear reinforcement in Article 5.8.3.3 (in.)
f_{fe} = effective stress of FRP shear reinforcement as determined in Article 5.8.3.3 (ksi)
s = spacing of stirrups (in.)
s_f = center-to-center spacing of FRP shear reinforcement in Article 5.8.3.3 (in.)
h_f = flange thickness in Article 5.8.3.3 (in.)
α = angle of inclination of transverse steel reinforcement to longitudinal axis (°)
α_f = angle of inclination of transverse FRP reinforcement to longitudinal axis in Article 5.8.3.3 (°)
A_f = sum of area of FRP reinforcement on both faces of the web within a distance s_f in Article 5.8.3.3 (in.^{2})
V_f = shear resistance provided by externally bonded FRP shear reinforcement in Article 5.8.3.3 (kip)
E_f = modulus of elasticity of FRP reinforcement in Article 5.8.3.3 (ksi)
ε_{fe} = effective strain of FRP reinforcement in Article 5.8.3.3
ε_{fu} = failure tensile strain of FRP reinforcement in Article 5.8.3.3
R_f = strain reduction factor to account for the effectiveness of FRP strengthening in Article 5.8.3.3
ρ_f = FRP shear reinforcement ratio in Article 5.8.3.3
n_f = number of plies of FRP reinforcement in Article 5.8.3.3
t_f = thickness of one ply of FRP reinforcement in Article 5.8.3.3 (in.)
w_f = width of FRP shear reinforcement in Article 5.8.3.3 (in.)

SPECIFICATIONS **COMMENTARY**

5.8.2.6 Types of Transverse Reinforcement

Transverse reinforcement may consist of

- Steel reinforcement in the form of:
  - Stirrups making an angle not less than 45° with the longitudinal tension reinforcement;
  - Welded wire fabric reinforcement, with wires located perpendicular to the axis of the member, provided that the transverse wires are certified to undergo a minimum elongation of 4 percent, measured over a gage length of at least 4.0 in. including at least one cross wire;
  - Anchored prestressed tendons, detailed and constructed to minimize seating and time-dependent losses, which make an angle not less than 45° with the longitudinal tension reinforcement;
  - Longitudinal bars bent to provide an inclined portion making an angle of 30° or more with the longitudinal tension reinforcement and inclined to intercept potential diagonal cracks;
  - Combinations of stirrups, tendons, and bent longitudinal bars; or
  - Spirals.
- Externally bonded FRP shear reinforcement making an angle not less than 45° with the longitudinal flexural tensile reinforcement in accordance with Article 5.8.3.5 and 5.8.3.6.3 as applicable.

Transverse reinforcement shall be detailed such that the shear force between different elements or zones of a member are effectively transferred.

Torsional reinforcement shall consist of both transverse and longitudinal steel reinforcement. Longitudinal steel reinforcement shall consist of bars and/or tendons. Transverse steel reinforcement shall consist of:

- Closed stirrups perpendicular to the longitudinal axis of the member,
- A closed cage of welded wire fabric with transverse wires perpendicular to the axis of the member, or
- Spirals.

Transverse torsion reinforcement shall be made fully continuous and shall be anchored by 135° standard hooks around longitudinal reinforcement.

SPECIFICATIONS

5.8.2.7 Maximum Spacing of Transverse Reinforcement

The center-to-center spacing of the transverse steel reinforcement and the center-to-center spacing between externally bonded FRP shear reinforcement shall not exceed the maximum permitted spacing, s_{max}, determined as:

- If $v_u < 0.125 f_c'$ then
  $s_{max} = 0.8 d_v \le 24.0$ in.

- If $v_u \ge 0.125 f_c'$ then
  $s_{max} = 0.4 d_v \le 12.0$ in.

where:

v_u = the shear stress calculated in accordance with 5.8.2.9 (ksi)
d_v = effective shear depth as defined in Article 5.8.2.9 (in.)

For segmental post-tensioned concrete box girder bridges, spacing of closed stirrups or closed ties required to resist shear effects due to torsional moments shall not exceed one-half of the shortest dimension of the cross section, or 12.0 in.

5.8.2.8 Design and Detailing Requirements

Transverse steel reinforcement shall be anchored at both ends in accordance with the provisions of Article 5.11.2.6. For composite flexural members, extension of beam shear reinforcement into the deck slab may be considered when determining if the development and anchorage provisions of Article 5.11.2.6 are satisfied.

The design yield strength of nonprestressed transverse steel reinforcement shall be taken equal to the specified yield strength when the latter does not exceed 60.0 ksi. For nonprestressed transverse steel reinforcement with yield strength in excess of 60.0 ksi, the design yield strength shall be taken as the stress corresponding to a strain of 0.0035, but not to exceed 75.0 ksi. The design yield strength of prestressed transverse steel reinforcement shall be taken as the effective stress, after allowance for all prestress losses, plus 60.0 ksi, but not greater than f_{py}.

When welded wire reinforcement is used as transverse reinforcement, it shall be anchored at both ends in accordance with Article 5.11.2.6.3. No welded joints other than those required for anchorage shall be permitted.

Components of inclined flexural compression and/or flexural tension in variable depth members shall be considered when calculating shear resistance.

Externally bonded FRP shear reinforcement shall be installed to a beam using:

- Side bonding, in which the FRP is only bonded

COMMENTARY

C5.8.2.7 Maximum Spacing of Transverse Reinforcement

Sections that are highly stressed in shear require more closely spaced reinforcement to provide crack control.

C5.8.2.8

Figure C5.8.2.8-1 shows different possible configurations of the FRP when applied to a beam.

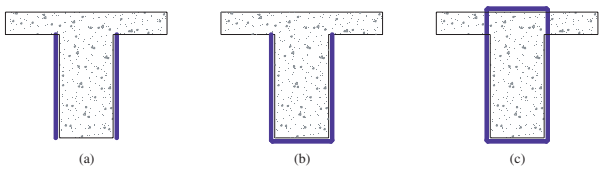

Figure C5.8.2.8-1 - Configuration of FRP Application: (a) Two-side bonding, (b) U-wrap, and (c) Complete wrap

SPECIFICATIONS

to the sides of the component;

- U-wrap, in which FRP U-jackets are bonded on both the sides and the soffit of the component; or
- Complete wrapping, in which the FRP is wrapped around the entire cross section.

The fibers in the FRP in its final position on the concrete component shall be oriented to provide the required resistance. The orientation of the fibers shall be shown on the contract documents.

Externally bonded FRP shear reinforcement may be anchored to the concrete. Mechanical anchorage systems consisting of FRP composite plates and concrete anchor bolts shall be proportioned such that the factored bearing resistance of the concrete anchor bolts used to anchor one end of a FRP strip is not less than the tensile force exerted from the FRP strip calculated on the basis of the failure tensile strain of the FRP. The use of additional horizontal strips of FRP as anchorage for FRP shear reinforcement shall not be permitted.

5.8.3.3 Nominal Shear Resistance

The nominal shear resistance, V_n, shall be determined as the lesser of:

$$V_n = V_c + V_s + V_f + V_p \qquad (5.8.3.3\text{-}1)$$

and

$$V_n = 0.25 f'_c b_v d_v + V_p \qquad (5.8.3.3\text{-}2)$$

in which:

$V_c = 0.0316 \beta \sqrt{f'_c}\, b_v d_v$, if the procedures of Articles 5.8.3.4.1 or 5.8.3.4.2 are used (5.8.3.3-3)

V_c = the lesser of V_{ci} and V_{cw}, if the procedure of Article 5.8.3.4.3 are used

$$V_s = \frac{A_v f_y d_v (\cot\theta + \cot\alpha)\sin\alpha}{s} \qquad (5.8.3.3\text{-}4)$$

$$V_f = \frac{A_f f_{fe} d_f}{s_f}(\sin\alpha_f + \cos\alpha_f) \qquad (5.8.3.3\text{-}5)$$

where:

A_f = area of FRP shear reinforcement within a distance s_f (in.^{2})

A_v = area of steel shear reinforcement (stirrups) within a distance s_v (in.^{2})

b_v = effective web width taken as the minimum web width within the depth dv as determined in Article 5.8.2.9 (in.)

COMMENTARY

The direction of the fibers relative to the direction of the stresses the FRP reinforcement is meant to resist will effect the effectiveness of the FRP reinforcement. The fibers should be oriented in the direction that maximizes the effectiveness of the FRP reinforcement.

Anchoring externally bonded FRP shear reinforcement helps reduce the potential for premature failure due to debonding. There are various types of anchorage systems available in the literature [NCHRP Report 12-75].

Examples of mechanical anchorage systems consisting of FRP composite plates and concrete anchor bolts are available in the literature [NCHRP Report 12-75].

C5.8.3.3

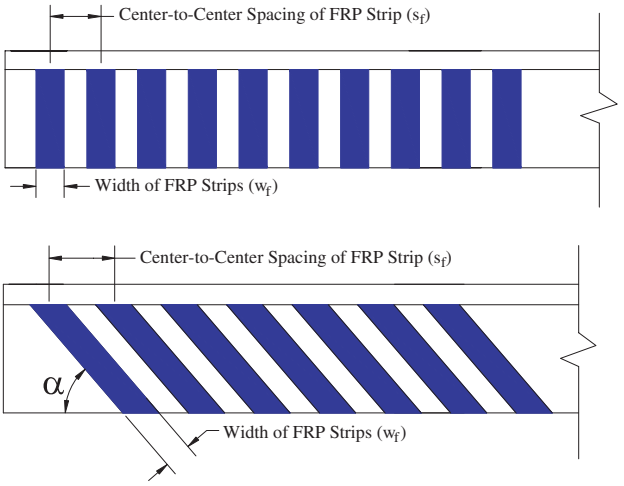

Figure C5.8.3.3-1 Illustration of the Terms s_f and w_f

SPECIFICATIONS

d_f = effective depth of FRP shear reinforcement equal to d_v for rectangular sections and d - h_f for T-sections(in.)

d_v = effective shear depth as determined in Article 5.8.2.9 (in.)

f_{fe} = effective stress of FRP shear reinforcement as determined in Article 5.8.3.3 (ksi)

h_f = flange thickness (in.)

s = spacing of stirrups (in.)

s_f = center-to-center spacing of FRP shear reinforcement (in.)

V_f = shear resistance provided by FRP shear reinforcement (kip); may only be used in conjunction with the provisions of Articles 5.8.3.4.1 and 5.8.3.4.2 when minimum steel shear reinforcement is provided or when the member depth or maximum spacing of distributed longitudinal reinforcement is less than 12 inches, and with the provisions of Article 5.8.3.4.3. V_f shall be taken as zero when $d_v/b_v > 4$

V_p = component in the direction of the applied shear of the effective prestressing force; positive if resisting the applied shear (kip)

α_f = angle of inclination of FRP transverse reinforcement to longitudinal axis (°)

β = factor indicating ability of diagonally cracked concrete to transmit tension as specified in Article 5.8.3.4.

θ = angle of inclination of diagonal compressive stresses as determined in Article 5.8.3.4 (°)

The effective stress of FRP shear reinforcement, f_{fe}, shall be determined as:

$$f_{fe} = E_f \varepsilon_{fe} \qquad (5.8.3.3\text{-}6)$$

in which

$$\varepsilon_{fe} = R_f \varepsilon_{fu} \qquad (5.8.3.3\text{-}7)$$

where:

E_f = modulus of elasticity of FRP reinforcement (ksi)

R_f = strain reduction factor to account for the effectiveness of FRP strengthening

ε_{fe} = effective strain of FRP reinforcement. it is limited to 0.012 when Eq. 5.8.3.3-9 is used.

ε_{fu} = failure tensile strain of FRP reinforcement

The strain reduction factor (R_f) shall be determined as:

- For completely wrapped or properly anchored U-wrap configurations

$$R_f = 0.088 \le 4(\rho_f E_f)^{-.67} \le 1.0 \qquad (5.8.3.3\text{-}8)$$

COMMENTARY

The application of FRP reinforcements on precast I-shaped sections with "slender webs" did not provide significant or reliable FRP contributions to shear capacity, V_f, and on occasion resulted in a decrease of strength relative to that of the member that did not have FRP shear reinforcement [NCHRP Project 12-75]. Changes in the experimental setup and girder details made to address this reduction was unsuccessful. It was concluded that the reason that the application of FRP shear reinforcements did not lead to strength gains in I-girders with slender webs was due to degradation of the diagonal compressive resistance of slender webs when stiff and well bonded FRP reinforcements are glued to the surface of these webs. While the members experiencing this web resistance degradation were all prestressed, it has been concluded that this degradation was due to the slenderness of the webs and not the effect of prestressing [NCHRP Project 12-75]. Based on an examination of strength gains as a function of the ratio of depth to web width (d/b_v), it was concluded that the shear resistance provided by FRP shear reinforcement, V_f , should be ignored for members with a web slenderness of $d/b_w > 4$ [NCHRP Project12-75].

According to the observation on the experimental database, the maximum effective strain that can be achieved in the beams failing due to debonding of FRP was 0.012.

The upper bound for the quantity $\rho_f E_f$ in Eqs. 5.8.3.3-8 and 5.8.3.3-9 is 300 ksi [NCHRP Project 12-75]. Substituting this value in the two equations results in the lower bound value of R_f shown in the two equations.

SPECIFICATIONS

COMMENTARY

- For Un-anchored U-wrap or Two-side bonding configurations

$$R_f = 0.066 \le 3(\rho_f E_f)^{-.67} \le 1.0 \qquad (5.8.3.3\text{-}9)$$

where:

ρ_f = FRP shear reinforcement ratio

The FRP shear reinforcement ratio, ρ_f, shall be determined as:

- For discrete strips

$$\rho_f = \frac{2n_f t_f w_f}{b_v s_f} \qquad (5.8.3.3\text{-}10)$$

- For continuous sheets

$$\rho_f = \frac{2n_f t_f}{b_v} \qquad (5.8.3.3\text{-}11)$$

where:

b_v = effective web width taken as the minimum web width within the depth d_v as determined in Article 5.8.2.9 (in.)
n_f = number of plies of FRP shear reinforcement
s_f = center-to-center spacing of FRP shear reinforcement strips (in.)
t_f = thickness of FRP plies (in.)
w_f = width of FRP shear reinforcement strips (in.)

The factor 2 in Equations 5.8.3.3-10 and 5.8.3.3-11 accounts for the presence of FRP reinforcement on both sides of a component.

5.8.3.5 Longitudinal Reinforcement

At each section, the tensile capacity of the longitudinal reinforcement on the flexural tension side of the member shall be proportioned to satisfy:

$$A_{ps} f_{ps} + A_s f_y \ge \frac{|M_u|}{d_v \phi_f} + 0.5\frac{N_u}{\phi_c} + \left(\left| \frac{V_u}{\phi_v} - V_p \right| - 0.5V_s - 0.5V_f \right) \cot\theta \qquad (5.8.3.5\text{-}1)$$

in which:

$$V_s + V_f \le V_u/\phi \qquad (5.8.3.5\text{-}2)$$

where:

V_s = shear resistance provided by the transverse steel reinforcement at the section under investigation as given by Eq. 5.8.3.3-4 (kip)

SPECIFICATIONS

COMMENTARY

V_f = shear resistance provided by the transverse FRP reinforcement at the section under investigation as given by Eq. 5.8.3.3-5 (kip)

θ = angle of inclination of diagonal compressive stresses used in determining the nominal shear resistance of the section under investigation as determined by Article 5.8.3.4 (°); if the procedures of Article 5.8.3.4.3 are used, cot θ is defined therein

$\phi_f\phi_v\phi_c$ = resistance factors taken from Article 5.5.4.2 as appropriate for moment, shear and axial resistance

The area of longitudinal reinforcement on the flexural tension side of the member need not exceed the area required to resist the maximum moment acting alone. This provision applies where the reaction force or the load introduces direct compression into the flexural compression face of the member.

Eq. 5.8.3.5-1 shall be evaluated where simply-supported girders are made continuous for live loads. Where longitudinal reinforcement is discontinuous, Eq. 5.8.3.5-1 shall be reevaluated.

At the inside edge of the bearing area of simple end supports to the section of critical shear, the longitudinal reinforcement on the flexural tension side of the member shall satisfy:

$$A_s f_y + A_{ps} f_{ps} \geq \left(\frac{V_u}{\phi_v} - 0.5V_s - 0.5V_f - V_p \right) \cot\theta \qquad (5.8.3.5\text{-}3)$$

Eqs. 5.8.3.5-1 and 5.8.3.5-2 shall be taken to apply to sections not subjected to torsion. Any lack of full development shall be accounted for.

ATTACHMENT B

Recommended Design Guidelines for Concrete Girders Strengthened in Shear with FRP

These proposed guidelines are the recommendations of the NCHRP Project 12-75 Research Team at the Missouri University of Science and Technology. These guidelines have not been approved by NCHRP or any AASHTO committee nor formally accepted for the AASHTO specifications.

SPECIFICATIONS

COMMENTARY

B1 GENERAL

This attachment presents recommended design guidelines for concrete girders strengthened in shear using externally bonded fiber reinforced polymers (FRPs). Design examples developed using these guidelines are presented in the appendix.

B1.1 Design Philosophy

The proposed design guidelines were based on the traditional reinforced concrete (RC) design principles adopted by the current *AASHTO LRFD Bridge Design Specifications* and the knowledge on the mechanical behavior of FRP obtained from work performed under the NCHRP Project 12-75. As such, the factored shear resistance, ϕV_n, of a concrete member should meet or exceed the factored shear force applied to the member, V_u. The applied factored shear force and the factored shear resistance should be computed based on the load and resistance factors specified in the *AASHTO LRFD Bridge Design Specifications*. The factored shear resistance shall be determined as:

$$\phi V_n \geq V_u \qquad \text{(B1-1)}$$

where:

V_n : Nominal shear resistance
V_u : Required shear strength
ϕ : Strength reduction factor (0.9)

Careful consideration for all possible failure modes and subsequent strains and stresses should be considered in determining the nominal shear strength of a member.

B1.2 Scope

These design guidelines focus on presenting design procedures including design equations. Specific limits of applying the proposed design guidelines are also presented in the relevant sections throughout this document.

B2 EVALUATION AND REPAIR OF EXISTING RC BEAMS

CB2

FRP strengthening is usually performed on structurally deficient or damaged RC beams. Before a strengthening procedure is implemented, the extent of deficiency and suitability of FRP strengthening should be evaluated. The necessary evaluation criteria for repair of existing concrete structures and post repair evaluation criteria are well established in the following documents.

Information, such as evaluation and repair of existing RC beams as well as proper application of FRP, is available; an attempt was made to provide references to other publications where additional details can be found.

SPECIFICATIONS

- *ACI 201.1R: Guide for Making a Condition Survey of Concrete in Service*
- *ACI 224.1R: Causes, Evaluation, and Repair of Cracks in Concrete*
- *ACI 364.1R-94: Guide for Evaluation of Concrete Structures Prior to Rehabilitation*
- *ACI 440.2R-08: Guide for the Design and Construction of Externally Bonded FRP Systems for Strengthening Concrete Structures*
- *ACI 503R: Use of Epoxy Compounds with Concrete*
- *ACI 546R: Concrete Repair Guide*
- *International Concrete Repair Institute (ICRI) ICRI 03730: Guide for Surface Preparation for the Repair of Deteriorated Concrete Resulting from Reinforcing Steel Corrosion*
- *International Concrete Repair Institute (ICRI) ICRI 03733: Guide for Selecting and Specifying Materials for Repairs of Concrete Surfaces*
- *NCHRP Report 609: Recommended Construction Specifications Process Control Manual for Repair and Retrofit of Concrete Structures Using Bonded FRP Composites*

Relevant specifications and guidelines provided by FRP manufacturers should also be carefully reviewed prior to the design of any strengthening system.

B3 STRENGTHENING SCHEMES

FRP shear reinforcement is commonly attached to a beam, as shown in Figure B3.1 with (a) side bonding, in which the FRP is only bonded to the sides, (b) U-wrap, in which FRP U-jackets are bonded to both the sides and soffit, and (c) complete wrapping, in which the FRP is wrapped around the entire cross section.

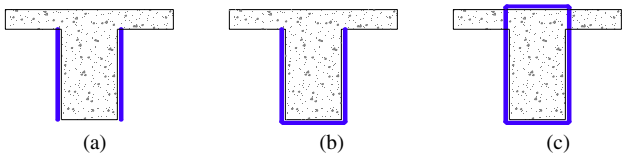

Figure B3.1 Strengthening Scheme: Cross-Sectional View (a) Side bonding, (b) U-wrap, and (c) Complete wrap

For all wrapping schemes, the FRP can be applied continuously along the portion of the member length to be strengthened or as discrete strips. The fibers of the FRP may also be oriented at various angles to meet a range of strengthening requirements as shown in Figure B3.2

CB3

Complete wrapping of the cross section is the most effective scheme and is commonly used in strengthening columns where there is sufficient access for such application. Beams are typically limited to U-wrap and side bonding applications since the integral slab makes it impractical to completely wrap such members. U-wrapping has been experimentally shown to be more effective in improving the shear resistance of a member than side bonding.

SPECIFICATIONS

COMMENTARY

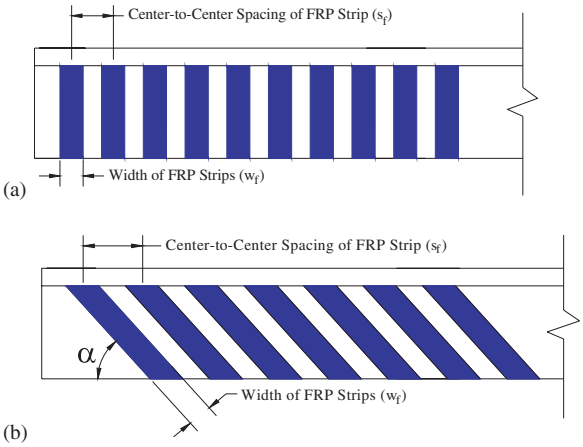

Figure B3.2 Strengthening Scheme: Side View — (a) Fibers at 90° Direction, and (b) Fibers at Inclined Direction

B4 APPLICATION OF FRP

B4.1 General

In general, procedures for the installation of FRP systems are developed by the manufacturer and can vary between different systems. Procedures may also vary depending on the type and condition of the structure to be strengthened. The application of FRP systems will not stop the ongoing corrosion of existing steel reinforcements. The cause of corrosion to internal steel reinforcements should be addressed and corrosion-related deterioration should be repaired prior to application of any FRP system.

CB4.1

It is recommended that FRP applications be performed by a contractor trained in accordance with the installation procedures specified by the manufacturer. Comprehensive guidelines in this regard are provided in *NCHRP Report 609*, Recommended Construction Specifications and Process Control Manual for Repair and Retrofit of Concrete Structures Using Bonded FRP Composites

B4.2 Surface Preparation

The concrete surface should be prepared to a minimum concrete surface profile (CSP) 3 as defined by the ICRI-surface-profile chips (ICRI 03732, *NCHRP Report 609*). Localized out-of-plane variations, including form lines, should not exceed 1/32 inch or the tolerances recommended by the FRP system manufacturer, whichever is smaller. Bug holes and voids should be filled with epoxy putty. It is recommended that surface preparation be accomplished using abrasive or water-blasting techniques. All laitance, dust, dirt, oil, curing compound, existing coatings, and any other matter that could interfere with the bond between the FRP system and concrete substrate should be removed.

When fibers are wrapped around corners, the corners should be rounded to a minimum 1/2 inch radius to prevent stress concentrations in the FRP system and voids between the FRP system and the concrete. Rough edges should also be smoothed by grinding or with putty prior to FRP application.

CB4.2

Bond behavior of the FRP system is highly dependent on a sound concrete substrate and can significantly influence the integrity of the FRP strengthening system. Proper preparation and profiling of the concrete substrate is necessary to achieve optimum bond strength. Improper surface preparation can lead to premature debonding or delamination.

SPECIFICATIONS

B4.3 Inspection, Evaluation, and Acceptance

Application of FRP systems should be inspected by a licensed engineer or qualified inspector knowledgeable in FRP systems and installation procedures. The following should be recorded at the time of installation:

- Date and time of installation
- Ambient temperature, relative humidity, and general weather observations and surface temperature of concrete
- Surface dryness, surface preparation methods and resulting profile using the ICRC-surface-profile-chips
- Qualitative description of surface cleanliness
- Type of auxiliary heat source, if applicable
- Widths of cracks not injected with epoxy
- Fiber or pre-cured laminate batch number(s) and approximate locations in structure
- Batch numbers, mixture ratios, mixing times, and qualitative descriptions of the appearance of all mixed resins, including primers, putties, saturants, adhesives, and coatings mixed for the day
- Observations of progress of cure of resins
- Conformance with installation procedures
- Location and size of any delaminations or air voids
- General progress of work
- Level of curing of resin in accordance with ASTM D3418.
- Adhesion strength

COMMENTARY

CB4.3

When concrete and atmospheric temperatures exceed 90°F, difficulties may be experienced in application of the epoxy compound owing to acceleration of the reaction and hardening rates. If ambient temperatures above 90°F are anticipated, work should be scheduled when the temperature is lower, such as in the early morning hours. If it is necessary to apply epoxy compounds at temperatures exceeding 90 °F, the work should be supervised by a person experienced in applying epoxy at high temperatures. Epoxy systems formulated for elevated temperature are available (ACI 530R-93).

At temperatures below 40°F, difficulties may occur due to deceleration of the reaction rates. The presence of frost or ice crystals may also be detrimental to the bond between the FRP and the concrete.

Evaluate moisture content or outgassing of the concrete by determining if moisture will collect at bond lines between old concrete and epoxy adhesive before epoxy has cured. This may be accomplished by taping a 4 x 4 ft (1 x 1 m) polyethylene sheet to concrete surface. If moisture collects on underside of polyethylene sheet before epoxy would cure, then allow concrete to dry sufficiently to prevent the possibility of a moisture barrier between old concrete and new epoxy (ACI 530R-93).

During installation, sample cups of mixed resin should be prepared according to a predetermined sampling plan and retained for testing to determine level of curing in accordance with ASTM D3418. The relative cure of the resin can also be evaluated on the project site by physical observation of resin tackiness and hardness of work surfaces or hardness of retained resin samples.

For bond-critical applications, tension adhesion testing of cored samples should be conducted using the methods in ACI 530R or ASTM D 4541 or the method described by ISIS (1998). The sampling frequency should be specified. Tension adhesion strengths should exceed 200 psi and exhibit failure of the concrete substrate before failure of the adhesive (ACI 440.2R-08).

B5 MATERIAL PROPERTIES OF FRP

The following mechanical properties should be obtained from manufacturers or coupon tests in accordance with ASTM D3039.

- E_f : the modulus of elasticity of FRP
- ε_{fu} : the ultimate strain of FRP.

Then, the nominal resistance, f_{fu}, can be determined assuming linear behavior of FRP stress-strain relationship up to failure as:

$$f_{fu} = E_f \varepsilon_{fu} \qquad \text{(B5-1)}$$

SPECIFICATIONS

COMMENTARY

B6 NOMINAL SHEAR RESISTANCE

An interaction is known to exist between the shear contributions of concrete, transverse steel reinforcement, and FRP. However, this interaction mechanism is not yet fully understood and thus is not reflected in the design procedures. Therefore, following the current reinforced concrete design principals, the nominal shear resistance (V_n) is determined by adding the contribution of the FRP reinforcement to the contributions from concrete and internal transverse steel reinforcement:

$$V_n = V_c + V_s + V_f \tag{B6-1}$$

where, V_c is the contributions of concrete, V_s is the contribution of transverse steel reinforcement (stirrups), and V_f is the contribution of FRP. The contributions from the concrete (V_c) and transverse steel reinforcement (V_s) can be computed based on the current AASHTO LRFD Bridge Design Specifications. Calculation of the FRP contribution (V_f) is presented in the following sections.

B7 SHEAR CONTRIBUTION OF FRP

B7.1 Calculation of Contribution of FRP

CB7.1

The contribution of FRP (V_f) can be computed using the 45° truss model as:

$$\begin{aligned} V_f &= \frac{A_f f_{fe} d_f (\sin\alpha_f + \cos\alpha_f)}{s_f} \\ &= \frac{A_f E_f \varepsilon_{fe} d_f (\sin\alpha_f + \cos\alpha_f)}{s_f} \\ &= \rho_f E_f \varepsilon_{fe} b_v d_f (\sin\alpha_f + \cos\alpha_f) \end{aligned} \tag{B7-1}$$

where, A_f is the area of FRP covering two sides of the beam and can be determined by $2n_f t_f w_f$ (n_f is number of FRP plies, t_f is the FRP reinforcement thickness, w_f is the width of the strip), f_{fe} is the effective stress of FRP, d_f is the effective depth of FRP measured from the top of FRP reinforcement to the centroid of the longitudinal reinforcement, s_f is the center-to-center spacing of FRP, α_f is the angle of inclination of FRP with respect to the longitudinal axis of the member as shown in Figure B3.2, E_f is the modulus of elasticity of FRP, ε_{fe} is the effective strain of FRP, ρ_f is the reinforcement ratio of FRP, and b_v is the effective web width taken as the minimum web width within the effective depth (d_f)

SPECIFICATIONS

The FRP shear reinforcement ratio, ρ_f, is determined as:

- For discrete strips

$$\rho_f = \frac{2n_f t_f w_f}{b_v s_f} \quad \text{(B7-2)}$$

- For continuous sheets

$$\rho_f = \frac{2n_f t_f}{b_v} \quad \text{(B7-3)}$$

The effective strain (ε_{fe}) represents the average strain experienced by the FRP at shear failure of the strengthened member and can be expressed as:

- For Full Anchorage (Rupture Failures Expected): Complete Wrap or U-Wrap with Anchors

$$\varepsilon_{fe} = R_f \varepsilon_{fu} \quad \text{(B7-4)}$$

where $R_f = 0.088 \le 4(\rho_f E_f)^{-.67} \le 1.0$

- For Other Anchorage (Non-Rupture Failures more likely): Side bonding or U-Wrap

$$\varepsilon_{fe} = R_f \varepsilon_{fu} \le 0.012 \quad \text{(B7-5)}$$

where $R_f = 0.066 \le 3(\rho_f E_f)^{-.67} \le 1.0$

COMMENTARY

The effective strain, ε_{fe}, is largely dependent on the failure modes as discussed in Appendix A - Sections A3 and A4. Therefore, the experimental database collected in this project was grouped by the failure mode of the test specimens, i.e., either as debonding or rupture of the FRP and then regression analyses were performed to obtain Eqn. B7-4 and B7-5.

The upper bound for the quantity $\rho_f E_f$ in Eqs. B7-4 and B7-5 is 300 ksi. Substituting this value in these two equations results in the lower bound value of R_f shown in the two equations.

SPECIFICATIONS

COMMENTARY

B7.2 Limitations

B7.2.1 Shear span-to-depth ratio

The reduction factors (R_f) were developed from tests in which the loading was at a distance from the support sufficient to assume plane sections before deformation remain plane after deformation, i.e. shallow beam behavior. Thus, these provisions are only applicable to beams with a shear span-to-depth ratio greater than 2.5.

B7.2.2 Maximum Amount of FRP Shear Reinforcement

CB7.2.2

The amount of FRP should be determined so that the nominal shear strength calculated by Eq. B 6-1 should not exceed the nominal shear strength calculated by

$$V_n = 0.25 f_c' b_v d_v + V_p \qquad \text{(AASHTO 5.8.3.3-2)}$$

This provision is required to avoid web crushing failure of FRP strengthened beams due to excessive transverse shear reinforcement (both FRP and steel stirrups).

B.7.2.3 Maximum Spacing of FRP Shear Reinforcement

The clear spacing between externally bonded FRP shear reinforcement shall not exceed the maximum permitted spacing ($s_{\max}$) in accordance with the current AASHTO LRFD Bridge Design Specifications, expressed as:

If $v_u < 0.125 f_c'$ then $s_{\max} = 0.8 d_v \le 24\,\text{in.}$ (AASHTO 5.8.2.7-1)

If $v_u \ge 0.125 f_c'$ then $s_{\max} = 0.4 d_v \le 12\,\text{in.}$ (AASHTO 5.8.2.7-2)

where v_u = the shear stress calculated in accordance with AASHTO LRFD – Article 5.8.2.9 (ksi) and d_v =effective shear depth as defined in AASHTO LRFD — Article 5.8.2.9 (in.)

B7.3 Use of Anchorage Systems

Different types of anchorage systems are available for shear strengthening with FRP. Examples of mechanical anchorage systems consisting of FRP composite plates and concrete anchor bolts are available in the literature [NCHRP Report 12-75]. However, it should be noted that additional horizontal FRP strips cannot ensure FRP rupture failure. Thus, it is recommended that Equation B7-5 be used to calculate the FRP contribution, realizing that such approach will result in conservative estimates.

APPENDIX

Design Examples

The following six design examples are presented to illustrate use of the recommended guidelines:

Example 1-1: RC T-beam without internal transverse steel reinforcement strengthened with FRP in U-wrap configuration without anchorage systems
Example 1-2: RC T-beam without internal transverse steel reinforcement strengthened with FRP in U-wrap configuration with an anchorage system
Example 2-1: RC T-beam with internal transverse steel reinforcement strengthened with FRP in U-wrap configuration without anchorage systems
Example 2-2: RC T-Beam with internal transverse steel reinforcement strengthened with FRP in U-wrap configuration with an anchorage system
Example 3-1: PC I-Beam with internal transverse steel reinforcement strengthened with FRP in U-wrap configuration without anchorage systems
Example 3-2: PC I-Beam with internal transverse steel reinforcement strengthened with FRP in U-wrap configuration with an anchorage system

DESIGN EXAMPLE 1-1: RC T-Beam without Internal Transverse Steel Reinforcement Strengthened with FRP in U-wrap Configuration without Anchorage Systems

1. INTRODUCTION

This example demonstrates the design procedures for externally bonded FRP shear reinforcement of an older reinforced concrete (RC) bridge using a U-wrap configuration without anchorage. The bridge consists of simply supported T-beams spanning 42 feet and spaced at 4.5 feet on center. The T-beams contain no transverse steel reinforcement. Additional details of the T-beam are provided in Figures 1 and 2.

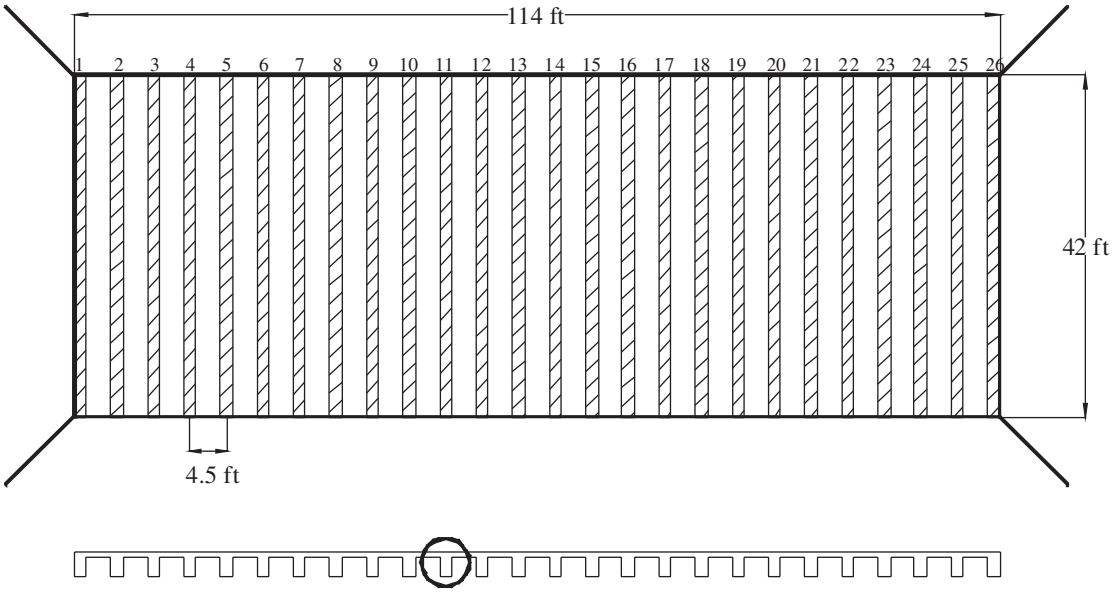

Figure 1. Bridge plan and transverse section.

2. MATERIAL PROPERTIES

The following material properties have been chosen to represent those anticipated in an older bridge for which shear deficiencies might be expected.

2.1. Concrete

Compressive strength $f'_c := 3.0$ ksi

Modulus of elasticity $E_c := 33 \cdot (1.5)^{1.5} \sqrt{f'_c \cdot 1000}$ ksi

$E_c = 3321$ ksi

$$\beta_1 := \begin{cases} 0.85 \text{ if } f'_c \le 4 \\ 0.65 \text{ if } f'_c \ge 8 \\ \left[0.85 - 0.05 \cdot \left(f'_c - 4\right)\right] \text{ otherwise} \end{cases}$$

$$\beta_1 = 0.85$$

2.2. Longitudinal Reinforcement

Yield strength $f_y := 60$ ksi

Modulus of elasticity $E_s := 29000$ ksi

2.3. FRP Reinforcement

Carbon Fiber Sheets are used in this example.

Thickness $t_f := 0.0065$ in.

Failure strength $f_{fu} := 550$ ksi

Modulus of elasticity $E_f := 33000$ ksi

Failure strain $\varepsilon_{fu} := \dfrac{f_{fu}}{E_f}$

$$\varepsilon_{fu} = 0.017 \text{ in/in}$$

3. GEOMETRICAL PROPERTIES

Total Height $h_T := 37$ in.

Flange Thickness $h_f := 7$ in.

Width of the web $b_v := 18$ in.

Effective Width of the Flange $b_{eff} := 54$ in.

Tensile reinforcement = 12#11 $A_s := 18.72$ in^2

Internal shear reinforcement = Not provided $A_v := 0.0$ in^2

Distance from the extreme compression fiber to the center of the steel at the section d := 32.7 in.

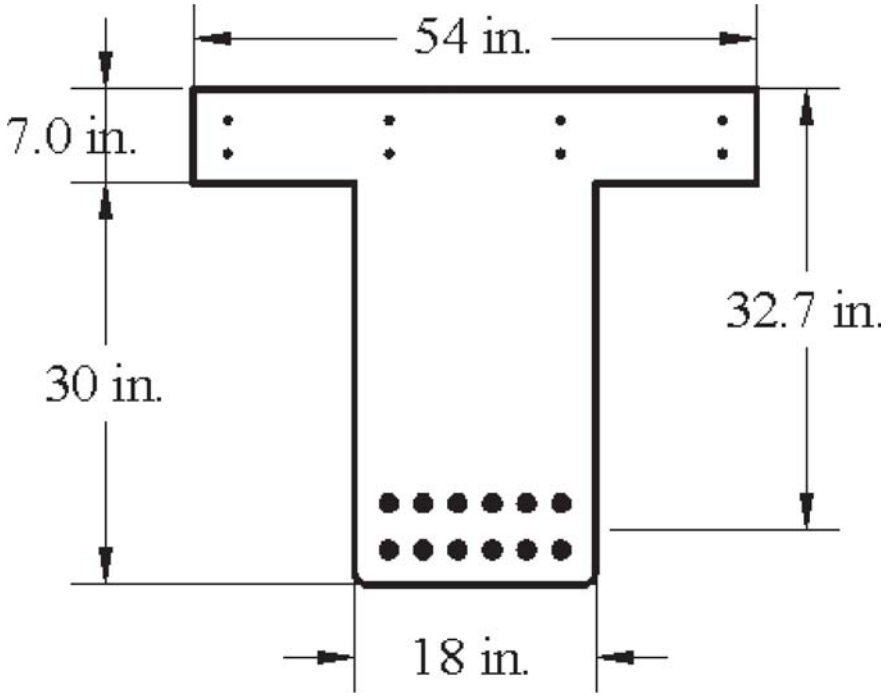

Figure 2. Cross-Section of an Intermediate Beam

4. CALCULATION OF THE FACTORED SHEAR FORCE AND NOMINAL SHEAR RESISTANCE

4.1 Factored Shear Force at the Critical Section

$V_{u\_crit} := 100 \text{ kips}$

4.2. Calculation of Nominal Shear Resistance

For this example, the simplified approach is followed.

$\theta := 45 \text{ deg}$ $\beta := 2$

The nominal shear resistance provided by the concrete, V_c, is calculated in accordance with LRFD Eqn.5.8.3.3-3 as:

Assuming rectangular section behavior with no compression steel, the distance from the extreme compression fiber to the neutral axis, c_c, may be calculated as:

$$c_{c1} := \frac{A_s \cdot f_y}{0.85 \cdot f'_c \cdot b_{eff} \cdot \beta_1} \qquad c_{c1} = 9.6 \text{ in.}$$

$a_{c1} := \beta_1 \cdot c_{c1}$ $\quad a_{c1} = 8.16$ in.

$$check\_a_{c1} := \begin{cases} \text{"Assumption is correct"} & \text{if } (a_{c1} \le h_f) \\ \text{"Not behave as rectangular"} & \text{otherwise} \end{cases}$$

$check\_a_{c1} = \text{"Not behave as rectangular"}$

Assuming T-beam section behavior with no compression steel, the distance from the extreme compression fiber to the neutral axis, c_c, may be calculated as:

$$c_{c2} := \frac{A_s \cdot f_y - 0.85 \cdot f'_c \cdot (b_{eff} - b_1) \cdot h_f}{0.85 \cdot f'_c \cdot b_v \cdot \beta_1} \qquad c_{c2} = 12.32 \text{ in.}$$

$a_{c2} := \beta_1 \cdot c_{c2}$ $\quad a_{c2} = 10.47$ in.

$$check\_a_{c2} := \begin{cases} \text{"Assumption is correct"} & \text{if } (a_{c2} \ge h_f) \\ \text{"Not behave as rectangular"} & \text{otherwise} \end{cases}$$

$check\_a_{c2} = \text{"Assumption is correct"}$

Therefore $c_c := c_{c2}$ $\quad c_c = 12.32$ in.

$a_c := a_{c2}$ $\quad a_c = 10.47$ in.

The effective shear depth d_V is taken as the distance, measured perpendicular to the neutral axis, between the resultants of the tensile and compressive forces due to flexure; it need not be taken less than the greater of $0.9d_e$ or $0.72h$ (LRFD Article5.8.2.9)

$$\left(d_{v1} := d - \frac{a_c}{2} \right) \quad (d_{v2} := 0.9 \cdot d) \quad (d_{v3} := 0.72 \cdot h_T)$$

$(d_v := \max(d_{v1}, d_{v2}, d_{v3}))$

$(d_v) = 29.4$ in.

The nominal shear resistance provided by the concrete is:

$v_c := 0.0316 \cdot \beta \cdot \sqrt{f'_c} \cdot b_v \cdot d_v$ (LRFD Eqn. 5.8.3.3-3)

$(v_c) = 58$ kips

The nominal shear resistance provided by the internal steel reinforcement is:

$v_s := 0$

The nominal shear resistance provided by the vertical component of prestressing strands is:

$(v_p := 0)$

The nominal shear resistance of the member is:

$v_n := v_c + v_s + v_p$ (LRFD Eqn. 5.8.3.3-1)

$v_n = 58$ kips

5. DESIGN OF FRP SHEAR REINFORCEMENT

5.1 Check if FRP Reinforcement is Necessary or Not

Strength reduction factor for shear ($\phi := 0.9$)

$$\text{Check\_FRP\_Needed} := \begin{cases} \text{"NOT need shear reinforcement"} & \text{if } \left(\phi \cdot V_n \geq V_{u\_crit}\right) \\ \text{"NEED shear reinforcement"} & \text{otherwise} \end{cases}$$

Check_FRP_Needed = "NEED shear reinforcement"

5.2 Computation of Required V_f

$$V_{f\_req} := \frac{V_{u\_crit}}{\phi} - V_n$$

$V_{f\_req} = 53.1$ kips

5.3 Selection of FRP Strengthening Scheme

U-wrap configuration is used without anchorage systems at the end of the sheets. The FRP sheets will be applied at 90 degree with respect to the longitudinal axis of the girder as shown in Figure 3. First, the spacing of FRP strips is chosen to meet the maximum spacing requirement. Then, the width of the FRP strips is selected to adjust the amount of FRP strips.

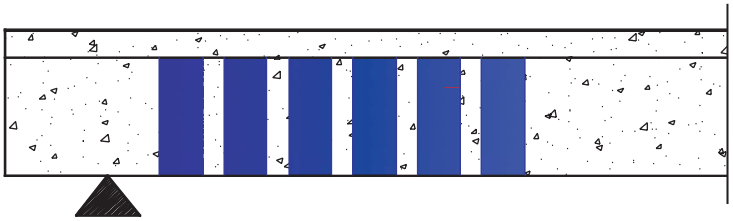

Figure 3 FRP strengthening scheme.

Use number of plies of FRP sheets $n_f := 1$

Use the width of FRP sheets $w_f := 8$ in.

Use the center-to-center spacing of FRP sheets $s_f := 15$ in.

Orientation of FRP sheets $\alpha_f := 90$ deg

Effective depth of FRP sheets $d_f := d - h_f$

$d_f = 25.7$ in.

Check if the selected spacing is acceptable or not

Shear stress on concrete is:

$$v_u := \frac{V_{u\_crit} - \phi \cdot V_p}{\phi \cdot b_v \cdot d_v} \qquad \text{(LRFD Eqn. 5.8.2.9-1)}$$

$(v_u) = 0.21$ ksi

The maximum spacing of the transverse reinforcement is:

$$s_{max} := \begin{cases} \min(0.8 \cdot d_v, 24) & \text{if } v_u < 0.125 \cdot f'_c \qquad \text{(LRFD Eqn. 5.8.2.7-1)} \\ \min(0.4 \cdot d_v, 12) & \text{otherwise} \qquad \text{(LRFD Eqn. 5.8.2.7-2)} \end{cases}$$

$s_{max} = 23.5$

$$Check\_Spacing := \begin{cases} \text{"Acceptable"} & \text{if } s_f \le s_{max} \\ \text{"NOT\_Acceptable\_Change\_the\_Spacing"} & \text{otherwise} \end{cases}$$

Check_Spacing = "Acceptable"

5.4 Calculation of Shear Resistance of FRP, V_f

The FRP reinforcement ratio is:

$$\rho_f := \frac{2 \cdot n_f \cdot w_f \cdot t_f}{b_v \cdot s_f} \qquad \text{(Attachment A Eqn. 5.8.3.3-10)}$$

$(\rho_f) = 3.852 \times 10^{-4}$

The FRP strain reduction factor is:

$$R_f := \min\left[3\cdot\left(\rho_f\cdot E_f\right)^{-0.67},\ 1.0\right] \qquad \text{(Attachment A Eqn. 5.8.3.3-9)}$$

$$R_f = 0.546$$

The effective strain of FRP is:

$$\varepsilon_{fe} := \min\left(R_f\cdot\varepsilon_{fu},\ 0.012\right) \qquad \text{(Attachment A Eqn. 5.8.3.3-7)}$$

$$\varepsilon_{fe} = 9.103\times 10^{-3}\ \text{in./in.}$$

The effective stress of FRP is:

$$f_{fe} := \varepsilon_{fe}\cdot E_f \qquad \text{(Attachment A Eqn. 5.8.3.3-6)}$$

$$\left(f_{fe}\right) = 300.4\ \text{ksi}$$

The shear contribution of the FRP can be then calculated.

$$V_f := \rho_f\cdot E_f\cdot\varepsilon_{fe}\cdot b_v\cdot d_f\cdot\left(\sin\left(\alpha_f\right)+\cos\left(\alpha_f\right)\right) \qquad \text{(Attachment A Eqn. 5.8.3.3-5)}$$

$$\left(V_f\right) = 53.5\ \text{kips}$$

$$V_{f\_check1} := \begin{cases} \text{"Change FRP Strengthening Scheme"} & \text{if } \left(V_f < V_{f\_req}\right) \\ \text{"Provided FRP Strength Large Enough"} & \text{otherwise} \end{cases}$$

$$V_{f\_check1} = \text{"Provided FRP Strength Large Enough"}$$

$$V_{f\_check2} := \begin{cases} \text{"Provided FRP amount is adequate"} & \text{if } \left(V_{f\_req} \le V_f < 1.1\cdot V_{f\_req}\right) \\ \text{"Change the FRP amount slightly"} & \text{otherwise} \end{cases}$$

$$\left(V_{f\_check2}\right) = \text{"Provided FRP amount is adequate"}$$

5.5 Calculation of Design Shear Resistance of the Member

The design strength of the member is:

$$\phi V_{n\_total} := \phi\cdot\left(V_c + V_p + V_s + V_f\right) \qquad \text{(Attachment A Eqn. 5.8.3.3-1)}$$

$$\left(\phi V_{n\_total}\right) = 100.4\ \text{kips}$$

$$Web\_crushing\_limit := 0.25 \cdot f'_c \cdot b_v \cdot d_v + V_p \qquad \text{(LRFD Eqn. 5.8.3.3-2)}$$

$$Web\_crushing\_limit = 397.3 \text{ kips}$$

$$Check\_web\_crushing\_limit := \begin{cases} \text{"OK"} & \text{if } \left(V_c + V_s + V_f + V_p\right) \le Web\_crushing\_limit \\ \text{"No Good"} & \text{otherwise} \end{cases}$$

$$Check\_web\_crushing\_limit = \text{"OK"}$$

6. SUMMARY

Externally bonded FRP sheets were designed in this example. The FRP sheets are applied at 90 degrees with respect to the longitudinal axis of the member with the U-wrap configuration and without anchorage systems as shown in Figure 4. The final design is summarized as:

Use number of plies of FRP sheets $n_f = 1$

Use the width of FRP sheets $w_f = 8$ in.

Use the center-to-center spacing of FRP sheets $s_f = 15$ in.

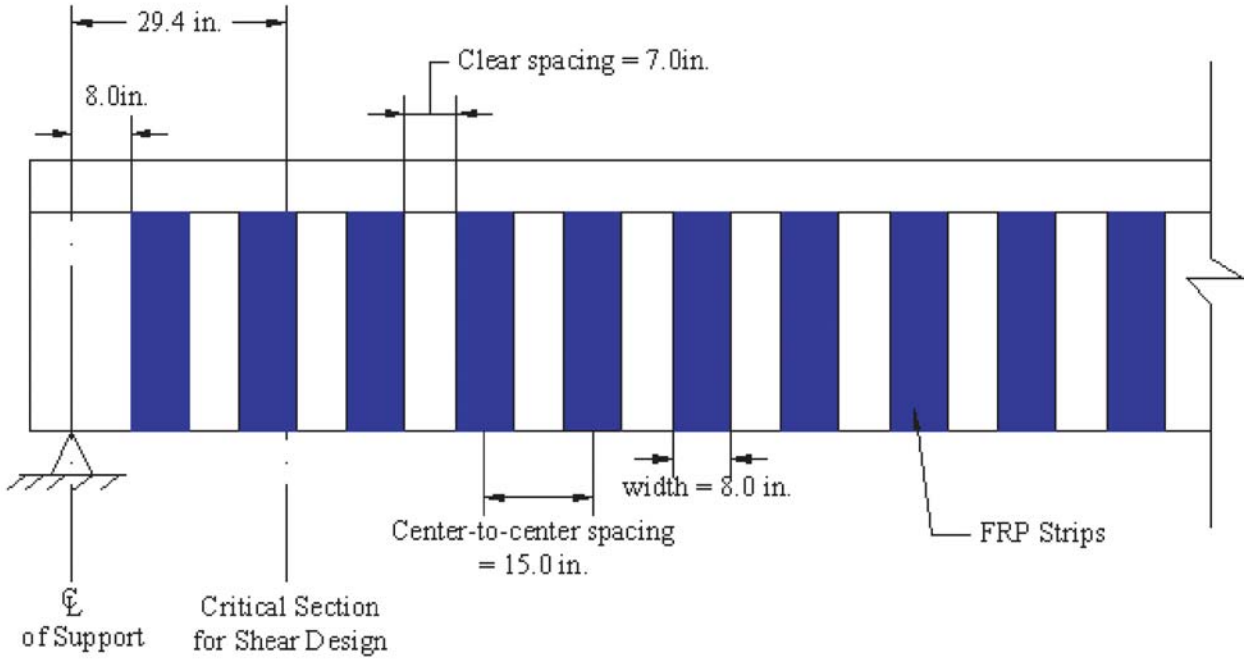

Figure 4. Final design of FRP strengthening.

DESIGN EXAMPLE 1-2: RC T-Beam without Internal Transverse Steel Reinforcement Strengthened with FRP in U-wrap Configuration with an Anchorage System

1. INTRODUCTION

This example demonstrates the design procedures for externally bonded FRP shear reinforcement of an older reinforced concrete (RC) bridge using a U-wrap configuration with anchorage. The bridge consists of simply supported T-beams spanning 42 feet and spaced at 4.5 feet on center. The T-beams contain no transverse steel reinforcement. Additional details of the T-beam are provided in Figures 1 and 2.

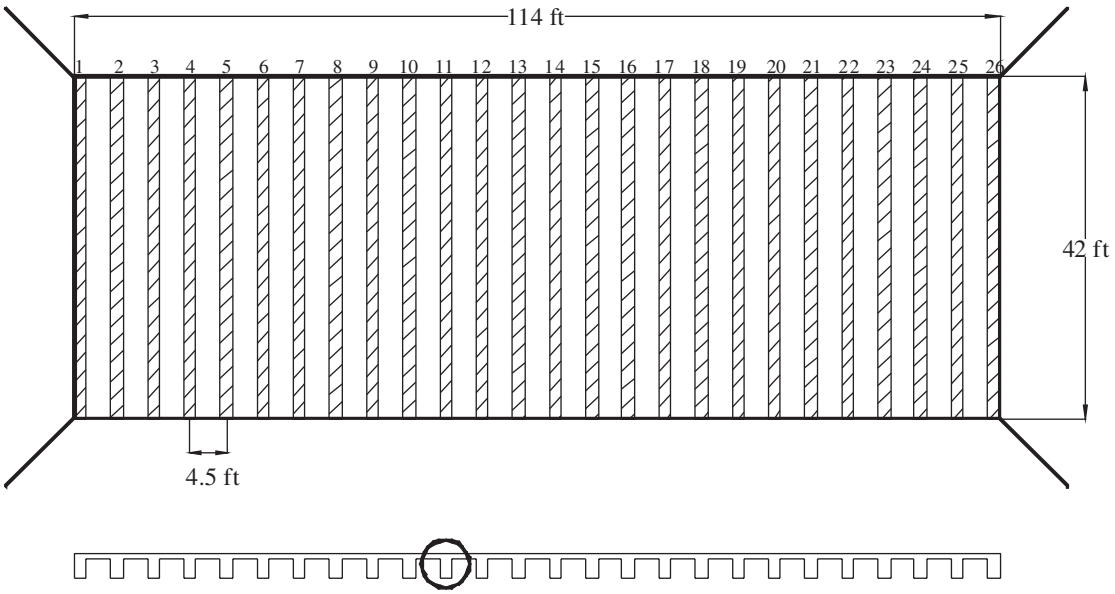

Figure 1. Bridge plan and transverse section.

2. MATERIAL PROPERTIES

The following material properties have been chosen to represent those anticipated in an older bridge for which shear deficiencies might be expected.

2.1. Concrete

Compressive strength $\left(f'_c := 3.0\right)$ ksi

Modulus of elasticity $\left(E_c := 33 \cdot (1.5)^{1.5} \sqrt{f'_c \cdot 1000}\right)$ ksi

$$\left(E_c\right) = 3321 \text{ ksi}$$

$$\beta_1 := \begin{cases} 0.85 & \text{if } f'_c \le 4 \\ 0.65 & \text{if } f'_c \ge 8 \\ \left[0.85 - 0.05 \cdot \left(f'_c - 4\right)\right] & \text{otherwise} \end{cases}$$

$$\beta_1 = 0.85$$

2.2. Longitudinal Reinforcement

Yield strength $f_y := 60$ ksi

Modulus of elasticity $E_s := 29000$ ksi

2.3. FRP Reinforcement

Carbon Fiber Sheets are used in this example.

Thickness $t_f := 0.0065$ in.

Failure strength $f_{fu} := 550$ ksi

Modulus of elasticity $E_f := 33000$ ksi

Failure strain $\varepsilon_{fu} := \dfrac{f_{fu}}{E_f}$

$$\varepsilon_{fu} = 0.017 \text{ in/in}$$

3. GEOMETRICAL PROPERTIES

Total Height $h_T := 37$ in.

Flange Thickness $h_f := 7$ in.

Width of the web $b_v := 18$ in.

Effective Width of the Flange $b_{eff} := 54$ in.

Tensile reinforcement = 12#11 $A_s := 18.72$ in^2

Internal shear reinforcement = Not provided $\left(A_v := 0.0\right)$ in^2

Distance from the extreme compression fiber to the center of the steel at the section d := 32.7 in.

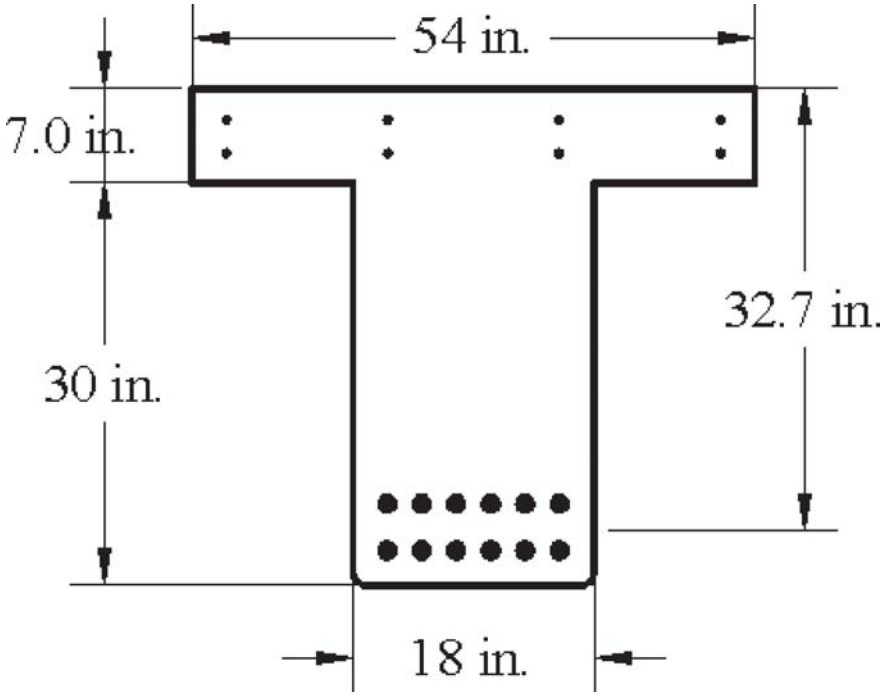

Figure 2. Cross-section of an intermediate beam.

4. CALCULATION OF THE FACTORED SHEAR FORCE AND NOMINAL SHEAR RESISTANCE

4.1 Factored Shear Force at the Critical Section

$V_{u\_crit} := 100$ kips

4.2. Calculation of Nominal Shear Resistance

For this example, the simplified approach is followed.

$(\theta := 45 \text{ deg})$ $(\beta := 2)$

The nominal shear resistance provided by the concrete, V_c, is calculated in accordance with LRFD Eqn.5.8.3.3-3 as:

Assuming rectangular section behavior with no compression steel, the distance from the extreme compression fiber to the neutral axis, c_c, may be calculated as:

$$\left(c_{c1} := \frac{A_s \cdot f_y}{0.85 \cdot f'_c \cdot b_{eff} \cdot \beta_1} \right) \qquad \left(c_{c1} \right) = 9.6 \text{ in.}$$

$$\left(a_{c1} := \beta_1 \cdot c_{c1} \right) \qquad \left(a_{c1} \right) = 8.16 \text{ in.}$$

$$\left(\text{check\_a}_{c1} := \left\| \begin{array}{ll} \text{"Assumption is correct"} & \text{if } \left(a_{c1} \le h_f\right) \\ \text{"Not behave as rectangular"} & \text{otherwise} \end{array} \right.\right)$$

$$\left(\text{check\_a}_{c1}\right) = \text{"Not behave as rectangular"}$$

Assuming T-beam section behavior with no compression steel, the distance from the extreme compression fiber to the neutral axis, c_c, may be calculated as:

$$\left(c_{c2} := \frac{A_s \cdot f_y - 0.85 \cdot f'_c \cdot \left(b_{eff} - b_v\right) \cdot h_f}{0.85 \cdot f'_c \cdot b_v \cdot \beta_1}\right) \qquad \left(c_{c2}\right) = 12.32 \text{ in.}$$

$$\left(a_{c2} := \beta_1 \cdot c_{c2}\right) \qquad \left(a_{c2}\right) = 10.47 \text{ in.}$$

$$\left(\text{check\_a}_{c2} := \left\| \begin{array}{ll} \text{"Assumption is correct"} & \text{if } \left(a_{c2} \ge h_f\right) \\ \text{"Not behave as rectangular"} & \text{otherwise} \end{array} \right.\right)$$

$$\left(\text{check\_a}_{c2}\right) = \text{"Assumption is correct"}$$

Therefore $\left(c_c := c_{c2}\right)$ $\left(c_c\right) = 12.32$ in.

$\left(a_c := a_{c2}\right)$ $\left(a_c\right) = 10.47$ in.

The effective shear depth d_v is taken as the distance, measured perpendicular to the neutral axis, between the resultants of the tensile and compressive forces due to flexure; it need not be taken less than the greater of $0.9d_e$ or $0.72h$ (LRFD Article5.8.2.9)

$$\left(d_{v1} := d - \frac{a_c}{2}\right) \qquad \left(d_{v2} := 0.9 \cdot d\right) \qquad \left(d_{v3} := 0.72 \cdot h_T\right)$$

$$\left(d_v := \max\left(d_{v1}, d_{v2}, d_{v3}\right)\right)$$

$$\left(d_v\right) = 29.4 \text{ in.}$$

The nominal shear resistance provided by the concrete is:

$V_c := 0.0316 \cdot \beta \cdot \sqrt{f'_c} \cdot b_v \cdot d_v$ (LRFD Eqn. 5.8.3.3-3)

$$\left(V_c\right) = 58 \text{ kips}$$

The nominal shear resistance provided by the internal steel reinforcement is:

$V_s := 0$

The nominal shear resistance provided by the vertical component of prestressing strands is:

$(V_p := 0)$

The nominal shear resistance of the member is:

$V_n := V_c + V_s + V_p$ (LRFD Eqn. 5.8.3.3-1)

$V_n = 58$ kips

5. DESIGN OF FRP SHEAR REINFORCEMENT

5.1 Check if FRP Reinforcement is Necessary or Not

Strength reduction factor for shear ($\phi := 0.9$)

$$\text{Check\_FRP\_Needed} := \begin{cases} \text{"NOT need shear reinforcement"} & \text{if } \left(\phi \cdot V_n \geq V_{u\_crit}\right) \\ \text{"NEED shear reinforcement"} & \text{otherwise} \end{cases}$$

Check_FRP_Needed = "NEED shear reinforcement"

5.2 Computation of Required V_f

$$V_{f\_req} := \frac{V_{u\_crit}}{\phi} - V_n$$

$V_{f\_req} = 53.1$ kips

5.3 Selection of FRP Strengthening Scheme

U-wrap configuration is used with anchorage systems at the end of the sheets. The FRP sheets will be applied at 90 degrees with respect to the longitudinal axis of the girder as shown in the Figure 3 below. Anchorage systems will be installed at the top end portion of the FRP sheets to increase the effectiveness of FRP shear strengthening. First, the spacing of FRP strips is chosen to meet the maximum spacing requirement. Then, the width of the FRP strips is selected to adjust the amount of FRP strips.

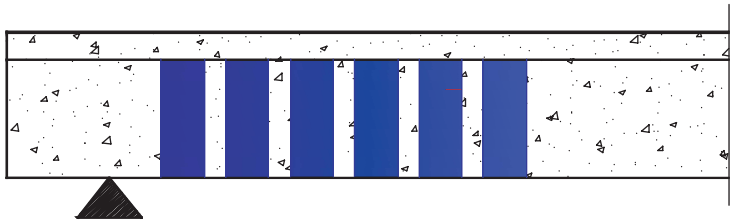

Figure 3. FRP strengthening scheme.

Use number of plies of FRP sheets $n_f := 1$

Use the width of FRP sheets $w_f := 5.5$ in.

Use the center-to-center spacing of FRP sheets $s_f := 18$ in.

Orientation of FRP sheets $\alpha_f := 90$ deg

Effective depth of FRP sheets $d_f := d - h_f$

$d_f = 25.7$ in.

Check if the selected spacing is acceptable or not

Shear stress on concrete is:

$$v_u := \frac{V_{u\_crit} - \phi \cdot V_p}{\phi \cdot b_v \cdot d_v} \qquad \text{(LRFD Eqn. 5.8.2.9-1)}$$

$(v_u) = 0.21$ ksi

The maximum spacing of the transverse reinforcement is:

$$s_{max} := \begin{cases} \min(0.8 \cdot d_v, 24) & \text{if } v_u < 0.125 \cdot f'_c \quad \text{(LRFD Eqn. 5.8.2.7-1)} \\ \min(0.4 \cdot d_v, 12) & \text{otherwise} \quad \text{(LRFD Eqn. 5.8.2.7-2)} \end{cases}$$

$s_{max} = 23.5$

$$Check\_Spacing := \begin{cases} \text{"Acceptable"} & \text{if } s_f \le s_{max} \\ \text{"NOT\_Acceptable\_Change\_the\_Spacing"} & \text{otherwise} \end{cases}$$

Check_Spacing = "Acceptable"

5.4 Calculation of Shear Resistance of FRP, V_f

The FRP reinforcement ratio is:

$$\rho_f := \frac{2 \cdot n_f \cdot w_f \cdot t_f}{b_v \cdot s_f} \qquad \text{(Attachment A Eqn. 5.8.3.3-10)}$$

$(\rho_f) = 2.207 \times 10^{-4}$

The FRP strain reduction factor is:

$$R_f := \min\left[4\cdot\left(\rho_f\cdot E_f\right)^{-0.67}, 1.0\right] \qquad \text{(Attachment A Eqn. 5.8.3.3-8)}$$

$$R_f = 1$$

The effective strain of FRP is:

$$\varepsilon_{fe} := R_f \cdot \varepsilon_{fu} \qquad \text{(Attachment A Eqn. 5.8.3.3-7)}$$

$$\varepsilon_{fe} = 0.017 \text{ in./in.}$$

The effective stress of FRP is:

$$f_{fe} := \varepsilon_{fe} \cdot E_f \qquad \text{(Attachment A Eqn. 5.8.3.3-6)}$$

$$\left(f_{fe}\right) = 550 \text{ ksi}$$

The shear contribution of the FRP can be then calculated.

$$\left(V_f := \rho_f \cdot E_f \cdot \varepsilon_{fe} \cdot b_v \cdot d_f \cdot \left(\sin\left(\alpha_f\right) + \cos\left(\alpha_f\right)\right)\right) \qquad \text{(Attachment A Eqn. 5.8.3.3-5)}$$

$$\left(V_f\right) = 56.1 \text{ kips}$$

$$V_{f\_check1} := \begin{cases} \text{"Change FRP Strengthening Scheme"} & \text{if } \left(V_f < V_{f\_req}\right) \\ \text{"Provided FRP Strength Large Enough"} & \text{otherwise} \end{cases}$$

$$V_{f\_check1} = \text{"Provided FRP Strength Large Enough"}$$

$$V_{f\_check2} := \begin{cases} \text{"Provided FRP amount is adequate"} & \text{if } \left(V_{f\_req} \le V_f < 1.1 \cdot V_{f\_req}\right) \\ \text{"Change the FRP amount slightly"} & \text{otherwise} \end{cases}$$

$$\left(V_{f\_check2}\right) = \text{"Provided FRP amount is adequate"}$$

5.5 Calculation of Design Shear Resistance of the Member

The design strength of the member is:

$$\phi V_{n\_total} := \phi \cdot \left(V_c + V_p + V_s + V_f\right) \qquad \text{(Attachment A Eqn. 5.8.3.3-1)}$$

$$\left(\phi V_{n\_total}\right) = 102.722 \text{ kips}$$

$$\phi V_{n\_check} := \begin{cases} \text{"Not Good"} & \text{if } V_{u\_crit} > \phi V_{n\_total} \\ \text{"OK"} & \text{otherwise} \end{cases}$$

$$\left(\phi V_{n\_check}\right) = \text{"OK"}$$

$$\text{Web\_crushing\_limit} := 0.25 \cdot f'_c \cdot b_v \cdot d_v + V_p \qquad \text{(LRFD Eqn 5.8.3.3-2)}$$

$$\text{Web\_crushing\_limit} = 397.3 \text{ kips}$$

$$\text{Check\_web\_crushing\_limit} := \begin{cases} \text{"OK"} & \text{if } \left(V_c + V_s + V_f + V_p\right) \le \text{Web\_crushing\_limit} \\ \text{"No Good"} & \text{otherwise} \end{cases}$$

$$\text{Check\_web\_crushing\_limit} = \text{"OK"}$$

6. SUMMARY

Externally bonded FRP sheets were designed in this example. The FRP sheets are applied at 90 degrees with respect to the longitudinal axis of the member with the U-wrap configuration as shown in Figure 4. In addition, an anchorage system is installed. The final design is summarized as:

Use number of plies of FRP sheets $n_f = 1$

Use the width of FRP sheets $w_f = 5.5$ in.

Use the center-to-center spacing of FRP sheets $s_f = 18$ in.

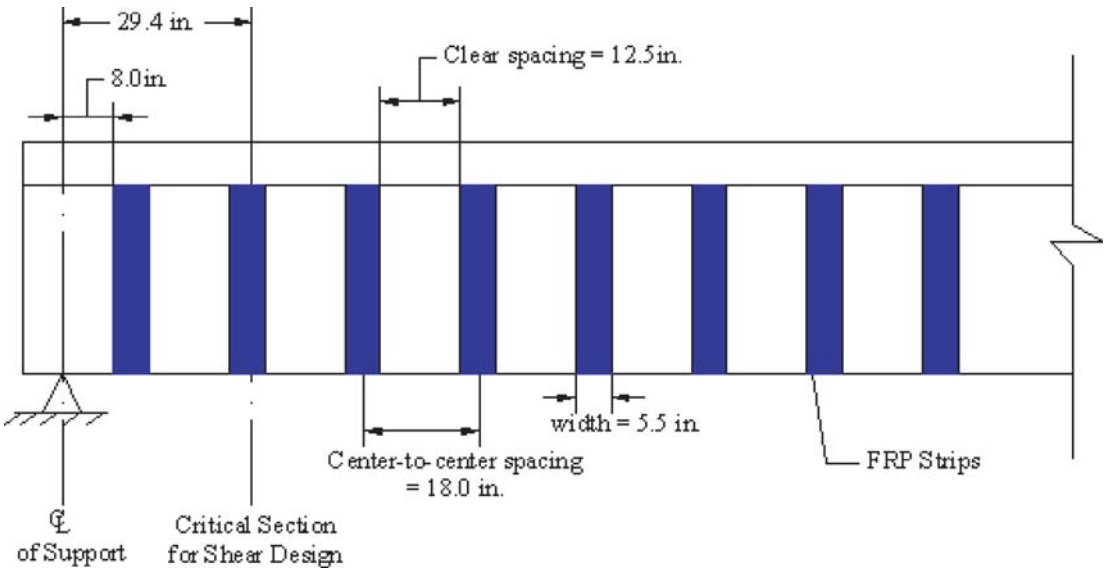

Figure 4. Final design of FRP strengthening.

DESIGN EXAMPLE 2-1: RC T-Beam with Internal Transverse Steel Reinforcement Strengthened with FRP in U-wrap Configuration without Anchorage Systems

1. INTRODUCTION

This example demonstrates the design procedures for externally bonded FRP shear reinforcement of an older reinforced concrete (RC) bridge using a U-wrap configuration without anchorage. The bridge consists of simply supported T-beams spanning 42 feet and spaced at 4.5 feet on center. The T-beams contain transverse steel reinforcement spaced at 12 inches on center. Additional details of the T-beam are provided in Figures 1 and 2.

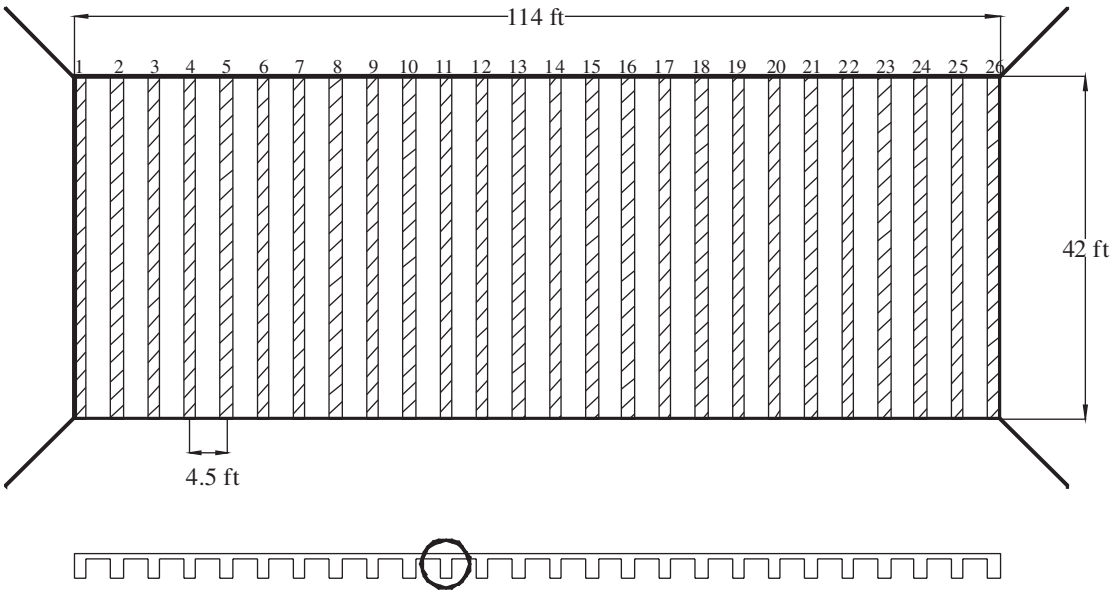

Figure 1. Bridge plan and transverse section.

2. MATERIAL PROPERTIES

The following material properties have been chosen to represent those anticipated in an older bridge for which shear deficiencies might be expected.

2.1. Concrete

Compressive strength $f'_c := 3.0$ ksi

Modulus of elasticity $\left(E_c := 33\cdot(1.5)^{1.5}\sqrt{f'_c\cdot 1000}\right)$ ksi

$$\left(E_c\right) = 3321 \text{ ksi}$$

$$\beta_1 := \begin{cases} 0.85 \text{ if } f'_c \le 4 \\ 0.65 \text{ if } f'_c \ge 8 \\ \left[0.85 - 0.05 \cdot \left(f'_c - 4\right)\right] \text{ otherwise} \end{cases}$$

$$\beta_1 = 0.85$$

2.2. Longitudinal Reinforcement

Yield strength $f_y := 60$ ksi

Modulus of elasticity $E_s := 29000$ ksi

2.3. Internal Steel Shear Reinforcement

Yield strength $f_{yt} := 60$ ksi

2.4. FRP Reinforcement

Carbon Fiber Sheets are used in this example.

Thickness $t_f := 0.0065$ in.

Failure strength $f_{fu} := 550$ ksi

Modulus of elasticity $E_f := 33000$ ksi

Failure strain $\varepsilon_{fu} := \frac{f_{fu}}{E_f}$

$$\varepsilon_{fu} = 0.017 \text{ in./in.}$$

3. GEOMETRICAL PROPERTIES

Total Height $h_T := 37$ in.

Flange Thickness $h_f := 7$ in.

Width of the web $b_v := 18$ in.

Effective width of the flange $b_{eff} := 54$ in.

Tensile reinforcement = 12#11 $A_s := 18.72 \text{ in.}^2$

Internal shear reinforcement = #3 at 12 in. spacing

$A_v := 0.22 \text{ in.}^2$ $s_v := 12$ in. $\alpha := 90 \cdot \text{deg}$

Distance from the extreme compression fiber to the center of the steel at the section d := 32.7 in.

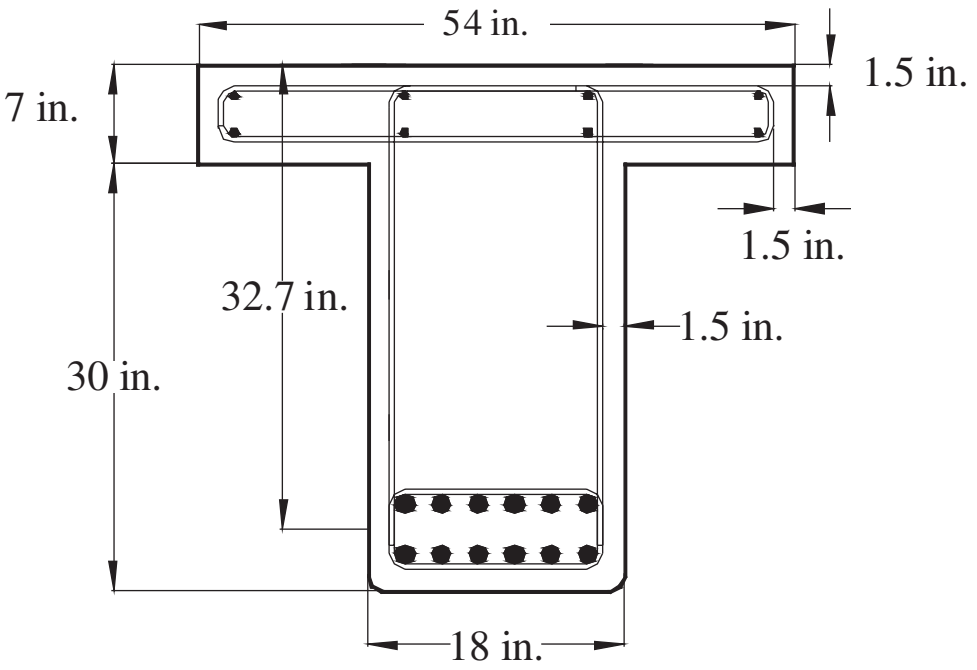

Figure 2. Cross-section of an intermediate beam.

4. CALCULATION OF THE FACTORED SHEAR FORCE AND NOMINAL SHEAR RESISTANCE

4.1 Factored Shear Force at the Critical Section

$V_{u\_crit} := 120$ kips

4.2. Calculation of Nominal Shear Resistance

For this example, the simplified approach is followed.

$(\theta := 45 \text{ deg})$ $(\beta := 2)$

The nominal shear resistance provided by the concrete, V_c, is calculated in accordance with LRFD Eqn.5.8.3.3-3 as:

Assuming rectangular section behavior with no compression steel, the distance from the extreme compression fiber to the neutral axis, c_c, may be calculated as:

$$\left(c_{c1} := \frac{A_s \cdot f_y}{0.85 \cdot f'_c \cdot b_{eff} \cdot \beta_1} \right) \qquad \left(c_{c1} \right) = 9.6 \text{ in.}$$

$$\left(a_{c1} := \beta_1 \cdot c_{c1} \right) \qquad \left(a_{c1} \right) = 8.16 \text{ in.}$$

$$\left(\text{check\_a}_{c1} := \left\| \begin{array}{ll} \text{"Assumption is correct"} & \text{if } \left(a_{c1} \le h_f\right) \\ \text{"Not behave as rectangular"} & \text{otherwise} \end{array} \right. \right)$$

$$\left(\text{check\_a}_{c1}\right) = \text{"Not behave as rectangular"}$$

Assuming T-beam section behavior with no compression steel, the distance from the extreme compression fiber to the neutral axis, c_c, may be calculated as:

$$\left(c_{c2} := \frac{A_s \cdot f_y - 0.85 \cdot f'_c \cdot \left(b_{eff} - b_v\right) \cdot h_f}{0.85 \cdot f'_c \cdot b_v \cdot \beta_1} \right) \qquad \left(c_{c2}\right) = 12.32 \text{ in.}$$

$$\left(a_{c2} := \beta_1 \cdot c_{c2}\right) \qquad \left(a_{c2}\right) = 10.47 \text{ in.}$$

$$\left(\text{check\_a}_{c2} := \left\| \begin{array}{ll} \text{"Assumption is correct"} & \text{if } \left(a_{c2} \ge h_f\right) \\ \text{"Not behave as rectangular"} & \text{otherwise} \end{array} \right. \right)$$

$$\left(\text{check\_a}_{c2}\right) = \text{"Assumption is correct"}$$

Therefore $\left(c_c := c_{c2}\right)$ $\left(c_c\right) = 12.32$ in.

$\left(a_c := a_{c2}\right)$ $\left(a_c\right) = 10.47$ in.

The effective shear depth d_v is taken as the distance, measured perpendicular to the neutral axis, between the resultants of the tensile and compressive forces due to flexure; it need not be taken less than the greater of $0.9d_e$ or $0.72h$ (LRFD Article5.8.2.9)

$$\left(d_{v1} := d - \frac{a_c}{2} \right) \left(d_{v2} := 0.9 \cdot d\right) \left(d_{v3} := 0.72 \cdot h_T\right)$$

$$\left(d_v := \max\left(d_{v1}, d_{v2}, d_{v3}\right)\right)$$

$$\left(d_v\right) = 29.43 \text{ in.}$$

The nominal shear resistance provided by the concrete is:

$$V_c := 0.0316 \cdot \beta \cdot \sqrt{f'_c} \cdot b_v \cdot d_v \qquad \text{(LRFD Eqn. 5.8.3.3-3)}$$

$$\left(V_c\right) = 57.988 \text{ kips}$$

The nominal shear resistance provided by the internal steel reinforcement is:

$$V_s := \frac{A_v \cdot f_{yt} \cdot d_v \cdot (\cot(\theta) + \cot(\alpha)) \sin(\alpha)}{s_v} \qquad \text{(LRFD Eqn. 5.8.3.3-4)}$$

$$V_s = 32.373 \text{ kips}$$

The nominal shear resistance provided by the vertical component of prestressing strands is:

$(V_p := 0)$

The nominal shear resistance of the member is:

$V_n := V_c + V_s + V_p$ (LRFD Eqn. 5.8.3.3-1)

$V_n = 90.36$ kips

5. DESIGN OF FRP SHEAR REINFORCEMENT

5.1 Check if FRP Reinforcement is Necessary or Not

Strength reduction factor for shear $(\phi := 0.9)$

$$\text{Check\_FRP\_Needed} := \begin{cases} \text{"NOT need shear reinforcement"} & \text{if } \left(\phi \cdot V_n \geq V_{u\_crit}\right) \\ \text{"NEED shear reinforcement"} & \text{otherwise} \end{cases}$$

Check_FRP_Needed = "NEED shear reinforcement"

5.2 Computation of Required V_f

$$V_{f\_req} := \frac{V_{u\_crit}}{\phi} - V_n$$

$V_{f\_req} = 43$ kips

5.3 Selection of FRP Strengthening Scheme

U-wrap configuration is used with anchorage systems at the end of the sheets. The FRP sheets will be applied at 90 degrees with respect to the longitudinal axis of the girder as shown in the Figure 3 below. First, the spacing of FRP strips is chosen to meet the maximum spacing requirement. Then, the width of the FRP strips is selected to adjust the amount of FRP strips.

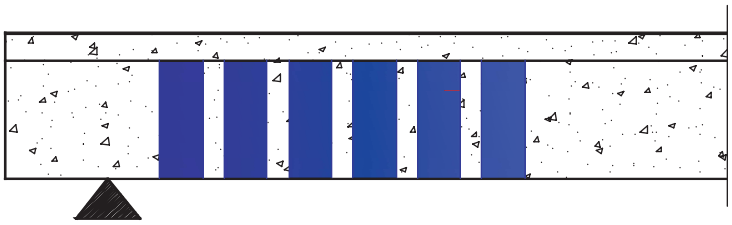

Figure 3. FRP strengthening scheme.

Use number of plies of FRP sheets $n_f := 1$

Use the width of FRP sheets $w_f := 4\ in.$

Use the center-to-center spacing of FRP sheets $s_f := 12\ in.$

Orientation of FRP sheets $\alpha_f := 90\ deg$

Effective depth of FRP sheets $d_f := d - h_f$

$$d_f = 25.7\ in.$$

Check if the selected spacing is acceptable

Shear stress on concrete is:

$$v_u := \frac{V_{u\_crit} - \phi \cdot V_p}{\phi \cdot b_v \cdot d_v} \qquad \text{(LRFD Eqn. 5.8.2.9-1)}$$

$$v_u = 0.252\ ksi$$

The maximum spacing of the transverse reinforcement is:

$$s_{max} := \begin{cases} \min(0.8 \cdot d_v, 24) & \text{if } v_u < 0.125 \cdot f'_c \qquad \text{(LRFD Eqn. 5.8.2.7-1)} \\ \min(0.4 \cdot d_v, 12) & \text{otherwise} \qquad \text{(LRFD Eqn. 5.8.2.7-2)} \end{cases}$$

$$s_{max} = 23.5$$

$$Check\_Spacing := \begin{cases} \text{"Acceptable"} & \text{if } s_f \le s_{max} \\ \text{"NOT\_Acceptable\_Change\_the\_Spacing"} & \text{otherwise} \end{cases}$$

$$Check\_Spacing = \text{"Acceptable"}$$

5.4 Calculation of Shear Resistance of FRP, V_f

The FRP reinforcement ratio is:

$$\rho_f := \frac{2 \cdot n_f \cdot w_f \cdot t_f}{b_v \cdot s_f} \qquad \text{(Attachment A Eqn. 5.8.3.3-10)}$$

$$\rho_f = 2.407 \times 10^{-4}$$

The FRP strain reduction factor is:

$$R_f := \min\left[3\cdot\left(\rho_f\cdot E_f\right)^{-0.67},\ 1.0\right] \qquad \text{(Attachment A Eqn. 5.8.3.3-9)}$$

$$R_f = 0.748$$

The effective strain of FRP is:

$$\varepsilon_{fe} := \min\left(R_f\cdot\varepsilon_{fu},\ 0.012\right) \qquad \text{(Attachment A Eqn. 5.8.3.3-7)}$$

$$\varepsilon_{fe} = 0.012 \text{ in./in.}$$

The effective stress of FRP is:

$$f_{fe} := \varepsilon_{fe}\cdot E_f \qquad \text{(Attachment A Eqn. 5.8.3.3-6)}$$

$$\left(f_{fe}\right) = 396 \text{ ksi}$$

The shear contribution of the FRP can be then calculated.

$$V_f := \rho_f\cdot E_f\cdot\varepsilon_{fe}\cdot b_v\cdot d_f\cdot\left(\sin\left(\alpha_f\right) + \cos\left(\alpha_f\right)\right) \qquad \text{(Attachment A Eqn. 5.8.3.3-5)}$$

$$\left(V_f\right) = 44.1 \text{ kips}$$

$$V_{f\_check1} := \begin{cases} \text{"Change FRP Strengthening Scheme"} & \text{if } \left(V_f < V_{f\_req}\right) \\ \text{"Provided FRP Strength Large Enough"} & \text{otherwise} \end{cases}$$

$$V_{f\_check1} = \text{"Provided FRP Strength Large Enough"}$$

$$V_{f\_check2} := \begin{cases} \text{"Provided FRP amount is adequate"} & \text{if } \left(V_{f\_req} \le V_f < 1.1\cdot V_{f\_req}\right) \\ \text{"Change the FRP amount slightly"} & \text{otherwise} \end{cases}$$

$$\left(V_{f\_check2}\right) = \text{"Provided FRP amount is adequate"}$$

5.5 Calculation of Design Shear Resistance of the Member

The design strength of the member is:

$$\phi V_{n\_total} := \phi\cdot\left(V_c + V_p + V_s + V_f\right) \qquad \text{(Attachment A Eqn. 5.8.3.3-1)}$$

$$\left(\phi V_{n\_total}\right) = 121.02 \text{ kips}$$

$$\phi V_{n\_check} := \begin{cases} \text{"Not Good"} & \text{if } V_{u\_crit} > \phi V_{n\_total} \\ \text{"OK"} & \text{otherwise} \end{cases}$$

$$\left(\phi V_{n\_total}\right) = \text{"OK"}$$

$$\text{Web\_crushing\_limit} := 0.25 \cdot f'_c \cdot b_v \cdot d_v + V_p \qquad \text{(LRFD Eqn. 5.8.3.3-2)}$$

$$\text{Web\_crushing\_limit} = 397.3 \text{ kips}$$

$$\text{Check\_web\_crushing\_limit} := \begin{cases} \text{"OK"} & \text{if } \left(V_c + V_s + V_f + V_p\right) \le \text{Web\_crushing\_limit} \\ \text{"No Good"} & \text{otherwise} \end{cases}$$

$$\text{Check\_web\_crushing\_limit} = \text{"OK"}$$

6. SUMMARY

Externally bonded FRP sheets were designed in this example. The FRP sheets are applied at 90 degrees with respect to the longitudinal axis of the member with the U-wrap configuration and without anchorage systems as shown in Figure 4. The final design is summarized as:

Use number of plies of FRP sheets $n_f = 1$

Use the width of FRP sheets $w_f = 4$ in.

Use the center-to-center spacing of FRP sheets $s_f = 12$ in.

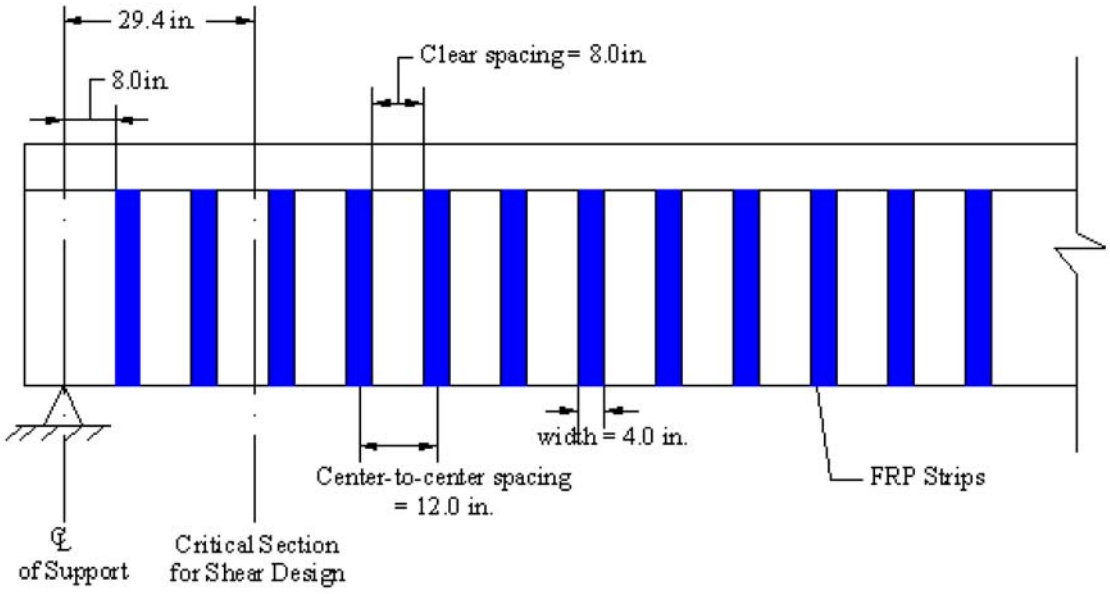

Figure 4. Final design of FRP strengthening.

DESIGN EXAMPLE 2-2: RC T-Beam with Internal Transverse Steel Reinforcement Strengthened with FRP in U-wrap Configuration with an Anchorage System

1. INTRODUCTION

This example demonstrates the design procedures for externally bonded FRP shear reinforcement of an older reinforced concrete (RC) bridge using a U-wrap configuration with anchorage. The bridge consists of simply supported T-beams spanning 42 feet and spaced at 4.5 feet on center. The T-beams contain transverse steel reinforcement spaced at 12 inches on center. Additional details of the T-beam are provided in Figures 1 and 2.

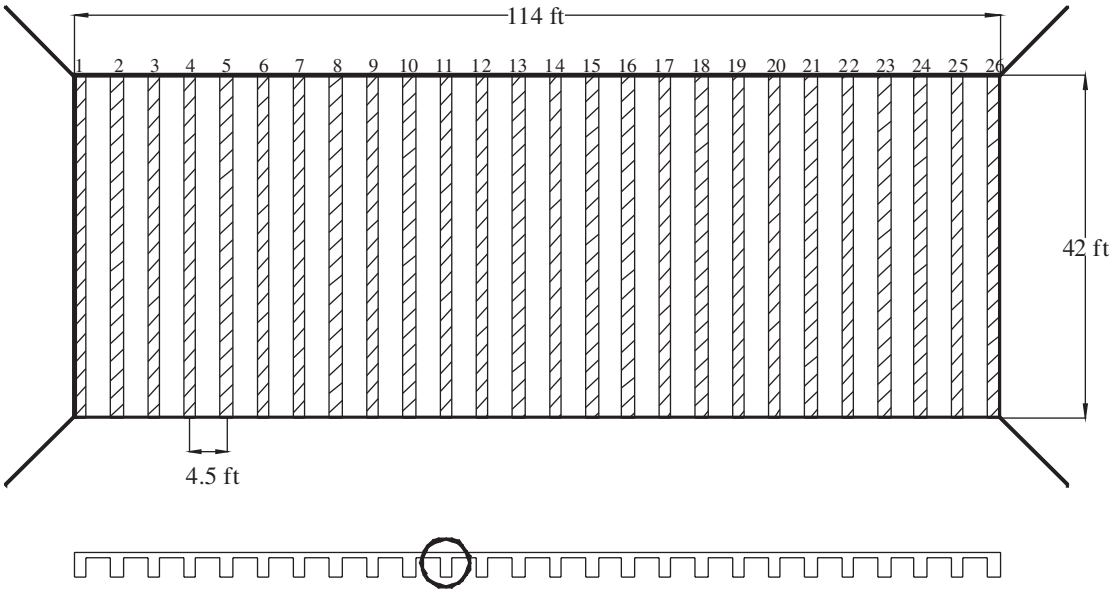

Figure 1. Bridge plan and transverse section.

2. MATERIAL PROPERTIES

The following material properties have been chosen to represent those anticipated in an older bridge for which shear deficiencies might be expected.

2.1. Concrete

Compressive strength $f'_c := 3.0$ ksi

Modulus of elasticity $\left(E_c := 33 \cdot (1.5)^{1.5} \sqrt{f'_c \cdot 1000} \right)$ ksi

$$\left(E_c\right) = 3321 \text{ ksi}$$

$$\beta_1 := \begin{cases} 0.85 \text{ if } f'_c \le 4 \\ 0.65 \text{ if } f'_c \ge 8 \\ \left[0.85 - 0.05 \cdot \left(f'_c - 4\right)\right] \text{ otherwise} \end{cases}$$

$$\beta_1 = 0.85$$

2.2. Longitudinal Reinforcement

Yield strength $f_y := 60$ ksi

Modulus of elasticity $E_s := 29000$ ksi

2.3. Internal Steel Shear Reinforcement

Yield strength $f_{yt} := 60$ ksi

2.4. FRP Reinforcement

Carbon Fiber Sheets are used in this example.

Thickness $t_f := 0.0065$ in.

Failure strength $f_{fu} := 550$ ksi

Modulus of elasticity $E_f := 33000$ ksi

Failure strain $\varepsilon_{fu} := \dfrac{f_{fu}}{E_f}$

$$\varepsilon_{fu} = 0.017 \text{ in./in.}$$

3. GEOMETRICAL PROPERTIES

Total Height $h_T := 37$ in.

Flange Thickness $h_f := 7$ in.

Width of the web $b_v := 18$ in.

Effective Width of the Flange $b_{eff} := 54$ in.

Tensile reinforcement = 12#11 $A_s := 18.72$ in.^{2}

Internal shear reinforcement = #3 at 12 in. spacing

$A_v := 0.22$ in^2 $\quad s_v := 12$ in. $\quad \alpha := 90$ deg

Distance from the extreme compression fiber to the center of the steel at the section d := 32.7 in.

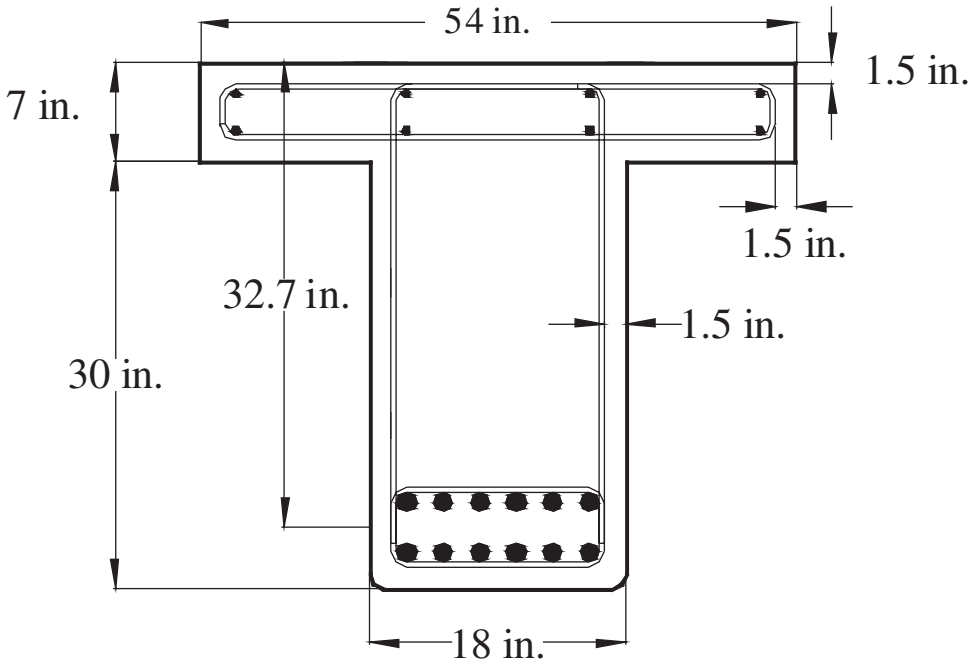

Figure 2. Cross-section of an intermediate beam.

4. CALCULATION OF THE FACTORED SHEAR FORCE AND NOMINAL SHEAR RESISTANCE

4.1 Factored Shear Force at the Critical Section

$V_{u\_crit} := 120 \text{ kips}$

4.2. Calculation of Nominal Shear Resistance

For this example, the simplified approach is followed.

$(\theta := 45 \text{ deg})$ $(\beta := 2)$

The nominal shear resistance provided by the concrete, V_c, is calculated in accordance with LRFD Eqn.5.8.3.3-3 as:

Assuming rectangular section behavior with no compression steel, the distance from the extreme compression fiber to the neutral axis, c_c, may be calculated as:

$$\left(c_{c1} := \frac{A_s \cdot f_y}{0.85 \cdot f'_c \cdot b_{eff} \cdot \beta_1} \right) \qquad \left(c_{c1} \right) = 9.6 \text{ in.}$$

$$\left(a_{c1} := \beta_1 \cdot c_{c1} \right) \qquad \left(a_{c1} \right) = 8.16 \text{ in.}$$

$$\left(\text{check\_a}_{c1} := \begin{cases} \text{"Assumption is correct"} & \text{if } \left(a_{c1} \le h_f\right) \\ \text{"Not behave as rectangular"} & \text{otherwise} \end{cases}\right)$$

$$\left(\text{check\_a}_{c1}\right) = \text{"Not behave as rectangular"}$$

Assuming T-beam section behavior with no compression steel, the distance from the extreme compression fiber to the neutral axis, c_c, may be calculated as:

$$\left(c_{c2} := \frac{A_s \cdot f_y - 0.85 \cdot f'_c \cdot \left(b_{eff} - b_v\right) \cdot h_f}{0.85 \cdot f'_c \cdot b_v \cdot \beta_1}\right) \qquad \left(c_{c2}\right) = 12.32 \text{ in.}$$

$$\left(a_{c2} := \beta_1 \cdot c_{c2}\right) \qquad \left(a_{c2}\right) = 10.47 \text{ in.}$$

$$\left(\text{check\_a}_{c2} := \begin{cases} \text{"Assumption is correct"} & \text{if } \left(a_{c2} \ge h_f\right) \\ \text{"Not behave as rectangular"} & \text{otherwise} \end{cases}\right)$$

$$\left(\text{check\_a}_{c2}\right) = \text{"Assumption is correct"}$$

Therefore $\left(c_c := c_{c2}\right)$ $\left(c_c\right) = 12.32$ in.

$\left(a_c := a_{c2}\right)$ $\left(a_c\right) = 10.47$ in.

The effective shear depth d_v is taken as the distance, measured perpendicular to the neutral axis, between the resultants of the tensile and compressive forces due to flexure; it need not be taken less than the greater of $0.9d_e$ or $0.72h$ (LRFD Article5.8.2.9)

$$\left(d_{v1} := d - \frac{a_c}{2}\right) \left(d_{v2} := 0.9 \cdot d\right) \left(d_{v3} := 0.72 \cdot h_T\right)$$

$$\left(d_v := \max\left(d_{v1}, d_{v2}, d_{v3}\right)\right)$$

$$\left(d_v\right) = 29.4 \text{ in.}$$

The nominal shear resistance provided by the concrete is:

$$V_c := 0.0316 \cdot \beta \cdot \sqrt{f'_c} \cdot b_v \cdot d_v \qquad \text{(LRFD Eqn. 5.8.3.3-3)}$$

$$\left(V_c\right) = 58 \text{ kips}$$

The nominal shear resistance provided by the internal steel reinforcement is:

$$V_s := \frac{A_v \cdot f_{yt} \cdot d_v \cdot (\cot(\theta) + \cot(\alpha)) \sin(\alpha)}{s_v} \qquad \text{(LRFD Eqn. 5.8.3.3-4)}$$

$$V_s = 32.4 \text{ kips}$$

The nominal shear resistance provided by the vertical component of prestressing strands is:

$\left(V_p := 0\right)$

The nominal shear resistance of the member is:

$V_n := V_c + V_s + V_p$ (LRFD Eqn. 5.8.3.3-1)

$V_n = 90.4 \text{ kips}$

5. DESIGN OF FRP SHEAR REINFORCEMENT

5.1 Check if FRP Reinforcement is Necessary or Not

Strength reduction factor for shear $(\phi := 0.9)$

$$\text{Check\_FRP\_Needed} := \begin{cases} \text{"NOT need shear reinforcement"} & \text{if } \left(\phi \cdot V_n \geq V_{u\_crit}\right) \\ \text{"NEED shear reinforcement"} & \text{otherwise} \end{cases}$$

Check_FRP_Needed = "NEED shear reinforcement"

5.2 Computation of Required V_f

$$V_{f\_req} := \frac{V_{u\_crit}}{\phi} - V_n$$

$V_{f\_req} = 43 \text{ kips}$

5.3 Selection of FRP Strengthening Scheme

U-wrap configuration is used with anchorage systems at the end of the sheets. The FRP sheets will be applied at 90 degrees with respect to the longitudinal axis of the girder as shown in the Figure 3 below. Anchorage systems will be installed at the top end portion of the FRP sheets to increase the effectiveness of FRP shear strengthening. First, the spacing of FRP strips is chosen to meet the maximum spacing requirement. Then, the width of the FRP strips is selected to adjust the amount of FRP strips.

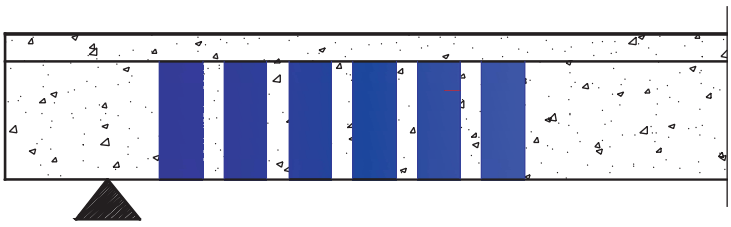

Figure 3. FRP strengthening scheme.

Use number of plies of FRP sheets $n_f := 1$

Use the width of FRP sheets $w_f := 4$ in.

Use the center-to-center spacing of FRP sheets $s_f := 16$ in.

Orientation of FRP sheets $\alpha_f := 90$ deg

Effective depth of FRP sheets $d_f := d - h_f$

$d_f = 25.7$ in.

Check if the selected spacing is acceptable or not

Shear stress on concrete is:

$$v_u := \frac{V_{u\_crit} - \phi \cdot V_p}{\phi \cdot b_v \cdot d_v} \qquad \text{(LRFD Eqn. 5.8.2.9-1)}$$

$(v_u) = 0.252$ ksi

The maximum spacing of the transverse reinforcement is:

$$s_{max} := \begin{cases} \min(0.8 \cdot d_v, 24) & \text{if } v_u < 0.125 \cdot f'_c \qquad \text{(LRFD Eqn. 5.8.2.7-1)} \\ \min(0.4 \cdot d_v, 12) & \text{otherwise} \qquad \text{(LRFD Eqn. 5.8.2.7-2)} \end{cases}$$

$s_{max} = 23.5$

$$Check\_Spacing := \begin{cases} \text{"Acceptable"} & \text{if } s_f \le s_{max} \\ \text{"NOT\_Acceptable\_Change\_the\_Spacing"} & \text{otherwise} \end{cases}$$

Check_Spacing = "Acceptable"

5.4 Calculation of Shear Resistance of FRP, V_f

The FRP reinforcement ratio is:

$$\rho_f := \frac{2 \cdot n_f \cdot w_f \cdot t_f}{b_v \cdot s_f} \qquad \text{(Attachment A Eqn. 5.8.3.3-10)}$$

$(\rho_f) = 1.806 \times 10^{-4}$

The FRP strain reduction factor is:

$$R_f := \min\left[4\cdot\left(\rho_f\cdot E_f\right)^{-0.67},\ 1.0\right] \qquad \text{(Attachment A Eqn. 5.8.3.3-8)}$$

$$R_f = 1$$

The effective strain of FRP is:

$$\varepsilon_{fe} := R_f\cdot\varepsilon_{fu} \qquad \text{(Attachment A Eqn. 5.8.3.3-7)}$$

$$\varepsilon_{fe} = 0.017 \text{ in./in.}$$

The effective stress of FRP is:

$$f_{fe} := \varepsilon_{fe}\cdot E_f \qquad \text{(Attachment A Eqn. 5.8.3.3-6)}$$

$$\left(f_{fe}\right) = 550 \text{ ksi}$$

The shear contribution of the FRP can be then calculated.

$$\left(V_f := \rho_f\cdot E_f\cdot\varepsilon_{fe}\cdot b_v\cdot d_f\cdot\left(\sin\left(\alpha_f\right) + \cos\left(\alpha_f\right)\right)\right) \qquad \text{(Attachment A Eqn. 5.8.3.3-5)}$$

$$\left(V_f\right) = 45.9 \text{ kips}$$

$$V_{f\_check1} := \begin{cases} \text{"Change FRP Strengthening Scheme"} & \text{if } \left(V_f < V_{f\_req}\right) \\ \text{"Provided FRP Strength Large Enough"} & \text{otherwise} \end{cases}$$

$$V_{f\_check1} = \text{"Provided FRP Strength Large Enough"}$$

$$V_{f\_check2} := \begin{cases} \text{"Provided FRP amount is adequate"} & \text{if } \left(V_{f\_req} \le V_f < 1.1\cdot V_{f\_req}\right) \\ \text{"Change the FRP amount slightly"} & \text{otherwise} \end{cases}$$

$$\left(V_{f\_check2}\right) = \text{"Provided FRP amount is adequate"}$$

5.5 Calculation of Design Shear Resistance of the Member

The design strength of the member is:

$$\phi V_{n\_total} := \phi\cdot\left(V_c + V_p + V_s + V_f\right) \qquad \text{(Attachment A Eqn. 5.8.3.3-1)}$$

$$\left(\phi V_{n\_total}\right) = 122.7 \text{ kips}$$

$$\phi V_{n\_check} := \begin{cases} \text{"Not Good"} & \text{if } V_{u\_crit} > \phi V_{n\_total} \\ \text{"OK"} & \text{otherwise} \end{cases}$$

$$\left(\phi V_{n\_check}\right) = \text{"OK"}$$

$$Web\_crushing\_limit := 0.25 \cdot f'_c \cdot b_v \cdot d_v + V_p \qquad \text{(LRFD Eqn. 5.8.3.3-2)}$$

$$Web\_crushing\_limit = 397.3 \text{ kips}$$

$$Check\_web\_crushing\_limit := \begin{cases} \text{"OK"} & \text{if } \left(V_c + V_s + V_f + V_p\right) \le Web\_crushing\_limit \\ \text{"No Good"} & \text{otherwise} \end{cases}$$

$$Check\_web\_crushing\_limit = \text{"OK"}$$

6. SUMMARY

Externally bonded FRP sheets were designed in this example. The FRP sheets are applied at 90 degrees with respect to the longitudinal axis of the member with the U-wrap configuration as shown in Figure 4. In addition, an anchorage system is installed. The final design is summarized as:

Use number of plies of FRP sheets $n_f = 1$

Use the width of FRP sheets $w_f = 4$ in.

Use the center-to-center spacing of FRP sheets $s_f = 16$ in.

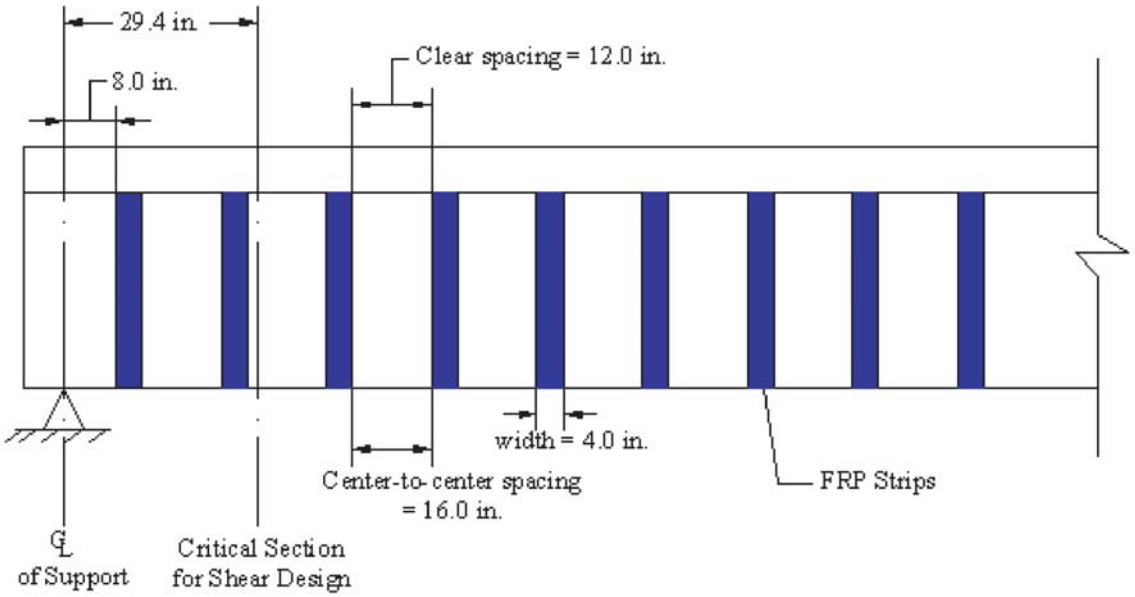

Figure 4. Final design of FRP strengthening.

DESIGN EXAMPLE 3-1: PC I-Beam with Internal Transverse Steel Reinforcement Strengthened with FRP in U-wrap Configuration without Anchorage Systems

1. INTRODUCTION

This example demonstrates the design procedures for externally bonded FRP shear reinforcement of a prestressed I-beam bridge using a U-wrap configuration without anchorage. The bridge consists of five simply supported pretensioned I-beams spanning 42 feet and spaced at 7.5 feet on center. The I-beams are lightly reinforced with transverse steel reinforcement. Additional details of the bulb-tees are provided in Figures 1 and 2.

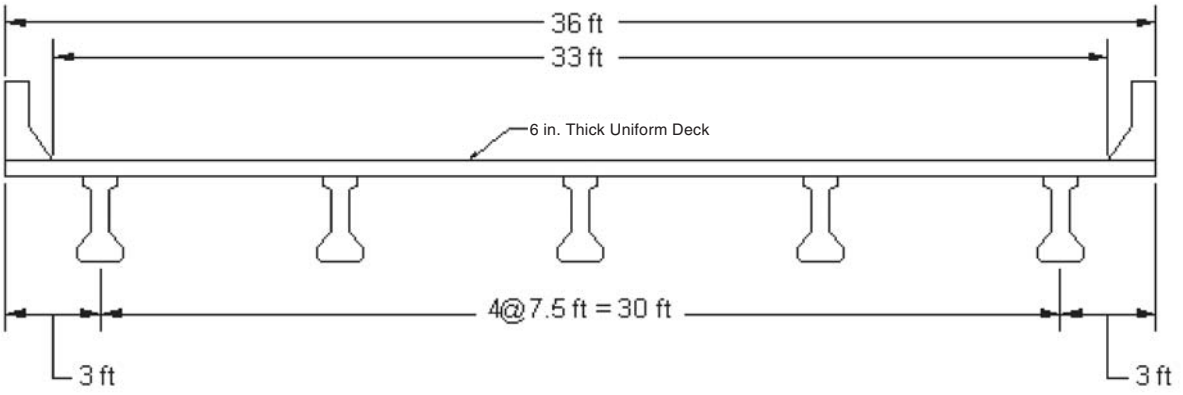

(a) Prestressed I-Beam Bridge Deck Cross-Section

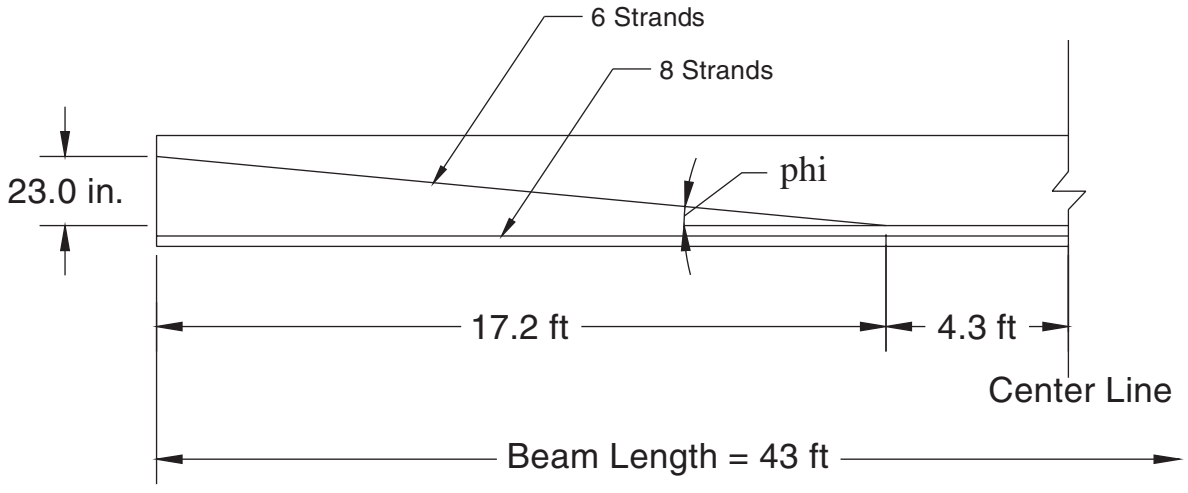

(b) Beam Tendon Geometry

Figure 1. AASHTO bulb-tee bridge deck bridge (Ref. PCI Bridge Design Manual).

2. MATERIAL PROPERTIES

2.1. Concrete

2.1.1 Deck

Compressive strength $f'_{cd} := 4.0\ ksi$

Modulus of elasticity $E_{cd} := 33 \cdot (1.5)^{1.5} \sqrt{f'_{cd} \cdot 1000}\ ksi$

$E_{cd} = 3834\ ksi$

$$\beta_{1d} := \begin{cases} 0.85 \text{ if } f'_{cd} \le 4 \\ 0.65 \text{ if } f'_{cd} \ge 8 \\ \left[0.85 - 0.05 \cdot \left(f'_{cd} - 4\right)\right] \text{ otherwise} \end{cases}$$

$\beta_{1d} = 0.85$

2.1.1 I-Beam

Compressive strength $f'_{cb} := 7.0\ ksi$

Modulus of elasticity $E_{cb} := 33 \cdot (1.5)^{1.5} \sqrt{f'_{cb} \cdot 1000}\ ksi$

$E_{cb} = 5072\ ksi$

$$\beta_{1b} := \begin{cases} 0.85 \text{ if } f'_{cb} \le 4 \\ 0.65 \text{ if } f'_{cb} \ge 8 \\ \left[0.85 - 0.05 \cdot \left(f'_{cb} - 4\right)\right] \text{ otherwise} \end{cases}$$

$\beta_{1b} = 0.7$

2.2. Prestressing Strands

Specified tensile strength $f_{pu} := 270$ ksi

Yield strength $f_{py} := 243$ ksi

Modulus of elasticity $E_{ps} := 28500$ ksi

Diameter = 0.5 in.

Total Area of the 14 strands $A_{ps} := 2.142$ in.^{2}

$k := 0.28$ for low-relaxation steel

2.3. Internal Steel Shear Reinforcement

Yield strength $f_{yt} := 60$ ksi

2.4. FRP Reinforcement

Carbon Fiber Sheets are used in this example.

Thickness $t_f := 0.0065$ in.

Failure strength $f_{fu} := 550$ ksi

Modulus of elasticity $E_f := 33000$ ksi

Failure strain $\varepsilon_{fu} := \dfrac{f_{fu}}{E_f}$

$\varepsilon_{fu} = 0.017$ in./in.

3. GEOMETRICAL PROPERTIES

Total height including deck slab $h_T := 38$ in.

Flange thickness $h_f := 6$ in.

Width of the web $b_v := 7$ in.

Effective width of the Flange $b_{eff} := 79.0$ in.

Internal shear reinforcement = #3 at 12 in. spacing

$A_v := 0.22$ in.^{2} $\quad s_v := 12$ in. $\quad \alpha := 90 \cdot$deg

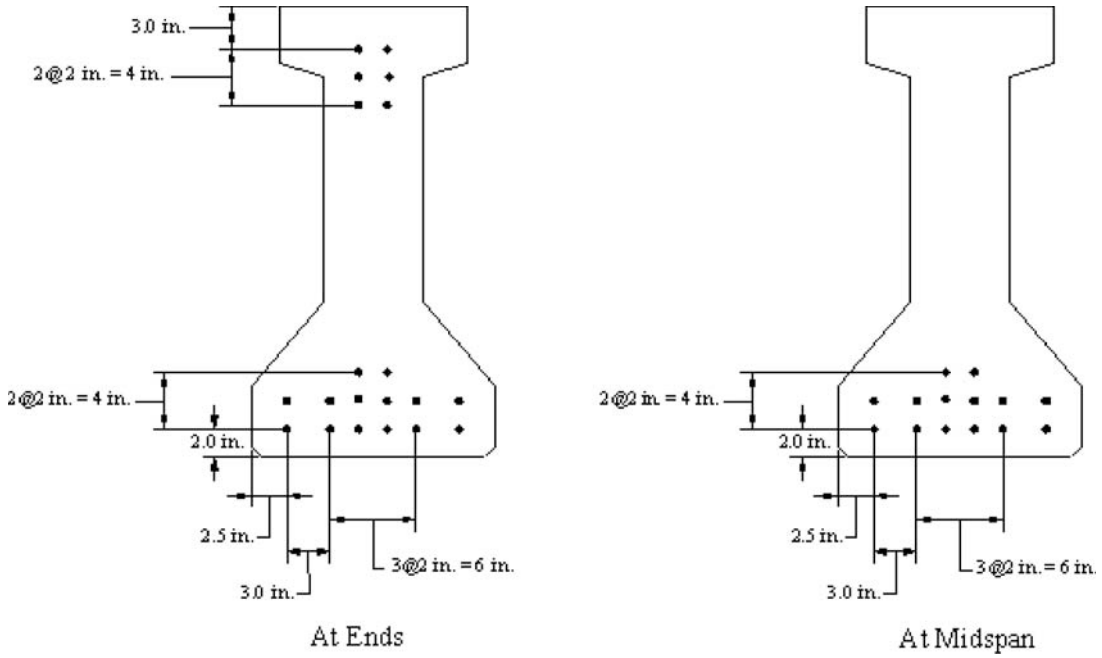

(a) I-Beam Prestressing Pattern.

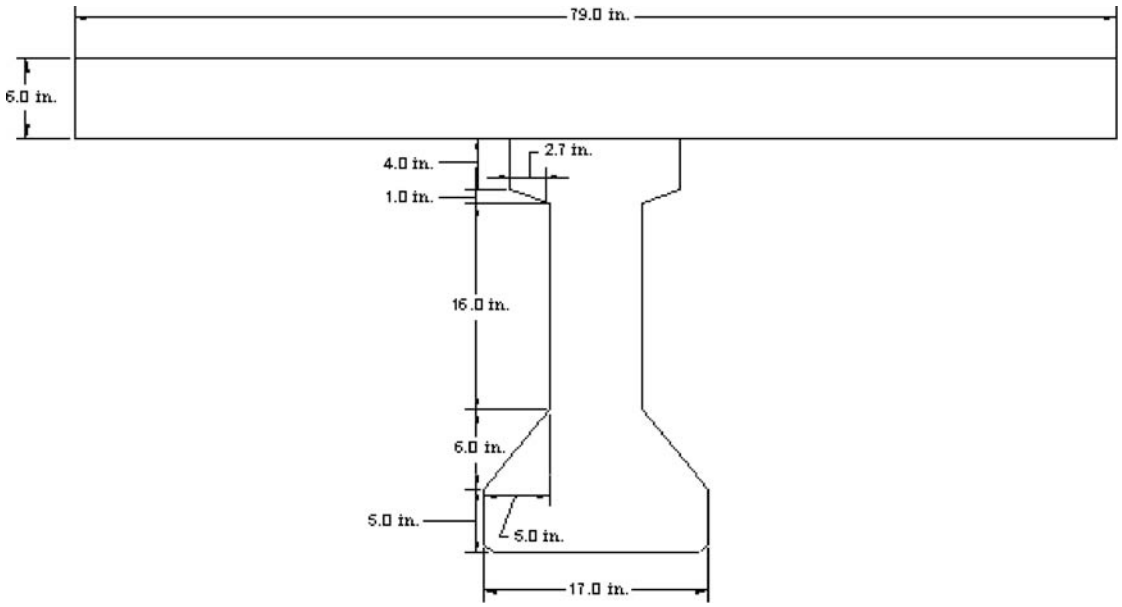

(b) Cross-Section of an Intermediate Beam

Figure 2. Cross-section of an intermediate beam.

4. CALCULATION OF THE FACTORED SHEAR FORCE AND NOMINAL SHEAR RESISTANCE

4.1 Factored Shear Force at the Critical Section

$V_{u\_crit} := 100\ kips$

4.2. Calculation of Nominal Shear Resistance

For this example, the simplified approach is followed.

$\theta := 45 \cdot deg \qquad \beta := 2$

The nominal shear resistance provided by the concrete, V_c, is calculated in accordance with LRFD Eqn.5.8.3.3-3 as:

The distance from the extreme compression fiber to the center of gravity of the strands at the midspan:

$d_p := 34.6\ in.$

Assuming rectangular section behavior with no compression steel, the distance from the extreme compression fiber to the neutral axis, c_c , may be calculated as:

$$c_c := \frac{A_{ps} \cdot f_{pu}}{0.85 \cdot f'_{cd} \cdot b_{eff} \cdot \beta_{1d} + k \cdot A_{ps} \cdot \frac{f_{pu}}{d_p}}$$

$\left(c_c\right) = 2.482\ in.$

$a_c := \beta_{1d} \cdot c_c$

$\left(a_c\right) = 2.11\ in.$

$$\left(check\_a_c := \left\| \begin{array}{ll} \text{"Assumption is correct"} & \text{if } \left(a_c \geq h_f\right) \\ \text{"Not behave as rectangular"} & \text{otherwise} \end{array} \right. \right)$$

$\left(check\_a_c\right) = \text{"Assumption is correct"}$

The effective shear depth d_v is taken as the distance, measured perpendicular to the neutral axis, between the resultants of the tensile and compressive forces due to flexure; it need not be taken to be less than the greater of $0.9d_e$ or 0.72h (LRFD Article5.8.2.9).

Since some of the strands are harped, the effective depth varies point-to-point. However, the effective depth must be calculated at the critical section in shear, which is not yet determined; therefore, an iterative procedure is required. For this example, only the final cycle of the iteration is shown.

Assume d_v $d_{v\_trial} := 27.36$ in.

Calculate the distance from the extreme compression face to the center of gravity of the strand, d_e at the location, d_v away from the centerline of the support.

$$e_{tr} := \frac{2\cdot 4 + 4\cdot 4 + \left[\frac{23}{206.4}\left(206.4 - d_{v\_trial}\right) + 2\right]\cdot 2 + \left[\frac{23}{206.4}\left(206.4 - d_{v\_trial}\right) + 4\right]\cdot 2 + \left[\frac{23}{206.4}\left(206.4 - d_{v\_trial}\right) + 6\right]\cdot 2}{6 + 6 + 2}$$

$d_e := h_T - e_{tr}$

$d_e = 26.021$ in.

Determine d_v $d_{v1} := d_e - \frac{a_c}{2}$ $d_{v2} := 0.9\cdot d_e$ $\left(d_{v3} := 0.72\cdot h_T\right)$

$\left(d_{v\_max} := \max\left(d_{v1}, d_{v2}, d_{v3}\right)\right)$

$\left(d_v := \max\left(d_{v\_max}, 0.5\cdot d_{v\_max}\cdot\cot(\theta)\right)\right)$

Final d_v $\left(d_v\right) = 27.36$ in.

$$Check\_dv1 := \begin{cases} \text{"OK"} & \text{if } 0.995 \le \frac{d_{v\_trial}}{d_v} \le 1.005 \\ \text{"Try Again"} & \text{otherwise} \end{cases}$$

Check_dv1 = "OK"

$$Check\_dv2 := \begin{cases} \text{"OK"} & \text{if } \frac{d_v}{b_v} \le 4 \\ \text{"NOT GOOD"} & \text{otherwise} \end{cases}$$

Check_dv2 = "OK"

The nominal shear resistance provided by the concrete is:

$V_c := 0.0316 \cdot \beta \cdot \sqrt{f'_c} \cdot b_v \cdot d_v$ (LRFD Eqn. 5.8.3.3-3)

$(V_c) = 32$ kips

The nominal shear resistance provided by the internal steel reinforcement is:

$$V_s := \frac{A_v \cdot f_{yt} \cdot d_v \cdot (\cot(\theta) + \cot(\alpha)) \sin(\alpha)}{s_v}$$ (LRFD Eqn. 5.8.3.3-4)

$V_s = 30.1$ kips

Harped tendon force = 6 x 0.153 x 149.0 = 136.8 kips (assuming f_{pe} = 149 ksi)

slope of the tendons $\psi := 0.111$

$V_p := 136.8 \cdot \psi$ $V_p = 15.2$ kips

The nominal shear resistance of the member is:

$V_n := V_c + V_s + V_p$ (LRFD Eqn. 5.8.3.3-1)

$V_n = 77.3$ kips

5. DESIGN OF FRP SHEAR REINFORCEMENT

5.1 Check if FRP Reinforcement is Necessary or Not

Strength reduction factor for shear ($\phi := 0.9$)

$$\text{Check\_FRP\_Needed} := \begin{cases} \text{"NOT need shear reinforcement"} & \text{if } (\phi \cdot V_n \geq V_{u\_crit}) \\ \text{"NEED shear reinforcement"} & \text{otherwise} \end{cases}$$

Check_FRP_Needed = "NEED shear reinforcement"

5.2 Computation of Required V_f

$$V_{f\_req} := \frac{V_{u\_crit}}{\phi} - V_n$$

$V_{f\_req} = 33.8$ kips

5.3 Selection of FRP Strengthening Scheme

U-wrap configuration is used with anchorage systems at the end of the sheets. The FRP sheets will be applied at 90 degrees with respect to the longitudinal axis of the girder as shown in the Figure 3 below. First, the spacing of FRP strips is chosen to meet the maximum spacing requirement. Then, the width of the FRP strips is selected to adjust the amount of FRP strips.

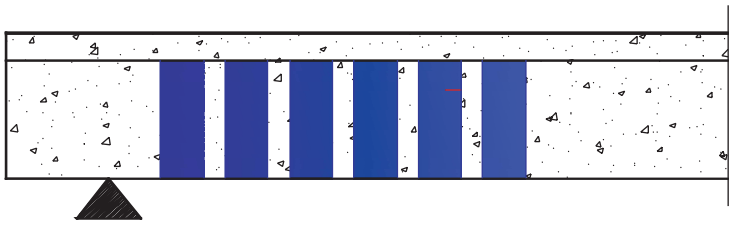

Figure 3. FRP strengthening scheme.

Use number of plies of FRP sheets $n_f := 1$

Use the width of FRP sheets $w_f := 8\ in.$

Use the center-to-center spacing of FRP sheets $s_f := 12\ in.$

Orientation of FRP sheets $\alpha_f := 90\ deg$

Effective depth of FRP sheets $d_f := d_p - h_f$

$$d_f = 28.6\ in.$$

Check if the selected spacing is acceptable or not

Shear stress on concrete is:

$$v_u := \frac{V_{u\_crit} - \phi \cdot V_p}{\phi \cdot b_v \cdot d_v} \qquad \text{(LRFD Eqn. 5.8.2.9-1)}$$

$$(v_u) = 0.501\ ksi$$

The maximum spacing of the transverse reinforcement is:

$$s_{max} := \begin{cases} \min(0.8 \cdot d_v,\ 24) & \text{if } v_u < 0.125 \cdot f'_{cb} \qquad \text{(LRFD Eqn. 5.8.2.7-1)} \\ \min(0.4 \cdot d_v,\ 12) & \text{otherwise} \qquad \text{(LRFD Eqn. 5.8.2.7-2)} \end{cases}$$

$$s_{max} = 21.9$$

$$\text{Check\_Spacing} := \begin{cases} \text{"Acceptable"} & \text{if } s_f \le s_{max} \\ \text{"NOT\_Acceptable\_Change\_the\_Spacing"} & \text{otherwise} \end{cases}$$

$$\text{Check\_Spacing} = \text{"Acceptable"}$$

5.4 Calculation of Shear Resistance of FRP, V_f

The FRP reinforcement ratio is:

$$\rho_f := \frac{2 \cdot n_f \cdot w_f \cdot t_f}{b_v \cdot s_f} \qquad \text{(Attachment A Eqn. 5.8.3.3-10)}$$

$$\left(\rho_f\right) = 1.238 \times 10^{-3}$$

The FRP strain reduction factor is:

$$R_f := \min\left[3 \cdot \left(\rho_f \cdot E_f\right)^{-0.67},\ 1.0\right] \qquad \text{(Attachment A Eqn. 5.8.3.3-9)}$$

$$R_f = 0.25$$

The effective strain of FRP is:

$$\varepsilon_{fe} := \min\left(R_f \cdot \varepsilon_{fu},\ 0.012\right) \qquad \text{(Attachment A Eqn. 5.8.3.3-7)}$$

$$\varepsilon_{fe} = 4.163 \times 10^{-3} \text{ in./in.}$$

The effective stress of FRP is:

$$f_{fe} := \varepsilon_{fe} \cdot E_f \qquad \text{(Attachment A Eqn. 5.8.3.3-6)}$$

$$\left(f_{fe}\right) = 137.4 \text{ ksi}$$

The shear contribution of the FRP can be then calculated.

$$\left(V_f := \rho_f \cdot E_f \cdot \varepsilon_{fe} \cdot b_v \cdot d_f \cdot \left(\sin\left(\alpha_f\right) + \cos\left(\alpha_f\right)\right)\right) \qquad \text{(Attachment A Eqn. 5.8.3.3-5)}$$

$$\left(V_f\right) = 34.1 \text{ kips}$$

$$V_{f\_check1} := \begin{cases} \text{"Change FRP Strengthening Scheme"} & \text{if } \left(V_f < V_{f\_req}\right) \\ \text{"Provided FRP Strength Large Enough"} & \text{otherwise} \end{cases}$$

$$V_{f\_check1} = \text{"Provided FRP Strength Large Enough"}$$

$$V_{f\_check2} := \begin{cases} \text{"Provided FRP amount is adequate"} & \text{if } \left(V_{f\_req} \le V_f < 1.1 \cdot V_{f\_req}\right) \\ \text{"Change the FRP amount slightly"} & \text{otherwise} \end{cases}$$

$$\left(V_{f\_check2}\right) = \text{"Provided FRP amount is adequate"}$$

5.5 Calculation of Design Shear Resistance of the Member

The design strength of the member is:

$$\phi V_{n\_total} := \phi \cdot \left(V_c + V_p + V_s + V_f\right) \qquad \text{(Attachment A Eqn. 5.8.3.3-1)}$$

$$\left(\phi V_{n\_total}\right) = 100.2 \text{ kips}$$

$$\phi V_{n\_check} := \begin{cases} \text{"Not Good"} & \text{if } V_{u\_crit} > \phi V_{n\_total} \\ \text{"OK"} & \text{otherwise} \end{cases}$$

$$\left(\phi V_{n\_check}\right) = \text{"OK"}$$

$$\text{Web\_crushing\_limit} := 0.25 \cdot f'_{cb} \cdot b_v \cdot d_v \cdot V_p \qquad \text{(LRFD Eqn. 5.8.3.3-2)}$$

$$\text{Web\_crushing\_limit} = 350.3 \text{ kips}$$

$$\text{Check\_web\_crushing\_limit} := \begin{cases} \text{"OK"} & \text{if } \left(V_c + V_s + V_f + V_p\right) \le \text{Web\_crushing\_limit} \\ \text{"No Good"} & \text{otherwise} \end{cases}$$

$$\text{Check\_web\_crushing\_limit} = \text{"OK"}$$

6. SUMMARY

Externally bonded FRP sheets were designed in this example. The FRP sheets are applied at 90 degrees with respect to the longitudinal axis of the member with the U-wrap configuration and without anchorage systems as shown in Figure 4. The final design is summarized as:

Use number of plies of FRP sheets $n_f = 1$

Use the width of FRP sheets $w_f = 8$ in.

Use the center-to-center spacing of FRP sheets $s_f = 12$ in.

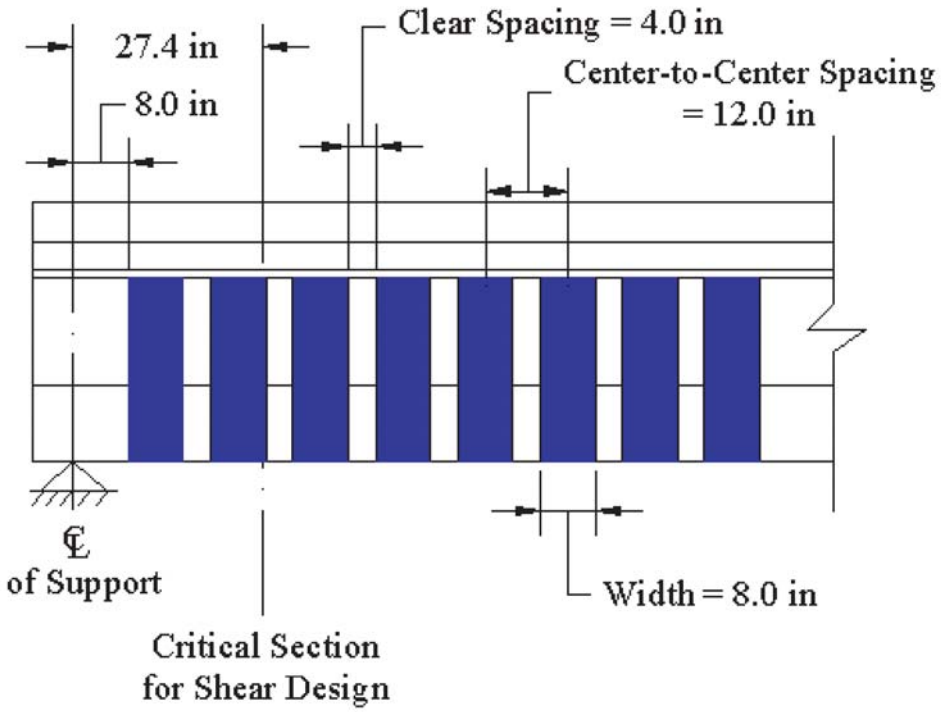

Figure 4. Final design of FRP strengthening.

DESIGN EXAMPLE 3-2: PC I-Beam with Internal Transverse Steel Reinforcement Strengthened with FRP in U-wrap Configuration with an Anchorage System

1. INTRODUCTION

This example demonstrates the design procedures for externally bonded FRP shear reinforcement of a prestressed I-beam bridge using a U-wrap configuration with anchorage. The bridge consists of five simply supported prestensioned I-beams spanning 42 feet and spaced at 7.5 feet on center. The I-beams are lightly reinforced with transverse steel reinforcement. Additional details of the bulb-tees are provided in Figures 1 and 2.

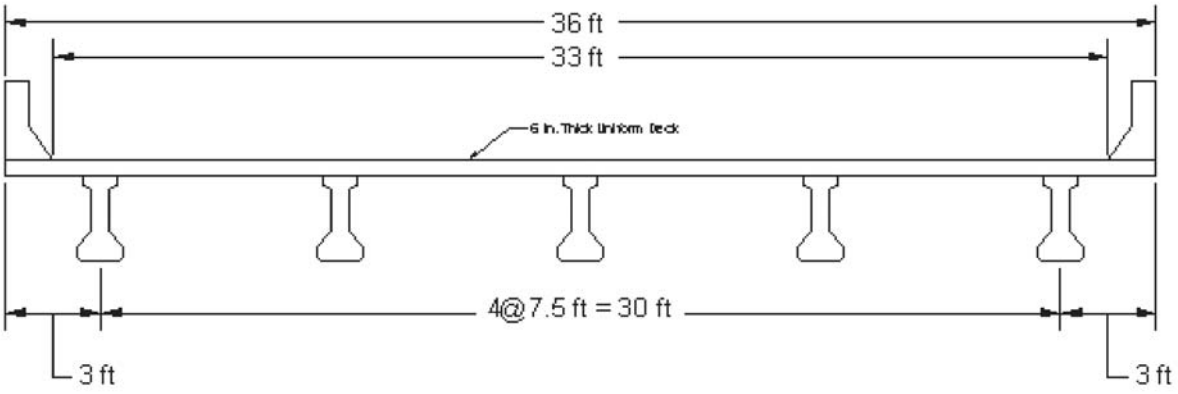

(a) Prestressed I-Beam Bridge Deck Cross-Section

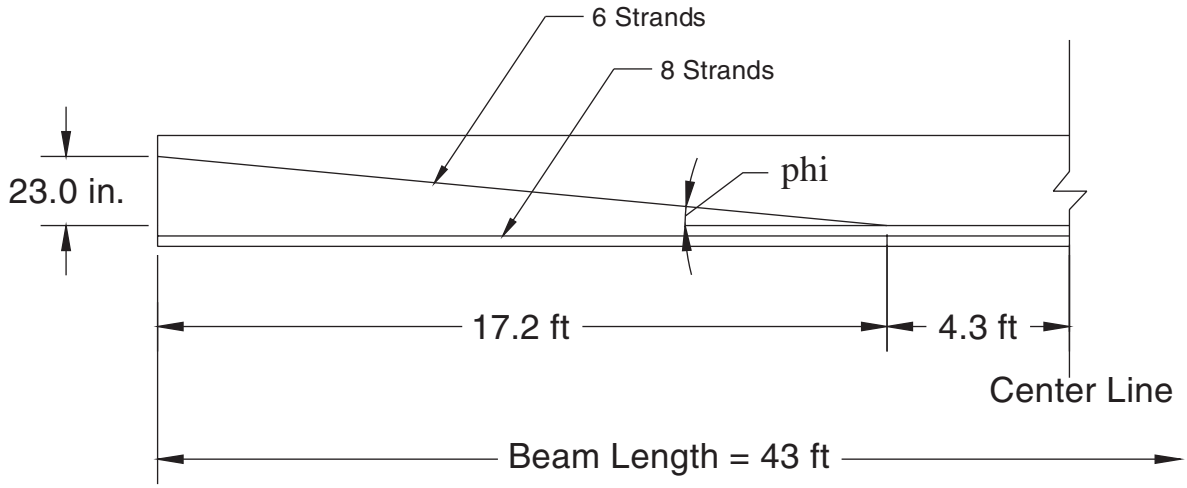

(b) Beam Tendon Geometry

Figure 1. AASHTO bulb-tee bridge deck bridge (Ref. PCI Bridge Design Manual).

2. MATERIAL PROPERTIES

2.1. Concrete

2.1.1 Deck

Compressive strength $f'_{cd} := 4.0\ ksi$

Modulus of elasticity $E_{cd} := 33 \cdot (1.5)^{1.5} \sqrt{f'_{cd} \cdot 1000}\ ksi$

$$E_{cd} = 3834\ ksi$$

$$\beta_{1d} := \begin{cases} 0.85 \text{ if } f'_{cd} \le 4 \\ 0.65 \text{ if } f'_{cd} \ge 8 \\ \left[0.85 - 0.05 \cdot \left(f'_{cd} - 4\right)\right] \text{ otherwise} \end{cases}$$

$$\beta_{1d} = 0.85$$

2.1.1 I-Beam

Compressive strength $f'_{cb} := 7.0\ ksi$

Modulus of elasticity $E_{cb} := 33 \cdot (1.5)^{1.5} \sqrt{f'_{cb} \cdot 1000}\ ksi$

$$E_{cb} = 5072\ ksi$$

$$\beta_{1b} := \begin{cases} 0.85 \text{ if } f'_{cb} \le 4 \\ 0.65 \text{ if } f'_{cb} \ge 8 \\ \left[0.85 - 0.05 \cdot \left(f'_{cb} - 4\right)\right] \text{ otherwise} \end{cases}$$

$$\beta_{1b} = 0.7$$

2.2. Prestressing Strands

Specified tensile strength $f_{pu} := 270\ ksi$

Yield strength $f_{py} := 243\ ksi$

Modulus of elasticity $E_{ps} := 28500\ ksi$

Diameter = 0.5 in.

Total Area of the 14 strands $A_{ps} := 2.142\ in^2$

k := 0.28 for low-relaxation steel

2.3. Internal Steel Shear Reinforcement

Yield strength $f_{yt} := 60$ ksi

2.4. FRP Reinforcement

Carbon-Fiber Sheets are used in this example.

Thickness $t_f := 0.0065$ in.

Failure strength $f_{fu} := 550$ ksi

Modulus of elasticity $E_f := 33000$ ksi

Failure strain $\varepsilon_{fu} := \frac{f_{fu}}{E_f}$

$\varepsilon_{fu} = 0.017$ in./in.

3. GEOMETRICAL PROPERTIES

Total height including deck slab $h_T := 38$ in.

Flange thickness $h_f := 6$ in.

Width of the web $b_v := 7$ in.

Effective width of the flange $b_{eff} := 79.0$ in.

Internal shear reinforcement = #3 at 12 in. spacing

$A_v := 0.22$ in^2 $\quad s_v := 12$ in. $\quad \alpha := 90 \cdot$ deg

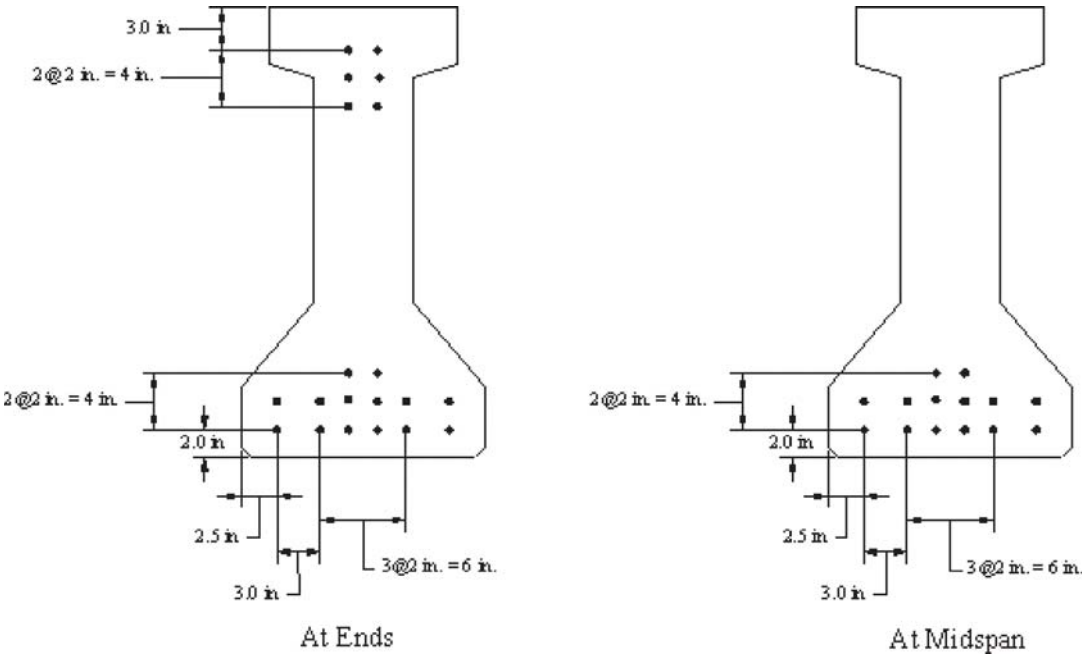

(a) I-Beam Prestressing Pattern

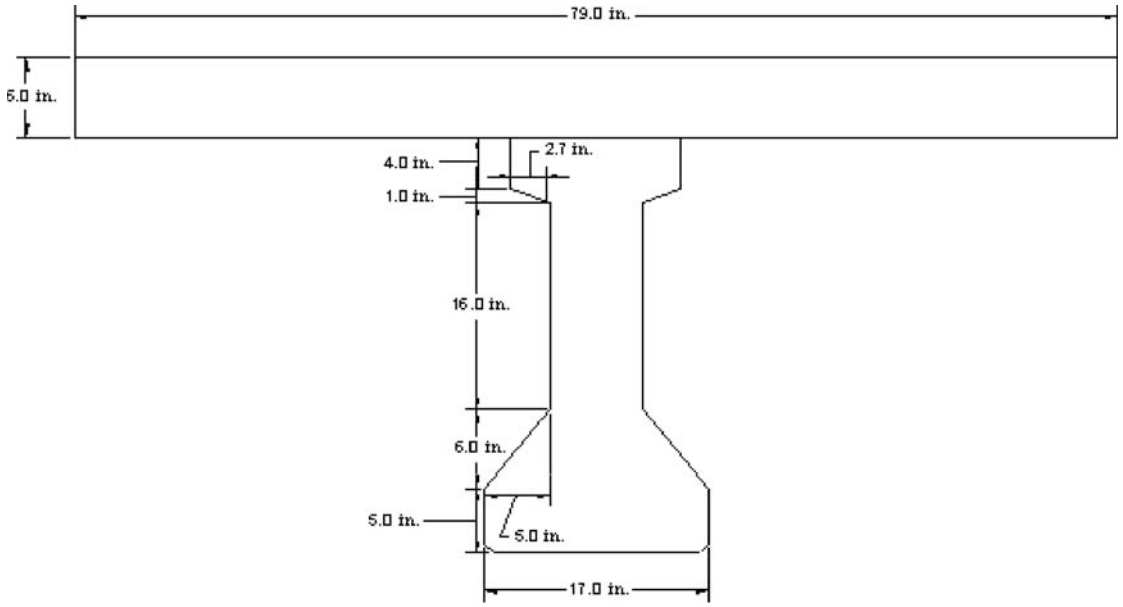

(b) Cross-Section of an Intermediate Beam

Figure 2. Cross-section of an intermediate beam.

4. CALCULATION OF THE FACTORED SHEAR FORCE AND NOMINAL SHEAR RESISTANCE

4.1 Factored Shear Force at the Critical Section

$V_{u\_crit} := 100$ kips

4.2. Calculation of Nominal Shear Resistance

For this example, the simplified approach is followed.

$\theta := 45 \cdot deg$ $\beta := 2$

The nominal shear resistance provided by the concrete, V_c, is calculated in accordance with LRFD Eqn.5.8.3.3-3 as:

The distance from the extreme compression fiber to the center of gravity of the strands at the midspan:

$d_p := 34.6$ in.

Assuming rectangular section behavior with no compression steel, the distance from the extreme compression fiber to the neutral axis, c_c, may be calculated as:

$$c_c := \frac{A_{ps} \cdot f_{pu}}{0.85 \cdot f'_{cd} \cdot b_{eff} \cdot \beta_{1d} + k \cdot A_{ps} \cdot \frac{f_{pu}}{d_p}}$$

$$(c_c) = 2.482 \text{ in.}$$

$$a_c := \beta_{1d} \cdot c_c$$

$$(a_c) = 2.11 \text{ in.}$$

$$\left(\text{check\_a}_c := \left\| \begin{array}{ll} \text{"Assumption is correct"} & \text{if } (a_c \geq h_f) \\ \text{"Not behave as rectangular"} & \text{otherwise} \end{array} \right. \right)$$

$$(\text{check\_a}_c) = \text{"Assumption is correct"}$$

The effective shear depth d_v is taken as the distance, measured perpendicular to the neutral axis, between the resultants of the tensile and compressive forces due to flexure; it need not be taken to be less than the greater of $0.9d_e$ or $0.72h$ (LRFD Article5.8.2.9).
Since some of the strands are harped, the effective depth varies point-to-point. However, the effective depth must be calculated at the critical section in shear, which is not yet determined; therefore, an iterative procedure is required. For this example, only the final cycle of the iteration is shown.

Assume d_v $\quad d_{v\_trial} := 27.36$ in.

Calculate the distance from the extreme compression face to the center of gravity of the strand, d_e at the location, d_v away from the centerline of the support.

$$e_{tr} := \frac{2 \cdot 4 + 4 \cdot 4 + \left[\frac{23}{206.4} \left(206.4 - d_{v\_trial} \right) + 2 \right] \cdot 2 + \left[\frac{23}{206.4} \left(206.4 - d_{v\_trial} \right) + 4 \right] \cdot 2 + \left[\frac{23}{206.4} \left(206.4 - d_{v\_trial} \right) + 6 \right] \cdot 2}{6 + 6 + 2}$$

$$d_e := h_T - e_{tr}$$

$$d_e = 26.021 \text{ in.}$$

Determine d_v $d_{v1} := d_e - \frac{a_c}{2}$ $d_{v2} := 0.9 \cdot d_e$ $\left(d_{v3} := 0.72 \cdot h_T\right)$

$\left(d_{v\_max} := \max\left(d_{v1}, d_{v2}, d_{v3}\right)\right)$

$\left(d_v := \max\left(d_{v\_max}, 0.5 \cdot d_{v\_max} \cdot \cot(\theta)\right)\right)$

Final d_v $\left(d_v\right) = 27.36$ in.

$$Check\_dv1 := \begin{cases} \text{"OK"} & \text{if } 0.995 \le \frac{d_{v\_trial}}{d_v} \le 1.005 \\ \text{"Try Again"} & \text{otherwise} \end{cases}$$

Check_dv1 = "OK"

$$Check\_dv2 := \begin{cases} \text{"OK"} & \text{if } \frac{d_v}{b_v} \le 4 \\ \text{"NOT GOOD"} & \text{otherwise} \end{cases}$$

Check_dv2 = "OK"

The nominal shear resistance provided by the concrete is:

$V_c := 0.0316 \cdot \beta \cdot \sqrt{f'_{cb}} \cdot b_v \cdot d_v$ (LRFD Eqn. 5.8.3.3-3)

$\left(V_c\right) = 32$ kips

The nominal shear resistance provided by the internal steel reinforcement is:

$$V_s := \frac{A_v \cdot f_{yt} \cdot d_v \cdot (\cot(\theta) + \cot(\alpha)) \sin(\alpha)}{s_v}$$ (LRFD Eqn. 5.8.3.3-4)

$V_s = 30.1$ kips

Harped tendon force = 6 x 0.153 x 149.0 = 136.8 kips (assuming f_{pe} = 149 ksi)

slope of the tendons $\psi := 0.111$

$V_p := 136.8 \cdot \psi$ $V_p = 15.2$ kips

The nominal shear resistance of the member is:

$V_n := V_c + V_s + V_p$ (LRFD Eqn. 5.8.3.3-1)

$V_n = 77.3$ kips

5. DESIGN OF FRP SHEAR REINFORCEMENT

5.1 Check if FRP Reinforcement is Necessary

Strength reduction factor for shear ($\phi := 0.9$)

$$Check\_FRP\_Needed := \begin{cases} \text{"NOT need shear reinforcement"} & \text{if } \left(\phi \cdot V_n \geq V_{u\_crit}\right) \\ \text{"NEED shear reinforcement"} & \text{otherwise} \end{cases}$$

Check_FRP_Needed = "NEED shear reinforcement"

5.2 Computation of Required V_f

$$V_{f\_req} := \frac{V_{u\_crit}}{\phi} - V_n$$

$V_{f\_req} = 33.8$ kips

5.3 Selection of FRP Strengthening Scheme

U-wrap configuration is used with anchorage systems at the end of the sheets. The FRP sheets will be applied at 90 degrees with respect to the longitudinal axis of the girder as shown in the Figure 3 below. First, the spacing of FRP strips is chosen to meet the maximum spacing requirement. Then, the width of the FRP strips is selected to adjust the amount of FRP strips.

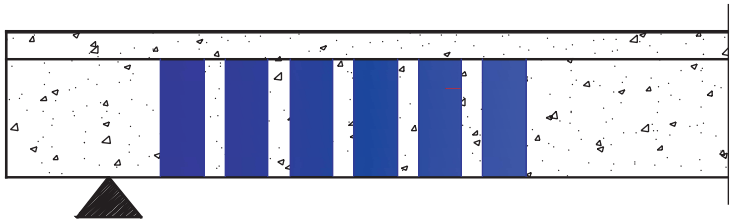

Figure 3. FRP strengthening scheme.

Use number of plies of FRP sheets $n_f := 1$

Use the width of FRP sheets $w_f := 4$ in.

Use the center-to-center spacing of FRP sheets $s_f := 12$ in.

Orientation of FRP sheets $\alpha_f := 90\ deg$

Effective depth of FRP sheets $d_f := d_p - h_f$

$d_f = 28.6$ in.

Check if the selected spacing is acceptable or not

Shear stress on concrete is:

$$v_u := \frac{V_{u\_crit} - \phi \cdot V_p}{\phi \cdot b_v \cdot d_v} \qquad \text{(LRFD Eqn. 5.8.2.9-1)}$$

$(v_u) = 0.501$ ksi

The maximum spacing of the transverse reinforcement is:

$$s_{max} := \begin{cases} \min(0.8 \cdot d_v, 24) & \text{if } v_u < 0.125 \cdot f'_{cb} \qquad \text{(LRFD Eqn. 5.8.2.7-1)} \\ \min(0.4 \cdot d_v, 12) & \text{otherwise} \qquad \text{(LRFD Eqn. 5.8.2.7-2)} \end{cases}$$

$s_{max} = 21.9$

$$Check\_Spacing := \begin{cases} \text{"Acceptable"} & \text{if } s_f \le s_{max} \\ \text{"NOT\_Acceptable\_Change\_the\_Spacing"} & \text{otherwise} \end{cases}$$

Check_Spacing = "Acceptable"

5.4 Calculation of Shear Resistance of FRP, V_f

The FRP reinforcement ratio is:

$$\rho_f := \frac{2 \cdot n_f \cdot w_f \cdot t_f}{b_v \cdot s_f} \qquad \text{(Attachment A Eqn. 5.8.3.3-10)}$$

$(\rho_f) = 6.19 \times 10^{-4}$

The FRP strain reduction factor is:

$$R_f := \min\left[4 \cdot (\rho_f \cdot E_f)^{-0.67}, 1.0\right] \qquad \text{(Attachment A Eqn. 5.8.3.3-8)}$$

$R_f = 0.53$

The effective strain of FRP is:

$\varepsilon_{fe} := R_f \cdot \varepsilon_{fu}$ (Attachment A Eqn. 5.8.3.3-7)

$\varepsilon_{fe} = 8.832 \times 10^{-3}$ in./in.

The effective stress of FRP is:

$f_{fe} := \varepsilon_{fe} \cdot E_f$ (Attachment A Eqn. 5.8.3.3-6)

$\left(f_{fe}\right) = 291.4$ ksi

The shear contribution of the FRP can be then calculated.

$\left(V_f := \rho_f \cdot E_f \cdot \varepsilon_{fe} \cdot b_v \cdot d_f \cdot \left(\sin\left(\alpha_f\right) + \cos\left(\alpha_f\right)\right)\right)$ (Attachment A Eqn. 5.8.3.3-5)

$\left(V_f\right) = 36.1$ kips

$$V_{f\_check1} := \begin{cases} \text{"Change FRP Strengthening Scheme"} & \text{if } \left(V_f < V_{f\_req}\right) \\ \text{"Provided FRP Strength Large Enough"} & \text{otherwise} \end{cases}$$

$V_{f\_check1} = \text{"Provided FRP Strength Large Enough"}$

$$V_{f\_check2} := \begin{cases} \text{"Provided FRP amount is adequate"} & \text{if } \left(V_{f\_req} \le V_f < 1.1 \cdot V_{f\_req}\right) \\ \text{"Change the FRP amount slightly"} & \text{otherwise} \end{cases}$$

$V_{f\_check2} = \text{"Provided FRP amount is adequate"}$

5.5 Calculation of Design Shear Resistance of the Member

The design strength of the member is:

$\phi V_{n\_total} := \phi \cdot \left(V_c + V_p + V_s + V_f\right)$ (Attachment A Eqn. 5.8.3.3-1)

$\left(\phi V_{n\_total}\right) = 102.1$ kips

$$\phi V_{n\_check} := \begin{cases} \text{"Not Good"} & \text{if } V_{u\_crit} > \phi V_{n\_total} \\ \text{"OK"} & \text{otherwise} \end{cases}$$

$\left(\phi V_{n\_check}\right) = \text{"OK"}$

$Web\_crushing\_limit := 0.25 \cdot f'_{cb} \cdot b_v \cdot d_v \cdot V_p$ (LRFD Eqn. 5.8.3.3-2)

$Web\_crushing\_limit = 350.3$ kips

$$Check\_web\_crushing\_limit := \begin{cases} \text{"OK"} & \text{if } \left(V_c + V_s + V_f + V_p\right) \le Web\_crushing\_limit \\ \text{"No Good"} & \text{otherwise} \end{cases}$$

$Check\_web\_crushing\_limit = \text{"OK"}$

6. SUMMARY

Externally bonded FRP sheets were designed in this example. The FRP sheets are applied at 90 degrees with respect to the longitudinal axis of the member with the U-wrap configuration and without anchorage systems as shown in Figure 4. The final design is summarized as:

Use number of plies of FRP sheets $n_f = 1$

Use the width of FRP sheets $w_f = 4$ in.

Use the center-to-center spacing of FRP sheets $s_f = 12$ in.

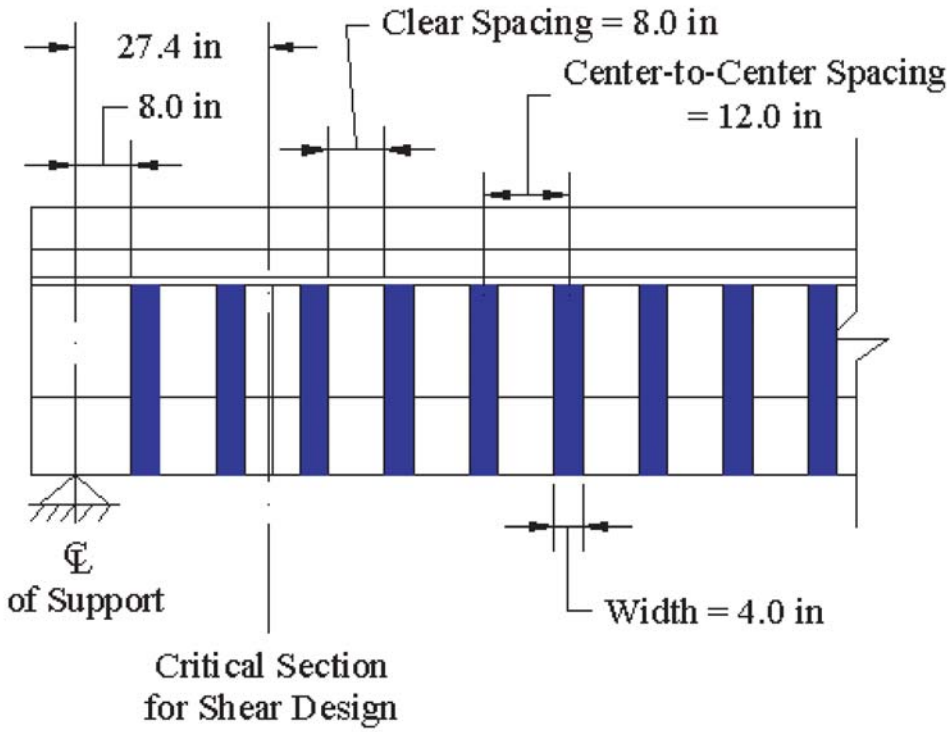

Figure 4. Final design of FRP strengthening.

Abbreviations and acronyms used without definitions in TRB publications:

AAAE	American Association of Airport Executives
AASHO	American Association of State Highway Officials
AASHTO	American Association of State Highway and Transportation Officials
ACI–NA	Airports Council International–North America
ACRP	Airport Cooperative Research Program
ADA	Americans with Disabilities Act
APTA	American Public Transportation Association
ASCE	American Society of Civil Engineers
ASME	American Society of Mechanical Engineers
ASTM	American Society for Testing and Materials
ATA	Air Transport Association
ATA	American Trucking Associations
CTAA	Community Transportation Association of America
CTBSSP	Commercial Truck and Bus Safety Synthesis Program
DHS	Department of Homeland Security
DOE	Department of Energy
EPA	Environmental Protection Agency
FAA	Federal Aviation Administration
FHWA	Federal Highway Administration
FMCSA	Federal Motor Carrier Safety Administration
FRA	Federal Railroad Administration
FTA	Federal Transit Administration
HMCRP	Hazardous Materials Cooperative Research Program
IEEE	Institute of Electrical and Electronics Engineers
ISTEA	Intermodal Surface Transportation Efficiency Act of 1991
ITE	Institute of Transportation Engineers
NASA	National Aeronautics and Space Administration
NASAO	National Association of State Aviation Officials
NCFRP	National Cooperative Freight Research Program
NCHRP	National Cooperative Highway Research Program
NHTSA	National Highway Traffic Safety Administration
NTSB	National Transportation Safety Board
PHMSA	Pipeline and Hazardous Materials Safety Administration
RITA	Research and Innovative Technology Administration
SAE	Society of Automotive Engineers
SAFETEA-LU	Safe, Accountable, Flexible, Efficient Transportation Equity Act: A Legacy for Users (2005)
TCRP	Transit Cooperative Research Program
TEA-21	Transportation Equity Act for the 21st Century (1998)
TRB	Transportation Research Board
TSA	Transportation Security Administration
U.S.DOT	United States Department of Transportation